CANADIAN THESES ON MICROFICHE

THESES CANADIENNES SUR MICROFICHE

I.S.B.N.

National Library of Canada
Collections Development Branch

Canadian Theses on
Microfiche Service

Ottawa, Canada
K1A 0N4

Bibliothèque nationale du Canada
Direction du développement des collections

Service des thèses canadiennes
sur microfiche

NOTICE

The quality of this microfiche is heavily dependent upon the quality of the original thesis submitted for microfilming. Every effort has been made to ensure the highest quality of reproduction possible.

If pages are missing, contact the university which granted the degree.

Some pages may have indistinct print especially if the original pages were typed with a poor typewriter ribbon or if the university sent us a poor photocopy.

Previously copyrighted materials (journal articles, published tests, etc.) are not filmed.

Reproduction in full or in part of this film is governed by the Canadian Copyright Act, R.S.C. 1970, c. C-30. Please read the authorization forms which accompany this thesis.

THIS DISSERTATION
HAS BEEN MICROFILMED
EXACTLY AS RECEIVED

AVIS

La qualité de cette microfiche dépend grandement de la qualité de la thèse soumise au microfilmage. Nous avons tout fait pour assurer une qualité supérieure de reproduction.

S'il manque des pages, veuillez communiquer avec l'université qui a conféré le grade.

La qualité d'impression de certaines pages peut laisser à désirer, surtout si les pages originales ont été dactylographiées à l'aide d'un ruban usé ou si l'université nous a fait parvenir une photocopie de mauvaise qualité.

Les documents qui font déjà l'objet d'un droit d'auteur (articles de revue, examens publiés, etc.) ne sont pas microfilmés.

La reproduction, même partielle, de ce microfilm est soumise à la Loi canadienne sur le droit d'auteur, SRC 1970, c. C-30. Veuillez prendre connaissance des formules d'autorisation qui accompagnent cette thèse.

LA THÈSE A ÉTÉ
MICROFILMÉE TELLE QUE
NOUS L'AVONS REÇUE

NL-339 (r. 82/08)

Canada

A HYBRID EQUALIZATION METHOD FOR QPSK DATA TRANSMISSION OVER NON-LINEAR SATELLITE CHANNELS

By

Basil Ghicopoulos, B.Eng., M.Eng., P.Eng.

THESIS

Submitted to the School of Graduate Studies
in partial fulfilment of the requirements
for the degree of Doctor of Philosophy

Department of Electrical Engineering
Faculty of Science and Engineering
University of Ottawa
Ottawa, Canada

July, 1980

ABSTRACT

The problem of intersymbol interference and its effects is considered. Of particular interest here is the transmission of data over non-linear satellite channels. Existing methods for combatting intersymbol interference, in the form of equalizers, are surveyed. The applicability of some equalization concepts, categorized as non-linear, is investigated. An extensive analytical development, considering some of the contributing factors, such as AM/AM and AM/PM, due to the presence of non-linear elements in the satellite channel, is presented.

A hybrid equalization scheme, incorporating a decision feedback equalization section followed by a reduced state maximum likelihood estimator, is here proposed. It is shown that such a combined approach effectively reduces the intersymbol interference. Consequently, the probability of error is also reduced. The performance of the proposed system has been evaluated by computing approximate upper and lower bounds of the probability of error vs. signal-to-noise ratio. Furthermore, the transmission system, which includes the earth and space segments of a non-linear satellite channel, as well as the proposed hybrid equalization scheme, has been modeled in a computer simulation.

The simulation results indicate a good agreement with the analytical ones. A comparison is also made between the performance achieved when a bit detector is used and the one with the proposed hybrid scheme: The improvement achieved with the later one is noticeable.

ACKNOWLEDGEMENTS

The author wishes to express his sincere graditude and respect to his thesis advisor Dr. W. Steenaart, for his patient guidance provided in the course of this work and for the stimulating discussions held throughout. My sincere thanks also to Professors S. G. Shiva and N. U. Ahmed for the encouragement and fruitful discussions held.

The co-operation and help of the staff of the Electrical Engineering department is appreciated. Equally, the patience and help received from the personnel of the Computer Sciences department, particularly Mr. W. Murray and Miss E. Sullivan, are gratefully acknowledged. Thanks are also due to Mr. J. Huang of Concordia University for cooperation, and to Mrs. M. Stavrianos for her patient and skillfull typing of the document.

TABLE OF CONTENTS

		PAGE
ABSTRACT		ii
ACKNOWLEDGEMENTS		iii
LIST OF SYMBOLS		vii
LIST OF FIGURES		x
LIST OF TABLES		xiii
PART 1:	ASPECTS OF DATA COMMUNICATIONS AND EQUALIZATION	1
CHAPTER I	INTRODUCTION	2
	1. Data communications	2
	2. Data transmission systems	3
	2.1 Signal characterization	9
	3. Scope of present work and Thesis organization	14
CHAPTER II	EQUALIZATION METHODS/TECHNIQUES	18
	1. General	18
	2. Background summary	19
	3. Decision feedback equalization	24
	4. Maximum likelihood detection	30
PART 2:	A HYBRID EQUALIZATION METHOD FOR DATA COMMUNICATIONS VIA NON-LINEAR SATELLITE CHANNELS	36

		PAGE
CHAPTER III	HYBRID EQUALIZATION/SEQUENCE ESTIMATION	37
	1. General	37
	2. Description and analysis of the hybrid receiver structure	39
	3. Performance analysis	55
	3.1 Error events	55
	3.2 Probability of error event	60
	3.3 Probability of symbol error	62
CHAPTER IV	SIMULATION OF A QPSK SATELLITE DATA LINK	66
	1. General	66
	2. System simulation description	67
	2.1 Transmitter chain	74
	2.1.1 Data generator	74
	2.1.2 Modulator and filter	78
	2.2 Satellite transponder	83
	2.2.1 AM/PM non-linearity	86
	2.2.2 TWT model	88
	2.3 Receiver chain	97
	3. System performance	104
	4. System flowchart	108
CHAPTER V	SIMULATION RESULTS	112
	1. Summary of results	112
	1.1 Bit-by-bit decision results	112
	1.2 Hybrid equalization/decision results	123
	2. Discussion	129

PAGE

3. Suggestions for further research 133

REFERENCES 135

APPENDIX I PROBABILISTIC DEVELOPMENT OF LIKELIHOOD RATIO 140

APPENDIX II SIMULATION PROGRAMS 144

LIST OF SYMBOLS

NOTATION	MEANING
A_κ	Amplitude of input random variable
B	Code word
C	Number of samples
E	Error vector
E_m	Error event
I_i	Input sequence to the MLD
L	Number of adjacent symbols
N	Time interval
P(E)	Probability of occurence of an error event
$P(\varepsilon)_u$	Upper bound of the probability of error
$P(\varepsilon)_\ell$	Lower bound of the probability of error
$P(\omega)$	Power spectrum
$\hat{S}_i(t)$	Input envelope voltage
$S_n(k)$	Class of states
$S_o[.]$	Output envelope voltage
$\hat{S}_o(t)$	Output envelope distortion
S_o^I	In-phase envelope non-linear component
S_o^Q	Quadrature envelope non-linear component

a_k	Received signal component
$\{c_j\}$	Sequence of tap gain coefficients
$c(t)$	Amplitude of transmitted signal $s_o(t)$
d	Distance between correct/incorrect path
$e_i(t)$	Input data signal
$g_1(x)$	AM/AM non-linear transfer function
$g_2(x)$	AM/PM non-linear transfer function
h	Channel impulse response (in complex form)
n	Channel length of n symbol intervals
p	Probability density function
$p(s)$	Tx/Rx lowpass filter characterization
$p(t)$	Main component of desired signal
$s(t)$	QPSK bandpass signal waveform
$[s_i(D)]$	Received sequence at the input of the FSM
s_k	State of the finite-state-machine (FSM)
$s_m(t)$	Modulated output signal
$[s_m(t)]$	Transmitted signal set
$s_o(t)$	Narrowband input signal to TWT
s_o^*	Complex baseband TWT output signal
$s_r(t)$	Received (distorted) signal
$u(t)$	Complex envelope representation of carrier f_o

$x(t)$	Bandpass signal input to TWT
x_k	Signal input to the Rx filter
$\{\hat{y}_i\}$	Decision feedback equalizer output sequence
$\{\tilde{y}_i\}$	Sequence of previously detected symbols
y_k	Signal output of the Rx filter
$[z(D)]$	Observed sequence at the output of the FSM
$\Gamma[.]$	Log likelihood representation of p
ε_d	Subset of error events
ε^2	Mean square error of DFE
ζ_k	State transition representation of the FSM
η_k	Additive Gaussian noise
Λ_i	Likelihood ratio
μ	Metric assigned to received signal sample
ξ	Signal-to-noise ratio at the DFE output
ρ	Signal-to-noise ratio
$\sigma^2_{\eta_o}$	Computed noise power (at the input of I&D)
ϕ	Relative phase shift in TWT
$\phi(t)$	Phase variation
$\hat{\phi}(t)$	AM/PM conversion factor

LIST OF FIGURES

FIGURE	TITLE	PAGE
1.1	Graphical representation of ISI	5
1.2	Simplified QPSK mathematical model and detectors	10
2.1	Decision feedback equalizer structure	25
3.1	General structure of hybrid equalization scheme	40
3.2	Hybrid equalizer input sequence	45
3.3	Trellis diagram	49
3.4	Error event path	57
4.1	Block diagram configuration of simulated system	68
4.2	Block diagram of simulated satellite transmission system	69
4.3	Block diagram of the major simulation subroutine blocks	73
4.4	Block diagram of transmitter chain simulator	75
4.5	Generator of a pseudorandom sequence with $p = 2^7 - 1$	75
4.6	QPSK signal constellation	77

4.7	Theoretical model of TWT	85
4.8	TWT Quadrature model as bandpass non-linear device	89
4.9	TWT envelope characteristics	94
4.10	Block diagram of the satellite TWT transponder simulator	96
4.11	Receiver model (front end)	99
4.12	Normalised sampled input to the equalizer	102
4.13	System flowchart	109
5.1	Probability of error vs. signal-to-noise ratio (no ISI present)	114
5.2	Probability of error vs. signal-to-noise ratio (without non-linearities)	115
5.3	Probability of error vs. signal-to-noise ratio (I/P backoff 1 db)	116
5.4	Probability of error vs. signal-to-noise ratio (I/P backoff 12 db)	117
5.5	Eye diagram - 90 Mb/s (I/P backoff 12 db)	120
5.6	Eye diagram -120 Mb/s (" " 1 db)	121
5.7	Eye diagram -180 Mb/s (" " 1 db)	122
5.8	Probability of error vs. signal-to-noise ratio (Hybrid equalization)	124

5.9	Probability of error vs. signal-to-noise ratio (Performance bounds)	125
5.10	Probability of error vs. signal-to-noise ratio (Composite figure)	127
5.11	Probability of error vs. signal-to-noise ratio (Composite figure - higher bit rates)	128
5.12	Eye diagrams - .80 Mb/s (I/P backoff 1 db, Composite figure)	130

LIST OF TABLES

TABLE	TITLE	PAGE
I	Values of the in-phase (a) and quadrature (b) envelope component coefficients	95
II	Channel response terms	105

PART I

ASPECTS OF DATA COMMUNICATIONS AND EQUALIZATION

CHAPTER I

INTRODUCTION

1. DATA COMMUNICATIONS

The rapid development of data communication systems in the past several years is largely due to the increasingly more economical development of the digital integrated circuits. The ensuing widespread use of digital signal processing techniques increased the demand for specialised transmission facilities. Some examples where digital data have to be transmitted from one point to another distant point include the extensive computing facilities to be found in business as well as educational institutions, the digital techniques employed in the (contemporary) telephone systems, sonar systems, computer processing of medical data, signal (voice, image and/or data) processing in space communications and a host of others. These various data sources create a large volume of data which have to be transmitted very rapidly and received quite accurately. These conditions demand an efficient utilisation of the already existing transmission facilities (through sometimes their upgrading) or the creation of new ones (where indicated economically) utilising newer concepts in the field wherever possible.

A major problem in data transmission is the presence of

Intersymbol Interference (ISI). This interference is created primarily due to imperfections in the physical realization of the various subsystems, such as filters, amplifiers, etc., and the characteristics of the transmission media. In order to understand the nature of the ISI problem, some basic data transmission concepts are presented in the next section.

2. DATA TRANSMISSION SYSTEMS

The physical channels used for data transmission include the telephone channels, overland or satellite microwave links, and radio channels. These channels tend to be limited in their use for data transmission at high rates due to bandwidth and noise restrictions: Bandwidth availability, as it is well known, is limited; whereas the noise is everpresent and affecting the data. The channel response is no longer restricted to the time allocated to the transmitted pulse: There is some (energy) spreading or, a time dispersion, to the adjacent symbols thus introducing intersymbol interference (ISI). This time dispersion is due to the bandlimited frequency response of the channel. Adding to it the noise corrupting the signal, one may visualise the "state" of the received signal. Increase of the data (transmission) rate results in even more distorted received signals consequently limiting the overall system reliability.

In the early development stages of data transmission,

equalization of amplitude and/or phase of the transmitted pulses was achieved in a relatively simple and uncomplicated way: In most cases, the influence of the (already known) channels could easily be compensated for through the use of existing (receiver) filtering techniques, primarily of linear nature.

As the higher transmission rates were in greater demand, the equalization problem became more complex. This problem is particularly pronounced in the digital communication environment whereby a sequence of discrete samples, of some periodic pulses, are transmitted over dispersive channels. The received pulses are highly affected by the dispersive channel characteristics because the latter introduce ISI. In essence this ISI is nothing else but symbol overlapping, which can be very severe, resulting at a significantly degraded system error rate performance. The main design objective of such receiver filters (= equalisers) is the minimization of the probability of error, by reducing the ISI and the noise interference.

To obtain an insight as to the nature of intersymbol interference, consider fig. 1.1. The time interval T_o of the signal pulses applied to the input of the channel is shorter when compared with the time interval T separating them (for a certain transmission rate), with most of the energy concentrated around T_o. At the receiving end, i.e.

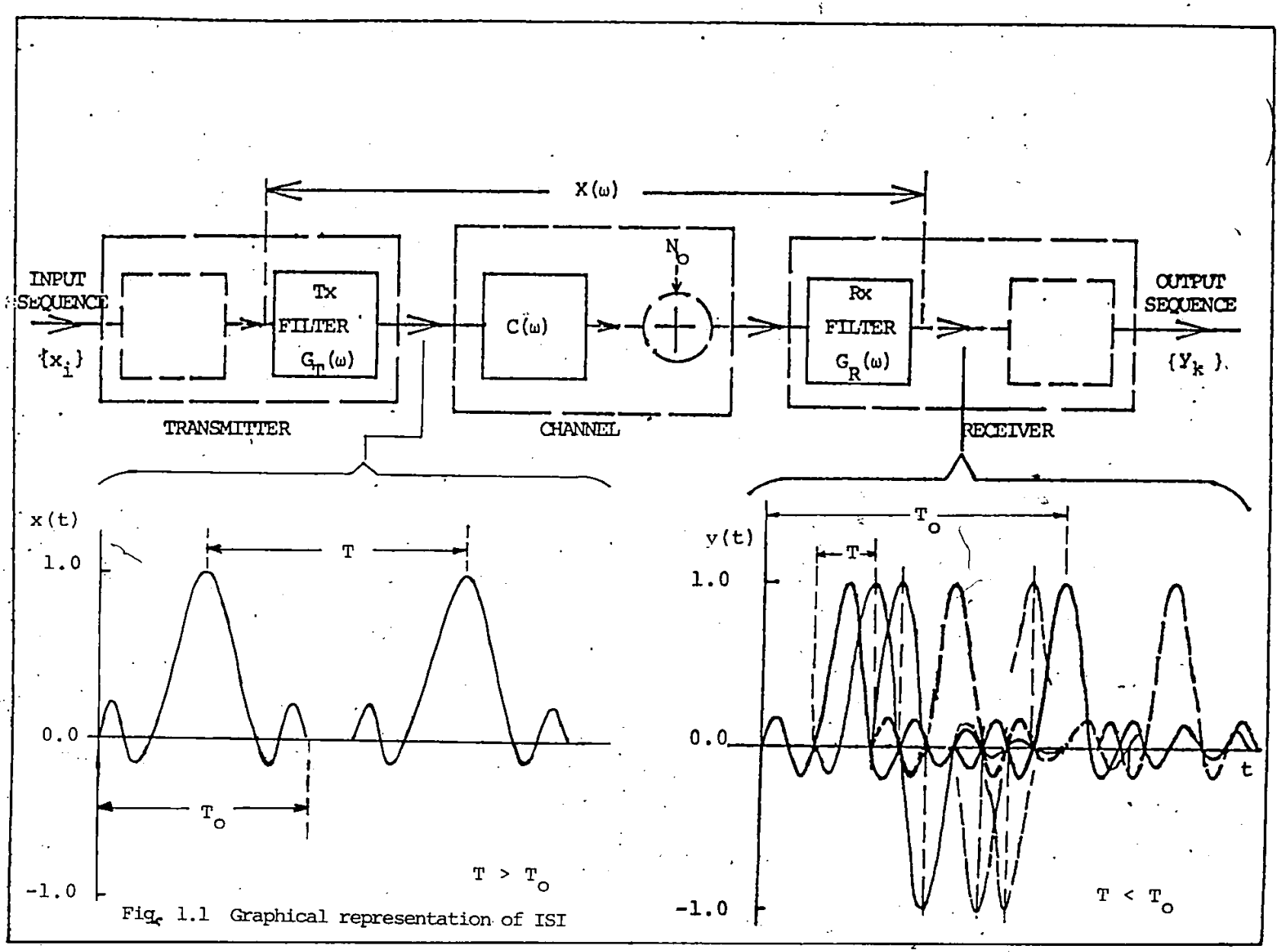

Fig. 1.1 Graphical representation of ISI

having passed through the channel, one observes that this energy is spread over a longer time interval thereby introducing overlapping between the pulses. In other words, some amplitude and/or phase distortion has been introduced by the physical channel. Also, the received signals are further contaminated by noise, which adds to the overall distortion. However, we neglect for the moment, further treatment of the noise component.

Of paramount importance in data communications is the pioneering work of Nyquist [1] who formulated that for intersymbol interference free transmission, signaling through an ideal low-pass filter is possible at a rate of $2f_c$ independent symbols/sec, where f_c is the filter cutoff frequency and provided the signal is sampled at the correct sampling instant.

In essence, intersymbol interference occurs whenever there is bandlimiting. An extensive analysis is to be found in [2]. The signal at the output of the receiver after sampling, will be [3]

$$y_\kappa = \sum_n a_n x_{\kappa-n} + \eta_\kappa \qquad (1.1)$$

where

a_κ = received signal component

x_κ = the input sequence

η_κ = additive white Gaussian noise

Equation (1.1) may be rewritten as

$$y_\kappa = x_o \left(a_\kappa + \frac{1}{x_o} \sum_{\substack{n \\ n \neq \kappa}} a_n \, x_{\kappa-n} + \frac{\eta_\kappa}{x_o} \right) \qquad (1.2)$$

where

x_o = attenuation or gain of the signal passing through the system. Equation (1.2) describes the received signal in terms of its desired component (first term), intersymbol interference (second term) and noise (third term). As the pulse is transmitted through the channel, a frequency dependent time delay is introduced causing its tail samples to interfere with previous as well as forthcoming pulses thus causing intersymbol interference. The effect, which is produced by the last two terms of equation (1.2), is minimized by designing suitable equalization filters.

The bandwidth restriction imposes further constraints on the dimensionality of the signal [4]. Thus, orthogonal pulses (i.e. non-overlapping) when transmitted in sequences through physical channels suffer distortion thereby losing their strict orthogonality property and consequently resulting in intersymbol interference which, in turn, forces a reduced transmission rate. Considering the overall (data) transmission system in our study, the generated signal at the source is propagated through some telephone channel, randomly selected, over land and space microwave links to the sink,

via another telephone channel, which is also randomly selected: All these time dispersive links have impulse or frequency characteristics which are unknown. In addition, there exists a variation of the channel characteristics with time. This time variation may be slow (on the telephone channels) or, significant (on the radio channels). These facts point to the additional receiver requirement of monitoring these characteristics so that adequate compensation may be performed (adaptive operation).

Emphasis is then placed in the suitability of the equalizing (filtering) scheme to compensate for intersymbol interference. The demand for higher efficiency as well as the limitations of the available physical channels, have necessitated the designing of such equalizer systems capable of reducing the intersymbol interference. It is in this area where this study effort is directed. In particular, the effort will be directed towards the investigation of the suitability of the decision theoretic approach towards equalization in connection with a Quaternary Phase Shift Keying (QPSK) modulation scheme as applied to a typical satellite communication channel. There are, basically, two categories under which these equalizer designs are classified: Linear and non-linear. The fundamental concepts, particularly of the latter category, will be reviewed in the next chapter, whereas the forms of the treated signals are reviewed in the next section.

2.1 SIGNAL CHARACTERIZATION

The Phase-Shift Keying (PSK) signals to be used in this work arise from rectangular pulse modulation of a carrier-wave to which one of M phase positions is assigned. The chosen value of M = 4 results in a Quadrature-Phase-Shift Keying (QPSK) modulated carrier. A steady sequence of these pulses is provided at the symbol rate $W = \frac{1}{T}$ where T is the symbol interval. The QPSK signal experiences distortion and creation of interference components due to the channel filters that are inserted between the data signal source and the data signal sink. The simplified low-pass model of a QPSK system is as shown in fig. 1.2. Coherent detection is assumed. Using complex envelope notation [5], the QPSK bandpass signal may be represented as

$$s(t) = \mathrm{Re}\left\{u(t)\exp[j2\pi f_o t]\right\}, \quad 0 < t < T \qquad (1.3)$$

where

$u(t)$ = complex envelope

f_o = carrier frequency

$\exp[.]$ = complex carrier

One avoids the use of sinusoidal carrier frequency terms by using the complex envelope notation in the treatment of the signal and noise quantities. Conceptually, the structure of the quadriphase signal evolves from the sum of two quadrature carriers (sine/cosine), each of which has been biphase modulated with an independent random data pulse. The resulting

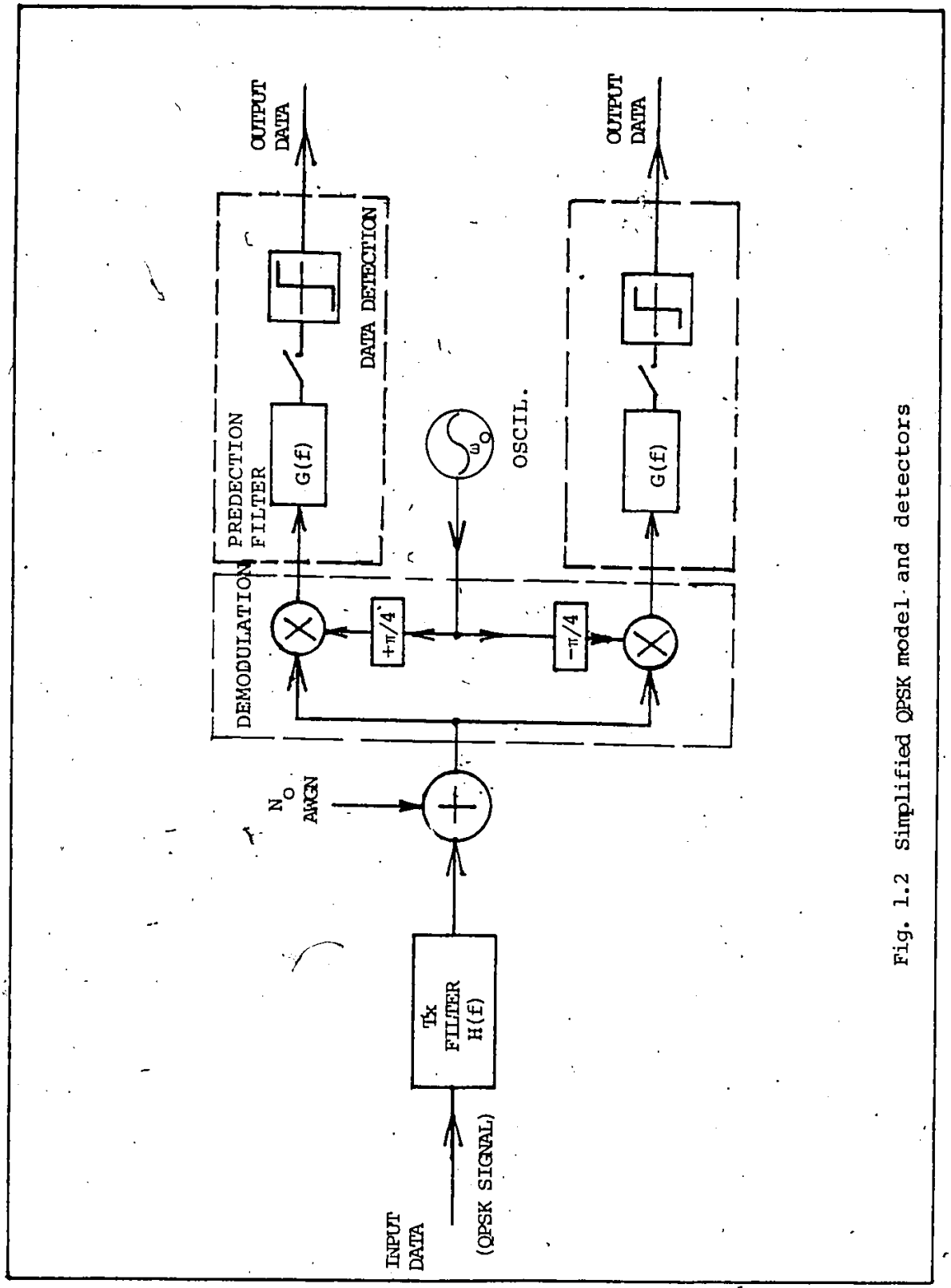

Fig. 1.2 Simplified QPSK model and detectors

quadriphase symbol will then be represented by the complex envelope

$$u(t) = \pm u_r(t) \pm j u_r(t) = \pm\sqrt{2}\, \exp(\pm\tfrac{j\pi}{4})\, u_r(t) \qquad (1.4)$$

where

$u_r(t)$ = Rectangular pulse with unit envelope, defined over $(0,T)$.

The QPSK complex signal envelope consists of a continuous sequence of symbols. The information is conveyed via the phase positions $[\pm \pi/4$ and $\pm 3\pi/4]$. This sequence passes, subsequently, through the transmission filter, which introduces ISI: The data signals become distorted and lengthened in duration causing an overlapping between adjacent symbols. The signal at the filter output, i.e. the modulated pulse waveform, in complex envelope notation and in response to u(t) is represented by

$$p(t) + \sum_{k=-K}^{K} \exp\left(\frac{j\,2\pi i_k}{M}\right) p(t + kT) \exp(2\pi j k f_o T) \qquad (1.5)$$

$$0 < t < T, \quad i_k = 0,1,\ldots M-1$$

where

K = number of interfering previous symbols

p(t) = main, desired pulse envelope

The resulting pulse p(t) in equation (1.5) will be given, in terms of the filter equivalent, low-pass impulse response h(t), by the expression

$$p(t) = \int_0^T u(t)h(t-\tau)d\tau \qquad (1.5a)$$

or, equivalently, in terms of low-pass equivalent spectra, by

$$P(f) = U(f)H(f) = \sqrt{2}\exp\left(\pm\frac{j\pi}{4}\right)U_r(f)H(f) \qquad (1.5b)$$

A fundamental assumption is made here in order to make the results independent of the carrier frequency: It is assumed that

$$\exp[\, j2\pi\, kf_oT\,] = 1 \quad \text{for all } k$$

implying that an integer number of carrier frequency periods is contained within the symbol length T. Using this assumption, the distorted pulse envelope plus intersymbol interference at the filter output, will be represented as

$$p(t) + \sum_{k=-K}^{K} \exp\left(\frac{j2\pi\, i_k}{M}\right) p(t + kT) \qquad (1.5c)$$

Violation of the above assumption, i.e. $f_oT \neq$ integer, will result in an increased number of possible combinations of interference patterns. In particular, for the QPSK signals treated here (M=4), there will be $M^k=4^k$ such possible combinations, since each of the k information carrying previous symbols may have been, independently, in anyone of the M-phase positions relative to the current pulse.

The use of coherent detection permits the low-pass data filter to be treated, via the multiplier operation, as though it were a (symmetrical) bandpass one. The predetection and data detection filter, as shown in fig. 1.2, will then be lumped together, as one filter, described by the low-pass impulse response $g(t)$. With an input then represented by equation (1.5c), the data filter output, at time $t = T$, will be given by

$$v(t) = \int_{-kT}^{T} \left[p(t) + \sum_{k=-K}^{K} \exp\left(\frac{j2\pi i_k}{M} \right) p(t+kT) \right] g(T-t)\,dt \qquad (1.5d)$$

In order to account for the effect of ISI from the sequence of K past and future symbols, the following function is introduced [5]:

$$z_k(f) = 1 + \sum_{k=-K}^{K} \exp\left[j2\pi \left(fkT + \frac{i_k}{M} \right) \right] \qquad (1.5e)$$

$$i_k = 0,1,\ldots,M-1$$

Consequently, equation (1.5d) may be re-written, in a more complete form, as follows:

$$v(t) = \int_{-\infty}^{+\infty} P(f)G(f)Z_k(f)\exp\left[j2\pi f(T) \right] df \qquad (1.5f)$$

An extensive analysis of the intersymbol interference, from the geometrical point of view, has been introduced by Messerschmitt [6], establishing the equivalence between the structure of ISI and a wide-sense stationary discrete random process. Also, the linear and decision feedback equalization methods are being equated to the prediction of a random process; in [7] the analysis is extended to that of the maximum likelihood detectors (MLD), for combatting ISI, whereby a canonical relationship is established between the minimum distance concept of MLD and the performance of the decision feedback equalizer.

The above discussions [6,7], allow for an insight, from a mathematical as well as physical viewpoint, into the nature of the intersymbol interference.

3. SCOPE OF WORK AND THESIS ORGANIZATION

The transmission of digital data signals over non-linear channels, such as the ones associated with a satellite communications link, poses a more difficult task, from equalisation point of view, than the transmission over linear channels. To-date, most efforts towards equalising such channels, have been oriented towards the linear channel environment. This is due to the fact that, the presence of the non-linearities create additional intersymbol interference, particularly at high transmission rates, thereby complicating

the study of such channels: The ensuing analytical complexity is quickly discouraging efforts towards extensive study.

However, it is the author's belief that, extensive theoretical study of an analytical nature, is of primary importance in attempting to optimize and predict the performance of a satellite communication system before its implementation.

Analysis and simulation, as accurate as possible, is more economical than the trial and error approach with hardware. Hence the motivation for undertaking this work. Naturally, the former approach has been adopted in the course of this investigation. On a more technical side, efforts in studying and/or simplifying various equalisation approaches, as applied to the problem of intersymbol interference, have been mainly directed towards the linear channel environment. In particular, efforts towards application of one such algorithm presented by Viterbi [33] , in the presence of the non-linearities in the transmission path, have been met with increased analytical complexity [67]. Consequently, attempts in applying this algorithm, in some modified form or another [41,42], have been limited. Given the optimality of the algorithm and the interest in reducing its complexity, further efforts in that direction are of interest.

The thesis presents a method to combat the ISI created when high-speed data are transmitted via satellite channels.

As a contribution to the solution of equalization problem of high-speed data transmitted via satellite channels, the work presented here addresses the problem of simplification of the Viterbi algorithm, in its simulated form, and in the presence of non-linearities of the channel. More specifically, the application of decision feedback as the pre-equalizing stages, results in a new hybrid equalizer configuration of reduced complexity and therefore more economical. The thesis work is organized in such a manner as to present the related topics, from the simple to the complex, defining new terms and concepts as they appear. Thus, the text proceeds with the background summary of the related work which is presented in chapter 2. In the same chapter, an introduction to possible equalization methods is presented while emphasis is placed in reviewing, in some detail, the two main methods to be further employed, i.e. the decision feedback equalization and the maximum likelihood detection. The application of these concepts to the equalization of data over satellite channels, using QPSK signals, is presented in chapter 3. The analytical development of the proposed receiver structure as well as its performance analysis is studied. That these two methods are chosen in combination is a new feature. In this way the desirable properties of the two methods are combined, while each one is kept simple in structure and therefore practical to apply.

The simulation of the satellite channel and equalizer is presented in chapter 4 where pertinent data, to both the satellite channel and the hybrid equalizer, are also provided. In the same chapter an overall flowchart of the total simulation is also provided.

The simulation results are summarized in chapter 5: These include performance curves, in terms of Probability of Error vs. signal-to-noise ratio, as well as eye diagrams. The latter are provided as a qualitative indication of the signal as received, over a satellite channel, in its distorted form at high bit rates. A summary and a concluding discussion, along with some suggestions for further research work, are to be found in the same chapter. There are also two appendices included: The probabilistic development of the likelihood ratio will be found in Appendix I, whereas Appendix II contains listings of the simulation programs used.

The novel approach in this thesis thus lies in a combination of two equalization methods; each of which alone would require more complex, i.e. higher order, structures to achieve the same result for the equalization of the satellite channel.

CHAPTER II

EQUALIZATION METHODS/TECHNIQUES

1. GENERAL

In data communications, the efforts for combatting the intersymbol interference have been mainly concentrated on improving the performance of the receivers. These efforts consisted primarily in devising various equalisation schemes to counteract the effects of the mainly linear channels. Several techniques have been developed and their principles and applications are presented in numerous publications, e.g. [2,3,9,12,14,5]. These techniques have been widely exploited and adapted to suit the purposes of particular situations. In a very general manner, these methods have been categorised either as linear, whereby mainly transversal filters are used, or as non-linear, whereby the use of quantizers and feed-back techniques are employed.

The aim of the linear methods is to minimize the mean-square error or the average probability of error, whereas that of the non-linear ones is the minimization of the probability of error of either the individual symbol or of an entire sequence. The intersymbol interference introduced during high-speed data transmission over non-linear channels, as in the present case, is considerable. It has been demonstrated

that, at high speeds [18,41], the linear type equalization methods, are not effective. Non-linear methods have proven more effective [15] in improving the overall system performance.

This work is mainly directed towards the non-linear equalizers. In particular, of the various approaches so far investigated, we will briefly review in this chapter, the basic operation of the decision-feedback equalizer as well as the maximum likelihood sequence estimation/equalizer. The first is classified as a symbol-by-symbol type whereas the second one is of the maximum likelihood sequence estimator type, i.e. it operates on sequences of symbols. It appears to be a reasonable approach, as it will be shown on chapter 3, to use these techniques in combination. In addition, we will present in summary form in the next section, the historical as well as the technical background of the related work on channel equalization.

2. BACKGROUND SUMMARY

The introduction of the transversal filter for equalization dates back to 1935 and is due to Wiener and Lee [3]. It was not until 1940 when Kallmann [9] actually made use of such a device.

This type of filter can be used to minimize, in the time domain, the intersymbol interference occuring in bandlimited

channels. However, the demand for higher data transmission rates, in the last decade or so, has really spurred an increased activity [3].

Concepts and techniques introduced by Lucky [10], [11] dominated and, to some extent still dominate today, the field of adaptive equalization, i.e. minimization of ISI based on continuous observation of the time varying linear channel. This technique, although quite effective in the case of private-line use for data transmission, is regarded as less so in the switched (telephone) network case. Indeed, various attempts by the industry to implement these concepts resulted in bulky and, occasionally, not so effective modems to be used in connection with dial-up facilities [11]. Further work by R. Gitlin [12] resulted in some improvements to the design of the proposed least-mean square algorithm. Here, the main concern is the choice of the correct algorithm form which is used for adjusting the tap-coefficients of the equalizer. Further investigation, by A. Gersho [13], dealt with the problem of equalizing an "unknown" channel, i.e. one that is selected randomly. The main idea of his proposal was the introduction of the concept of operating the equalizer in a tracking mode so that, its coefficients are continuously updated and minimization of the error criterion at the output is sought. This contribution is considered as a fundamental solution for adaptive equalization in digital communications, along with previous similar work, of a more general nature,

by M. Di Toro [19].

An equally fundamental paper on the random variation aspects of the linear channels is that by P. Bello [20]. This work is primarily directed to the characterization of the channels, resulting in the derivation of some useful channel models. A significant development in the design of equaliser-structures is the work reported by W. Steenaart and R. Ramachandran [14] which applies to discrete time signals transmitted through random channels. The resulting simplified equaliser structure seems to be particularly suitable in the environment of the dial-up (automatic, switched telephone) network. Extensive analytical work has been performed by many researchers in the design aspect of the various networks associated with data transmission. A good example of such work is the one reported by F. Assal [21]. Here, the analytical as well as practical aspects of linear channel transfer functions are discussed.

So far the equalization methods mentioned are linear. However, linear methods are less effective when large and extensive intersymbol interference is present. More efficient methods have been developed utilising non-linear approaches. One of the most important such method is decision feedback equalization. Of particular interest here is the work reported by P. Monsen [22], where he considers the non-linear equalization concept for data transmission through a fading

dispersive channel: Furthermore, he demonstrates the superiority of the decision feedback receiver. Work by K. Abend and B. Fritchman [23] and R. Price [24] develops the symbol detection through the use of decision feedback equalization further. A more recent contribution, by R. Gitlin and E.Y. Ho [25] extends the concept of decision feedback equalization in conjunction with maximum likelihood bit detection. The concepts of decision feedback equalization and maximum likelihood bit detection are presented in sections 3 and 4 respectively.

The interest in adaptive equalization is sustained, as evidenced in the work reported by H. Berger and H. Poza [26] as well as that of D. Falconer et al [27]. The first relates to investigation on data transmission at very high data rates in space transmission environment, whereas the second one reports on work related to data transmission on two-wire dialed lines. There have been some advances and developments in both linear and non-linear equalization techniques. The most representative work has been reported in [16], [18], [28], [29], [30]. Furthermore, some new approaches to the equalization aspects have been reported by K. Mueller and Spaulding [17] and by P. Butler and A. Cantoni [31].

All previously mentioned methods have been based on the symbol by symbol detection technique. A different approach, based on the observation of the entire received sequence, was

introduced by Forney [32]: The maximum likelihood sequence estimator (MLSE) uses, for efficient computation and sequence decisions, the Viterbi algorithm (VA) [33]. Although this algorithm is primarily a concept for decoding convolutional codes, the idea that the operation of the channel can be viewed as that of a convolutional coder [34], [35] gained acceptance. Its natural consequence was that, the equalization process, for reducing ISI, could be considered as that of decoding. Consequently, the VA could be successfully used as the optimum equaliser/decoder for an entire received sequence. It is to be noticed, however, that the VA algorithm itself is a special form of dynamic programming introduced by Bellman [36]. Application of this concept had also been reported by Kobayashi [37], [38], while its extension, in adaptive configuration has been reported, among others, by Ungerboeck [39] and Qureshi [40].

Recently, Mesiya et al, [41] and Hermann [42] have investigated the suitability of the maximum likelihood sequence estimation as applied to receivers which attempt to compensate for intersymbol interference in the case where the transmission channel is of non-linear nature: In [41], the application and performance of MLSE for binary phase-shift-keying (BPSK) is investigated for input data sequences with equal a priori probabilities; in [42] an attempt is made to examine, always through simulation, the performance of MLSE, for a finite memory non-linear channel, and compare it to a

known receiver structure with bit-by-bit decision rule. The work outlined indicates that there is a sustained interest in the "equalization" aspects of data transmission. In particular, as the demand for higher bit rates and the proliferation of satellite communication systems increases, further efforts and interest seem to be well justified.

3. Decision feedback equalisation

The main concept of the decision feedback scheme is based on the cancellation of the tail associated with the received pulses to eliminate the ISI of these pulses at the sampling time of the present pulse, which is sampled at the peak of the matched filter output. The structure of such equalizers using digital filters is as shown in fig. 2.1

In the configuration shown, the filter taps of the feed-forward and feedback section are spaced at equal symbol intervals T. Denoting the sequence of the detected symbols as

$$\{ \tilde{y}_{i-1} , \cdots , \tilde{y}_{i-n_2} \}$$

the estimate of the i^{th} symbol as $\hat{y}_i$, and
the sequence of the tap-gain coefficients of the filters as $\{c_k\}$
the output of the equalizer may be expressed as

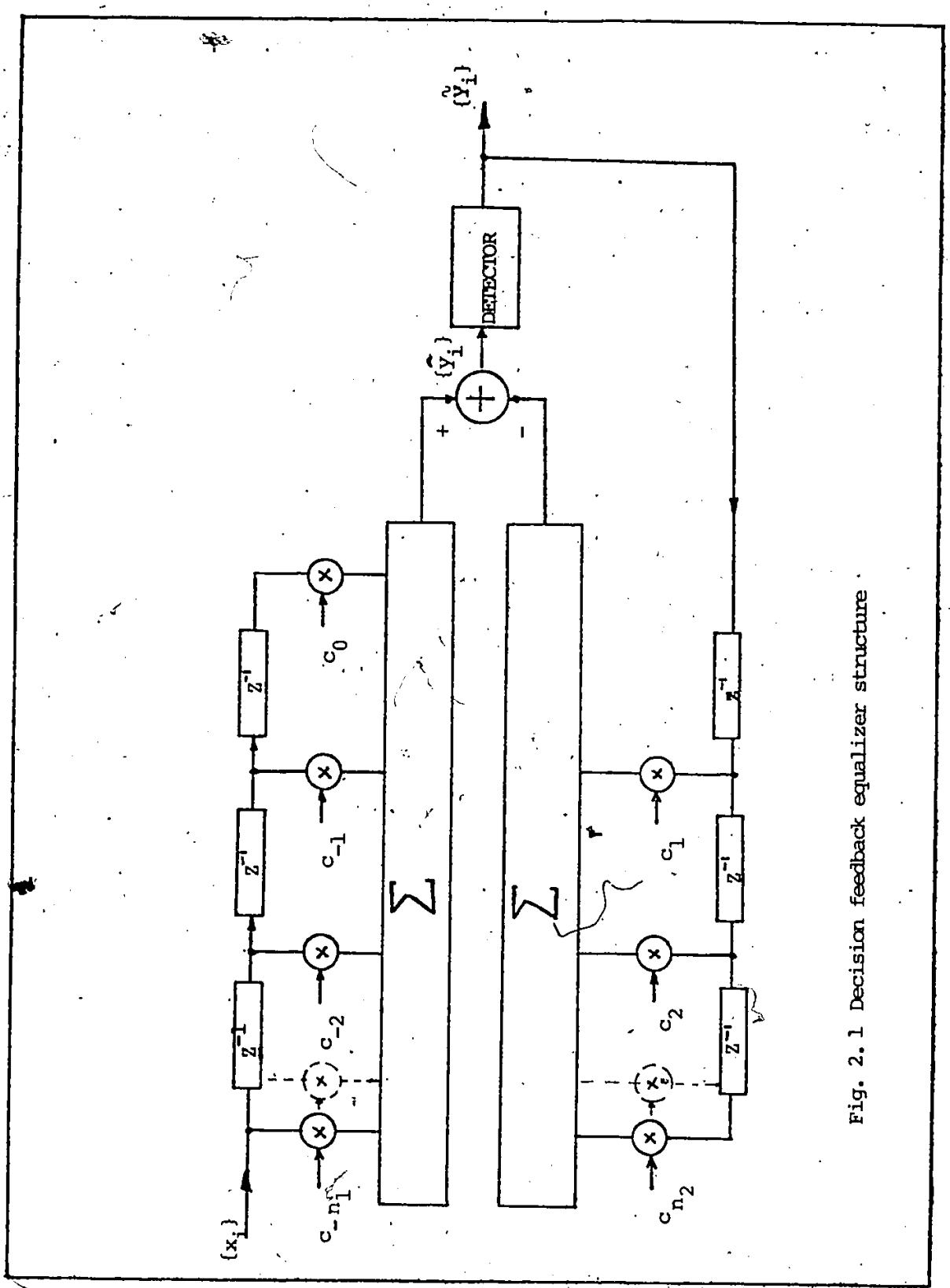

Fig. 2.1 Decision feedback equalizer structure

$$\tilde{y}_i = \sum_{k=-n_1}^{0} c_k x_{i-k} + \sum_{k=1}^{n_2} c_k \tilde{y}_{i-k} \qquad (2.1)$$

where $\{x_i\}$ is the input sequence, and the feedforward filter section is assumed to have $(n_1 + 1)$ taps whereas the feedback has n_2.

The calculation of the coefficients c_k is facilitated by using the mean-square error criterion and their selection is based on a set of linear equations as shown in [15], where it is shown that the values of the feedback filter coefficients are given in terms of the coefficients of the feed-forward section. It is claimed, in [15], that these values of the feedback coefficients result in cancellation of the ISI due to the preceding pulses under the assumption that the decisions on their polarities were made correctly.

The uncertainty in the decision-directed detection of the symbols, combined with the residual ISI and the channel noise, is of primary importance in evaluating the performance of such an equalizer. There are various criteria of performance requiring optimal tap-gain setting of both, the feed-forward as well as the feed-back digital filters. The adopted criteria are:

(1) The minimum mean-square distortion [8]

(2) The zero-forcing (complete elimination of ISI) criterion [24]

(3) The minimum mean-square error [6,22]

(4) The minimum probability of error [7]

In comparing the performance of the decision feedback equalizer with that of the linear type, a convenient assumption is made i.e. that the input signals to the decision feedback equalizer are correct and therefore no errors have occurred. Later on, this assumption will be waived and the effect of decision errors will be examined. Under this assumption then, the calculation of the average probability of error will produce a lower bound. It has been shown [3], that in considering a M-Φ communication system, operating over a linear channel perturbed by Gaussian noise, the P(e) is given by

$$P(e) = 2\left(1 - \frac{1}{M}\right) Q\left[\sqrt{\xi}\right] \qquad (2.2)$$

where

$$Q(x) = \frac{1}{\sqrt{2\pi}} \int_{x}^{+\infty} e^{-t^2/2}\, dt \quad , \text{ the error function}$$

$$\xi = \left(\frac{3}{M^2-1}\right) a \left(\frac{S}{N}\right) \quad , \text{ equalizer output SNR}$$

a = signal-to-noise ratio enhancement factor. Since considerable detail is involved in the expression of this factor, the reader is referred to [3] for further particulars.

M = 4 for a QPSK system

Now, the resulting signal-to-noise ratio for the decision feedback equalizer, i.e. the parameter ξ in equation (2.2), for a system operating over a noisy channel, is given by [24]

$$\xi = \frac{2}{N_o T} \exp\left\{ \frac{1}{2T} \int_0^{1/2T} \ln \left[\sum_{k=-\infty}^{+\infty} \left| R\left(f - \frac{k}{T}\right) \right|^2 \right] df \right\} \qquad (2.3)$$

where

$R(f)$ = Fourier transform of the received pulse.

Furthermore, it has been shown [24] that ξ, as given in (2.3), is always greater than the one given in (2.2) under the stated assumption, i.e. there are no decision errors present in the input to the decision-feedback equalizer. Consequently, one may state that the performance of a decision feedback equalizer is superior to that of a linear equalizer when employed in systems operating over bandlimited channels.

Further comparison is possible by examining alternative performance criteria. Thus, considering minimisation of the mean-square error ε, it has been found [52] that

$$\overline{\varepsilon^2}\ (\text{FEEDBACK EQUALIZER}) \leq \overline{\varepsilon^2}\ (\text{LINEAR EQUALIZER})$$

The above statement applies when comparing the respective operating equalizers over a linear channel.

As an alternative criterion consider that of minimisation of probability of error [7]. Comparative studies [54] have in-

dicated a good agreement between the performance of a decision feedback equalizer operating over linear as well as non-linear channels with severe ISI, under the mean-square error criterion and that of the same equalizer under the probability of error criterion. The overall conclusion then may be drawn that the feedback equalization scheme will perform better than a linear equalization scheme.

The above discussion was based on the assumption that the symbols presented to the input of the equalizer had been correctly decided upon. By waiving this assumption, however, the indicated superiority of the DFE type of equalization is somewhat lessened. This is due to the fact that, if there is an error made on the decision of the input signals, then this error tends to propagate through the feedback loop, thus reducing the effectiveness of the equalizer in cancelling entirely the ISI. Reduced effectiveness, however, is interpreted also as increased possibility of making additional errors on the subsequent symbols. This error propagation then, due to residual intersymbol interference, reduces the margin against noise and decisions for future symbols are prone to errors.

Lest we believe that the above paragraph cancels out the superiority of the decision feedback equalizer when it is employed in real channel situations, we hasten to mention some further developments. In dealing with the error propagation problem, upper bounds on the error probability have

been derived analytically [55] and further extensive comparative studies have been made of standard equalization techniques over bandlimited channels [18,54]: It has been demonstrated that, assuming identical conditions for both, the linear as well as the feedback equalizer, as far as the noise sequence samples are concerned (i.e. independent, hence, uncorrelated) and stationary and Gaussian channel noise, the "error probability of the decision feedback equalizer is smaller than that of the linear equalizer at high signal-to-noise ratios". Furthermore, the decision feedback equalizer apparently is insensitive to timing and carrier phase [18] and Doppler shifts [22]. These results seem to cover the conditions for most of the practical channels. Hence the superiority of performance of the decision feedback equalizer is maintained.

4. Maximum likelihood detection

The concept of detection based on the maximum likelihood rule is well documented and has been extensively dealt with [56]. However, its applicability to decoding of convolutional codes was identified by Viterbi [33]. Subsequently, Forney [32] realized that this method could be used as an effective means in combatting intersymbol interference in digital communications. Since the concept of maximum likelihood detection (or, sequence estimation) incorporating the

computationally efficient Viterbi algorithm (VA), will be used in the proposed hybrid equalizer structure, we will review it here briefly.

This approach differs from the previously described in that, the detection is based not on the symbol-by-symbol minimization of the probability of error, but on a decision made on an entire sequence of N symbols. Observing a received signal sequence (acting as input to the equalizer) $x_1, x_2, x_3, \ldots\ldots x_n$, the most probable sequence will be retained and its a posteriori probability will be computed with the aid of the VA. Assuming that all sequences are equally likely, the maximum a posteriori detection scheme is equivalent to the maximum likelihood criterion: The "surviving" (detected) sequence will be the one possessing the maximum joint probability density. Having for example, a sequence $\{y_i\}$ of κ symbols, these symbols being chosen from a Q alphabet, then there will be Q^{κ} possible such sequences. It is clear that Q^{κ} a posteriori probability calculations are required. However, application of the VA reduces this amount of calculation, as it will be shown later on. The decision then as to which sequence, from all the Q equally likely ones, will be the correct one, is made in favour of that sequence that will maximize the expression [15]

$$p[x_{\kappa}|y_{\kappa}] \triangleq p[x_{\kappa}, x_{\kappa-1}, \ldots, x_1|y_{\kappa}, y_{\kappa-1}, \ldots, y_1] \quad (2.4)$$

Further to the fundamental assumption that all sequences are to be equally likely, we also assume that the noise sequence is Gaussian, white and statistically independent of the signal. Based on these assumptions, the joint probability density, for real valued symbols transmitted through a non-linear channel with impulse response samples h_k, will be given [15]

$$p[x_\kappa|y_\kappa] = \frac{1}{\sqrt{2\pi}\sigma} \exp\left\{-\frac{1}{2\sigma^2}\left(x_\kappa - \sum_{j=o}^{N} h_j y_{\kappa-j}\right)^2\right\}_{k<N} \qquad (2.5)$$

Equation (2.5) suggests that, if no intersymbol interference is present, there will be only $Q\kappa$ probabilities calculated for the detection of κ symbols, instead of Q^κ : This is primarily due to the fact that the signal x_κ depends only on the signal y_κ, i.e. there is a requirement for maximizing only the individual probability densities $p[x_\kappa|y_\kappa]$. Thus, one may also write

$$p[x_\kappa|y_\kappa] = \prod_{j=1}^{N} p[x_j|y_j, y_{j-1}, \ldots, y_{j-N}] \qquad (2.6)$$

If there is intersymbol interference present with N interfering components, maximization of the quantity indicated by equation (2.6) will be most effectively performed by applying the VA [33].

Many articles have been published on the VA. Forney

[57] and Proakis [15], among others, presented in a rather detailed format the application of VA in digital communication. A practical modification [15] to equation (2.6) is to consider the natural logarithm of both sides of the equation. From Q^{N+1} possible sequences, which have been subdivided into Q^N groups, there is one sequence, from each group, that has the largest probability. This sequence is retained and a quantity, called metric μ, is assigned to it. The metric, in its general form, and for y_{N+i} symbols is given by [15]

$$\mu_i(y_{i+N}) = \max_{y_i} \left\{ \ln p(x_{i+N}|y_{i+N}, \ldots, y_i) + \mu_{i-1}(y_{N+i-1}) \right\} \qquad (2.7)$$

The metric values calculated according to the above equation, will provide the probabilities of the Q^N surviving sequences. In its actual operation the VA computes, for each received signal sample, the Q^{N+1} probabilities, i.e.

$$\ln p\,(x_{i+N}|y_{i+N}, \ldots, y_i) + \mu_{i-1}(y_{N+i-1}) \qquad (2.8)$$

These probabilities correspond, of course, to the Q^{N+1} signal sequences which are thought of as the continuation of the Q^N previous (and, therefore, surviving) sequences. Subsequently, the Q^{N+1} sequences are subdivided into Q^N groups. Each and every group contains Q sequences (with the only difference from sequence to sequence, being the symbol y_i). From each

of those Q groups, the sequence with the largest probability or, equivalently, the sequence with the minimum assigned metric, is selected and the remaining Q - 1 sequences are ignored. The end result is that Q^N sequences are, again, left with their corresponding metric assignments. It is easy to see that, for κ symbols to be detected, a total of κQ^{N+1} probabilities' calculations are necessary. This contrasts with the Q^κ probabilities that they would have been necessary to calculate if the symbol-by-symbol detection/estimation method were to be used. Typical values of all parameters are given in chapter 4.

In adopting the VA for solving the problem of intersymbol interference, Forney [32] introduced the concept of the channel representation as a Finite State Machine (FSM). Thus, in its most general form, the concept considers the machine as having Q^N finite states, for a Q - size symbol alphabet. The VA is then to be viewed as the procedure which identifies, at all times, the state of that finite-state machine (i.e. the channel) producing the Q^N most probable sequences. The error-rate performance of the above algorithm, is expressed [32] with rather tight upper and lower bounds.
In its most general form, the probability of error P(e) for such a system, operating over a linear channel, will be given by [32]

$$K_l Q\left[\frac{3}{N^2-1}\, r_e\right]^{1/2} \leq P(e) \leq K_u Q\left[\frac{3}{N^2-1}\, r_e\right]^{1/2} \qquad (2.9)$$

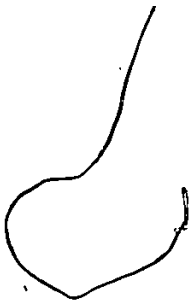

where

K_u, K_ℓ are constants, independent of SNR

r_e is the effective signal-to-noise ratio

$Q[.]$ is the complementary error function

The concept of an error event is of particular interest in analysing the algorithm's performance. An error event occurs when there is a deviation between the actual state sequence and that estimated by the VA. The usefulness of this concept is that it permits us to calculate [57] the error probability per unit time, thus facilitating the calculation of the error probability for a lengthy sequence. These calculations lead to upper and lower bounds for the probability of error events. This concepts will be utilised extensively in the next chapter in deriving the performance bounds.

PART II

A HYBRID EQUALIZATION METHOD

FOR

DATA COMMUNICATIONS VIA NON-LINEAR SATELLITE CHANNELS

CHAPTER III

HYBRID EQUALISATION/SEQUENCE ESTIMATION

1. GENERAL

The application of the DFE and MLSE concepts to the reception of data transmitted via satellite channels will be presented.

We propose a new hybrid equalizer structure which will be analysed and it will be shown that, this structure is quite effective for the purpose of minimizing the probability of error in the presence of down-link noise and intersymbol interference due to a non-linear TWT in a satellite data link.

Applicability of the non-linear equalization is suitable because of the fact that intersymbol interference between noiseless signal pulses is discrete [32]. The exploitation of this discreteness through the use of non-linear methods, such as DFE and MLSE (or VA), as opposed to the use of linear ones, results in considerable noise suppression and reduced intersymbol interference. In addition, the optimal performance of the VA, albeit with an increasing complexity as the number of intersymbol interference terms increases, merits an attempt to reduce this complexity. Efforts to that effect

have been initiated by Forney [32], whose structure includes a whitening matched filter for "pre-equalization" purposes and by Qureshi [40] who used a decision feedback scheme to "pre-equalize" linear channels. Others [39, 59-62] have studied the possibility of reducing the complexity of the VA by analysing various approaches to optimizing individual stages for shaping the channel impulse response presented to the VA. However, attempts to apply these concepts in the satellite transmission environment, for counteracting the effects of intersymbol interference, have been limited to-date. The non-linear nature of the channel makes attempts to precisely analyse it difficult. Thus the accepted recourse is the use of digital simulation so that a relatively complete model can be studied. For BPSK, the maximum likelihood sequence estimation concept, for minimizing the probability of error of the received sequences over non-linear channels, has been studied [41] whereas in [42] an extension has been attempted, for comparison purposes, to other modulation schemes, e.g. OQPSK, MSK. However, the equalization schemes proposed use linear elements as their pre-equalizing stage (prior to VA) with the exception of [40,62] where, although non-linear (DFE) equalizing methods are proposed (similar, in principle, to the one we will apply), they are applied towards linear channels.

2. DESCRIPTION AND ANALYSIS OF HYBRID RECEIVER STRUCTURE

The received signal is distorted due to ISI and downlink noise: This distorted signal will be represented by

$$s_r(t) = s_o^*(t) + \eta(t) \qquad (3.1)$$

where $s_o^*(t)$ = the complex baseband equivalent representation of the transmitted signal, described by equation (4.14).

$\eta(t)$ = the downlink noise

We assume that the channel is characterised by a finite impulse response of ν-symbol intervals, i.e. ν is the smallest integer such that

$$h(nT) = 0 \quad \text{for } t \geq \nu T \qquad (3.2)$$

In accordance with Forney [32], this impulse response may further be viewed as a sequence, i.e.

$$h_i(t) = h_o(t) - h_i(t-T) + \ldots + h_\nu(t-\nu T)$$

$$= \sum_{i=0}^{\nu} h(it)\, \delta(t-iT) \qquad (3.3)$$

The general representation of the proposed hybrid equaliser structure is as shown in fig. 3.1. Referring to fig. 3.1,

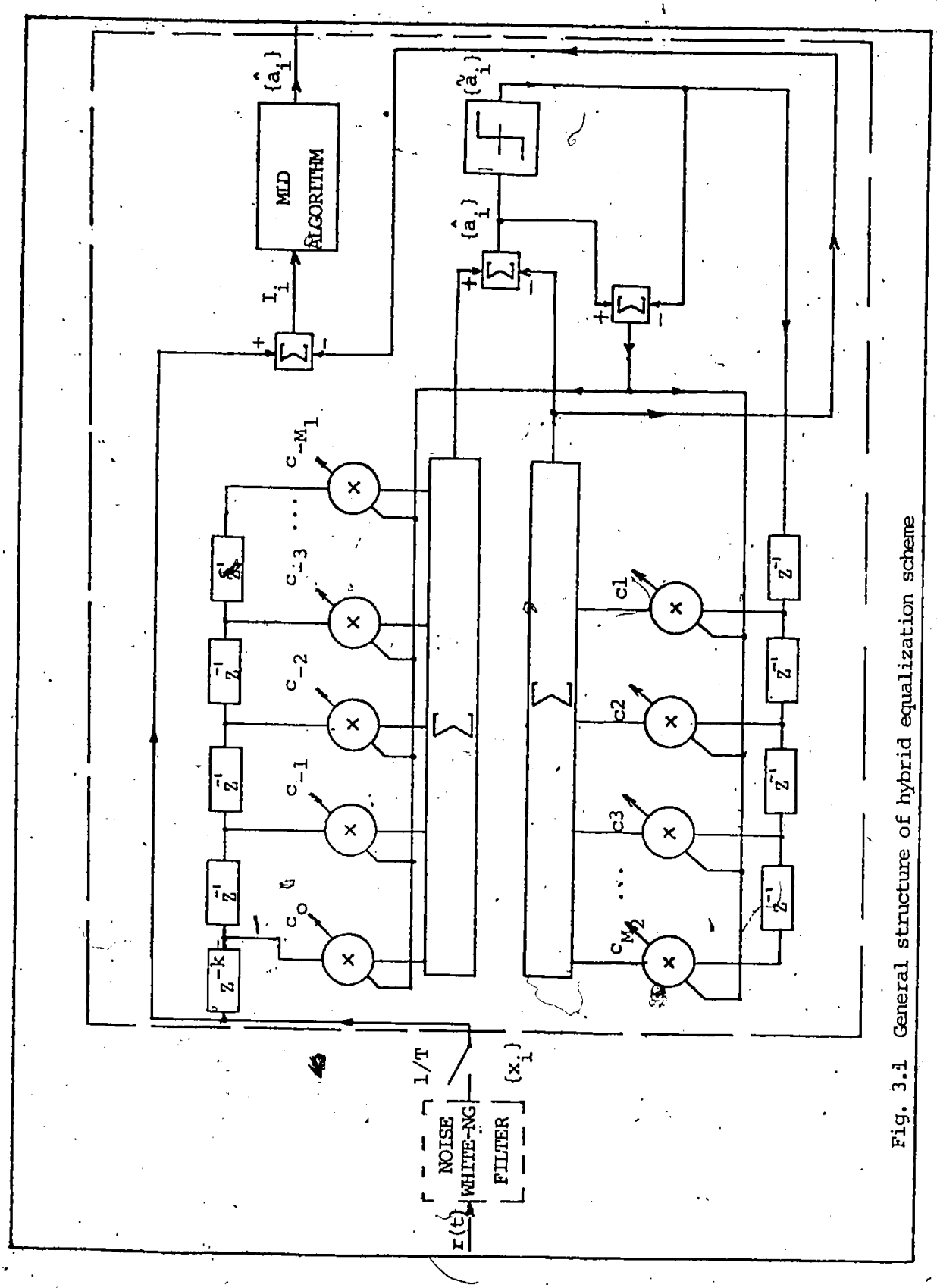

Fig. 3.1 General structure of hybrid equalization scheme

$s_r(t)$ represents the received input signal, with $\{x_i\}$ the input sample sequence to the equalizer receiver section, whereas $\{\tilde{a}_i\}$ will be the (tentative) output sequence of the decision-feedback section and $\{I_i\}$ the input sequence to the VA (here termed "Maximum Likelihood Detector (MLD) Algorithm").

The use of the filter which is equal to the transmit filter, is for bandlimiting and whitening the noise sequence sample. The sampled output of the filter, represented by $\{x_i\}$, is

$$\{x_i\} = \sum_{k=o}^{\nu} a_{i-k}\, h_k + n_i \qquad (3.4)$$

where

a_{i-k} = amplitude samples of the transmitted pulses
$= S_o^*(t)$
h_k = total channel impulse response
n_i = additive white noise samples

The structure of the DFE, as shown in Fig. 3.1, consists of two sections: A feedforward section and a feedback section. The feedforward section is a transversal filter with taps spaced at the symbol interval T and with input sequence $\{x_i\}$. The feedback section is also a transversal filter with taps spaced at the symbol interval. The inputs to the feedback section are decisions on previously detected symbols. Functionally, the feedback section is used to remove that

portion of ISI caused by previously detected symbols from the estimates of future symbols.

The equalizer output, in analogy with equation (2.1), can be expressed as

$$\hat{a}_i = \sum_{k=o}^{-M_1} c_k x_{i-k} + \sum_{k=1}^{M_2} c_k \tilde{a}_{i-k} \qquad (3.5)$$

where $\hat{a}_i$ is an estimate of the i^{th} information symbol, $\{c_k\}$ are the tap coefficients of the filter, $\{\tilde{a}_{i-k}\}, 1 \leq k \leq M_2$, are previously detected symbols and, $\{x_{i-k}\}$ is the input sequence to the equalizer, a function of the channel response, as indicated by equation (3.4). It is to be noted that, the equalization process is performed in a continuous manner in order to obtain the best tentative decisions $\{\tilde{a}_i\}$.

The equalizer has $(M_1 + 1)$ taps in its feedforward section and M_2 taps in its feedback section, as indicated by equation (3.5). A practical means for determining the coefficients $\{c_k\}$, is the use of the mean square error [15] criterion. Based on the assumption that previously detected symbols are correct, the minimization of the mean square error leads to a set of linear equations for setting the tap coefficients of the feedforward section:

$$\sum_{k=0}^{-M_1} c_k b_{kn} = h' \quad , \qquad m = 0,-1,\ldots,M_1 \qquad (3.5a)$$

Where h' is the complex conjugate of the channel response h as given by equation (3.3), and

$$b_{kn} = \sum_{n=o} h_n' h_{n+m-k} + N_o \delta_{km} \quad , \quad m,k=o,\ldots-M_1$$

The coefficients of the feedback section are given in terms of the coefficients of the feedforward section according to the following equation [15]

$$c_i = \sum_{k=o}^{-M_1} c_k h_{i-k} \quad , \quad i=1,2,\ldots M_2 \qquad (3.6)$$

The operation of the proposed new hybrid structure will be explained with the aid of Fig. 3.2, which shows (a) the impulse response of the whole channel (length ν) and (b) the impulse response presented to the MLD input. We define as complexity constraint, denoted by C, that only C+1 samples preceding and including the reference sample, are to be operated on by the MLD algorithm (signal section identified as "MLD" in Fig. 3.2a). Then, given this constraint, the previous samples must be equalized by the decision-feedback equalizer (signal section identified as "DFE" in Fig. 3.2a).

To achieve this, the decision-feedback equalizer, having set the taps of its feedforward section, makes a tentative decision $\tilde{a}_i$ on the transmitted symbol. This tentative decision, based on the "DFE" signal portion shown in Fig. 3.2a, is used as input to its feedback section where the setting of the transversal filter taps of this section will remove that portion of ISI caused by previously detected symbols from the estimates of future symbols.

The output of the feedback section of the equalizer, together with the remaining signal portion, identified as "MLD" in Fig, 3.2a, constitute the input to the MLD algorithm. Referring to Fig. 3.1,

$$I_i = x_i - \sum_{k=c+1}^{\nu} \tilde{a}_{i-k}\, h_k \qquad (3.7)$$

Substituting (3.4) into (3.7) we get

$$I_i = \sum_{k=o}^{c} a_{i-k}\, h_k + n_i + \sum_{k=C+1}^{\nu} (a_{i-k} - \tilde{a}_{i-k}) h_k \qquad (3.8)$$

Equation (3.8) suggests that, when $\tilde{a}_i = a_i$, for $C+1 \leq i \leq \nu$, or, in other words, there is no intersymbol interference in the output of the DFE, all the intersymbol interference terms, after the C term, will disappear at the input to the MLD

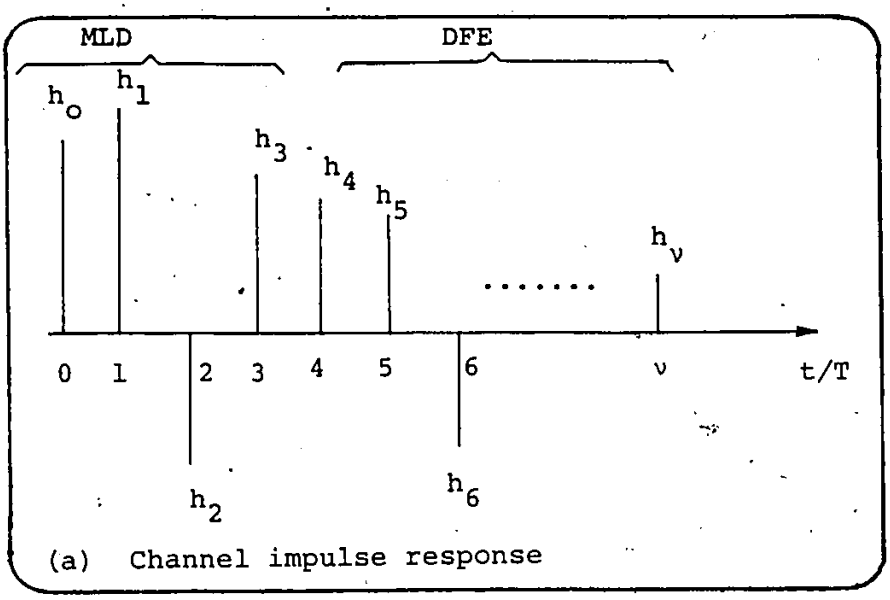

(a) Channel impulse response

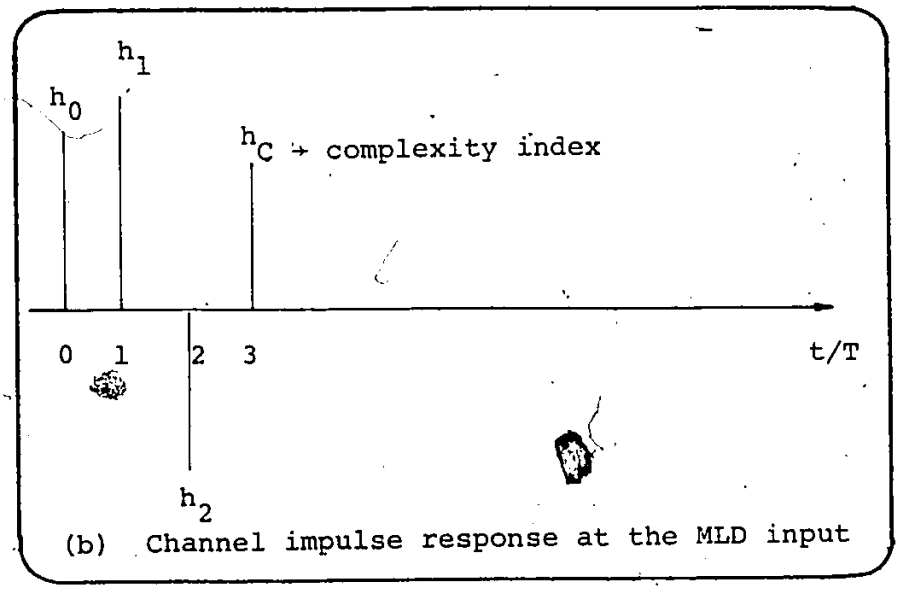

(b) Channel impulse response at the MLD input

Fig. 3.2 Hybrid equalizer input sequence

algorithm: Thus, the MLD algorithm is designed for the equalized channel of reduced length of $\nu' = C+1$ response terms, as shown in Fig. 3.2b. The MLD algorithm then performs maximum likelihood sequence estimation, on this equalized signal, in the usual manner.

The choice of the complexity constraint index, in terms of the channel response, is further discussed in chapter 4, where the concept is applied to the equalisation of the satellite channel used in this work.

The proposed equaliser structure could be made adaptive, as an extension of this work, by incorporating a channel parameter identification algorithm and subsequent filter tap adjustment.

Using the state representation of the finite state machine (ch. 2, sect. 4), denoted by s_k, one may conveniently represent the function to be maximized by the MLD algorithm, as shown in chapter 2 (sect. 4) in the following manner:

$$\sum_{i=0}^{N} p[\, I_i | s_k, \{a_i\}\,] = \exp\left\{ -\frac{1}{2N_o} \sum_{i=0}^{N} (I_i - h_o a_i - h_i a_{i-1} - \ldots - h_i a_{i-k})^2 \right\} \qquad (3.9)$$

or, if we use the log likelihood function, equation (3.9) may be rewritten as

$$\sum_{i=1}^{N} \ln p[\, I_i | s_k, \{a_i\}\,] = -\frac{1}{2N_o} \sum_{i=1}^{N} (\, I_i - h_i a_{i-k}\,)^2 \qquad (3.10)$$

where

$N = \nu$, the length of the channel response

I_i is the given input signal to the MLD algorithm

h is the channel impulse response (in complex form)

a_i is the equalizer output signal

The objective then will be to estimate $\{a_i\}$ from the given signal I_i. The development followed here, as far as possible, is analogous to that in [32, 39]. Using the metric μ and defining

$\mu(s_{k+1}) \triangleq$ maximum likelihood function of the path between

$$0 < k \leq k + 1$$

one may write this metric as follows

$$\mu(s_{k+1}) = \max_{a_1 \to a_{k-N}} \left(\sum_{k=1}^{N} \ln p[\, I_k | s_k a_k\,] \right) \qquad (3.11)$$

For a Q-level system, the function expressed by equation (3.11) has Q^N values. Using equation (3.10) one may also say that for Q states s_k,

$$\mu(s_{k+1}) = \max_{a_{k-N}} \left(\mu(s_k) - \left(I_i - \sum_{i=0}^{N} h_i a_{i-k} \right)^2 \right) \qquad (3.12)$$

By inspecting equation (3.12) we can observe that the term I_i^2 is independent of a_i and therefore, by ignoring it, we may rewrite equation (3.12) as follows

$$\mu(s_{k+1}) = \max_{a_{k-N}} \left(\mu(s_k) + 2I_i(h_o a_i + h_1 a_1 + \ldots + h_i a_{i-k}) - \right.$$

$$\left. - (h_o a_i + h_1 a_1 + \ldots + h_i a_{i-k})^2 \right) \qquad (3.13)$$

It has been shown [63] that, by following similar arguments, the number of metric computations required may be reduced to ca.50% of those required in the original algorithm.

The graphic representation of the various paths that describe the transitions from one state to another, may take the form of a trellis diagram. We will briefly describe this operation, with the aid of fig. 3.3.

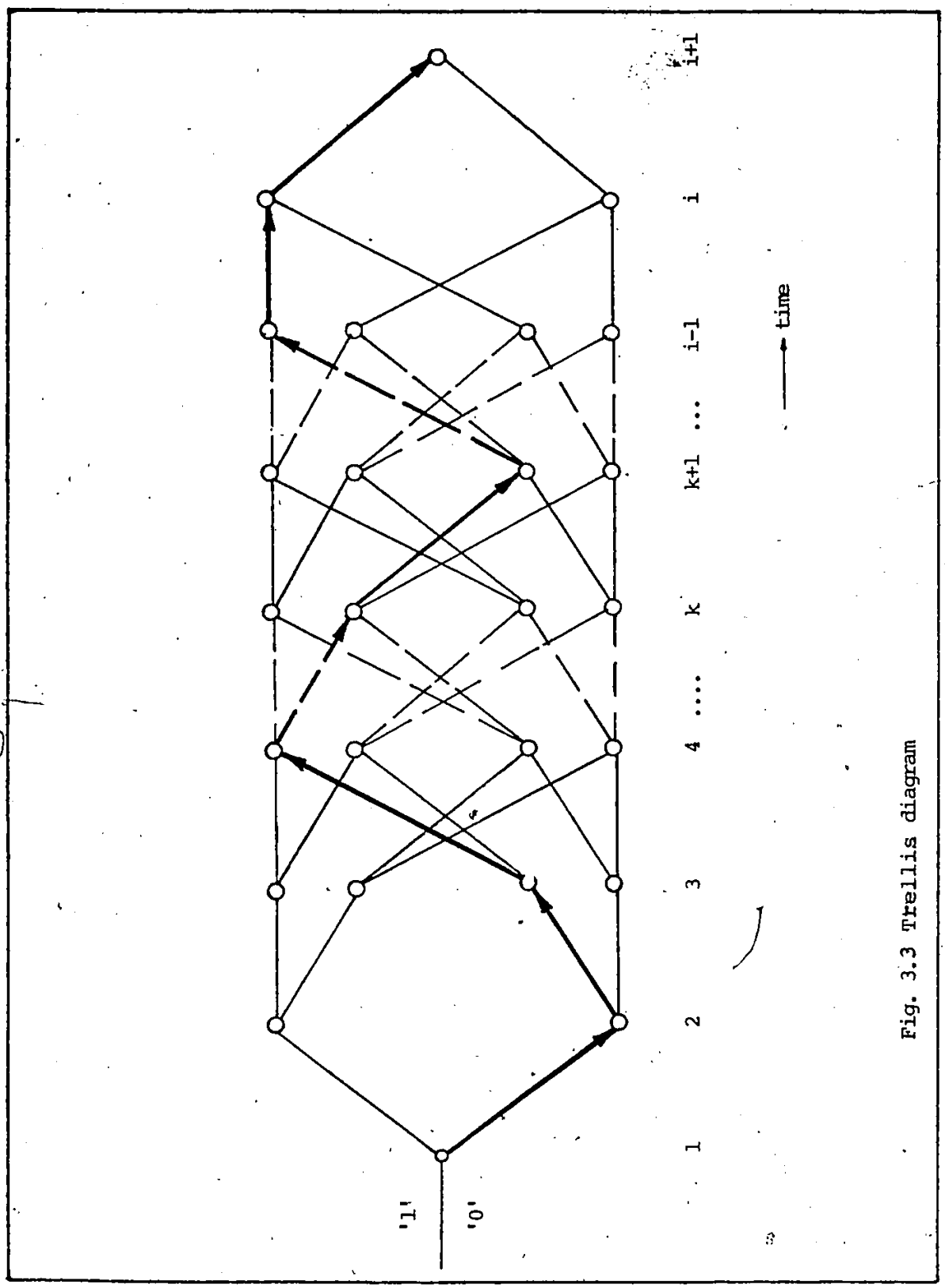

Fig. 3.3 Trellis diagram

We define the overall class of states as

$$S_n(k) = \sum_{n,k=1}^{Q^i} s(k) \qquad (3.14)$$

It is evident that there will then be a total of Q^i classes.

In the trellis diagram, a trace towards the upper half of the diagram signifies a ' 1 ' whereas a trace towards the lower half signifies a ' 0 ' . The operation is described by progressing in time (horizontally) from node to node, (i.e. the same state class) and from one state class to another (vertically). The algorithm is used to compute the path histories of the state transitions. There is a tendency among them to merge to some common path. The metric associated with each symbol, as previously defined, is the branch length between nodes. The algorithm then calculates these metric assignments, for each branch, and looks for the shortest path between them, i.e. each instant in time-retains that path that possesses the minimum metric value. Consequently, among all those paths converging at each node, only one will be assigned the smallest metric value. This path then will form part of the overall shortest route, which, in turn, will possess the (overall) minimum metric value in the trellis diagram. The remaining paths are then eliminated. The retained (shortest) path is also called the survivor. If, by chance, there exists a minimum value for more than one shortest

paths then, the survivor is arbitrarily chosen between them. For additional insight into the operation of the algorithm we note that the survivor up to each node is really a symbol sequence whereby each individual symbol is considered as a temporary decision. When the overall survivor path has been determined, i.e. the minimum distances have been calculated, then one may declare the corresponding final symbol sequence as the estimated one for the one originally transmitted.

The shortest path or, the merged common path history is indicated by the solid line in fig. 3.2. The calculation of the various paths from state to state, as described above, requires a considerable amount of storage and computing time. However, application of Bellman's [36] dynamic programming principle reduces considerably the computational effort required. To indicate the method, we proceeded as follows. The likelihood ratio definition is being given by

$$\Lambda_i = \frac{p[\, I_i | a_k = 1 \,]}{p[\, I_i | a_k = -1]} \qquad (3.15)$$

where

I_i = the input signal to the MLD algorithm

a_k = the equalizer output signal amplitude

and the log likelihood ratio given by

$$\lambda_i = \ln \Lambda_i$$

Now, if we approximate equation (3.15) by

$$\Lambda_i \approx \frac{\max p[\, I_i | a_k = +1 \,]}{\max p[\, I_i | a_k = -1 \,]} \qquad (3.16)$$

and proceed in a manner analogous to the analysis presented in [32], by restricting the analysis over L adjacent signals, we obtain

$$p[\, I_i | a_k \,] = K \exp\left\{ -\frac{1}{2\sigma^2} \sum_{i=-L}^{L} a_i \Big[\, I_i - \sum_{k=-L}^{L} a_k s_{k-i} \,\Big] \right\} \qquad (3.17)$$

The general derivation of (3.17) is to be found in Appendix I. Substituting (3.17) into (3.16), cancelling identical terms and taking the logarithm for Λ_i, we get [63]

$$\lambda_i = 2l_o + K(I_{-L}, \ldots, I_{-1}, I_1, \ldots, I_L) \qquad (3.18)$$

where

$$K = \ln \sum_{a_k} \exp\left\{ -\frac{1}{2} \sum_{i=-L}^{L}{}' a_i (I_i - s_{-i}) - \sum_{i=-L}^{L}{}' \sum_{\substack{k=-L \\ k\neq i}}^{L}{}' a_i a_k s_{k-i} \right\}$$

$$- \ln \sum_{a_k} \exp\left\{ -\frac{1}{2} \sum_{i=-L}^{L}{}' a_i (I_i + s_{-i}) - \sum_{i=-L}^{L}{}' \sum_{\substack{k=-L \\ k\neq i}}^{L}{}' a_i a_k s_{k-i} \right\} \qquad (3.19)$$

Thus, the calculation of the log likelihood function, based on the received signal, requires solution of equations (3.18) and (3.19). By applying now the maximization approximation, indicated by equation (3.16), we may rewrite equation (3.19) as follows

$$K \approx \max_{a_k} \left\{ -\frac{1}{2} \sum_{i=-L}^{L}{}' a_i (I_i - s_{-i}) - \sum_{i=-L}^{L}{}' \sum_{k=-L}^{L}{}' a_i a_k s_{k-i} \right\}$$

$$-\max_{a_k} \left\{ -\frac{1}{2} \sum_{i=-L}^{L}{}' a_i (I_i + s_{-i}) - \sum_{i=-L}^{L}{}' \sum_{\substack{k=-L \\ k \neq i}}^{L}{}' a_i a_k s_{k-i} \right\} \qquad (3.20)$$

It must be noted that, it is at this point where the dynamic programming method becomes a valuable tool for calculating the constant K as expressed by equation (3.20). It has been shown [63] that alternate application of the recursive formulae

$$W_{m+1,n} = W_{m,n} + a_m \left(I_m - \sum_{k=1}^{n-m} a_{m+k} s_k \right)$$

$$(3.21)$$

$$W_{m,n-1} = W_{m,n} + a_n \left(I_n - \sum_{k=1}^{n-m} a_{n-k} s_{-k} \right)$$

for $m \leq 0$, $n \geq 0$

will produce as a result

$$W_{0,0} = \sum_{i=-L}^{L}{}' a_i (I_i - a_o s_{-i}) - \frac{1}{2} \sum_{i=-L}^{L}{}' \sum_{\substack{k=-L \\ k \neq i}}^{L}{}' a_i a_k s_{k-i} \qquad (3.22)$$

which, when compared with equation (3.20), suggests that

$$K = \max_{a_k} \left\{ W_{0,0}(a_o = 1) \right\} - \max_{a_k} \left\{ W_{0,0}(a_o = -1) \right\} \qquad (3.23)$$

Substituting equation (3.23) into equation (3.21), we get

$$W_{m+1,n} = \max_{a_m} \left\{ W_{m,n} + a_m (I_m - \sum_{k=1}^{n-m} a_{m+k} s_k) \right\}$$

$$W_{m,n-1} = \max_{a_n} \left\{ W_{m,n} + a_n (I_m - \sum_{k=1}^{n-m} a_{n-k} s_{-k}) \right\} \qquad (3.24)$$

Thus, starting the calculation from a point where $W_{-L,L} = 0$, the successive application of equation (3.24) will ultimately produce the value of $W_{0,0}$.

The analysis has been based on the assumption that, the partially equalized sequence segment, presented by the decision feedback section to the MLD, is error free. That is, it has been assumed that the decision feedback equalizer section has been operating without errors. However, in actual practice, there will be occasional decision errors made on the polarity of a particular symbol. Consequently, the MLD will operate on sequences which contain error events which, in turn, will affect the performance of the overall receiver. In the next two sections, an elaboration of the notion of an error event will be developed as well as the calculation of the probability of occurrence of a particular error event leading to the calculation of the performance bounds for the overall proposed receiver structure.

3. PERFORMANCE ANALYSIS

The performance of the system will be analysed with the aid of the concept of the error events as introduced below. The probability of occurrence of such error events will be first calculated. Subsequently, the bounds for the symbol error probability will be derived. This analysis is presented in the following sections, respectively.

3.1 ERROR EVENTS

The decisions made by the MLD algorithm are directly

affected by the performance of the DFE section. Now, the tentative decisions made by the DFE, forming a reshaped pulse sequence to the input of the MLD, might be incorrect due to noise and ISI: This leads to the concept of an error event.

An error event ε is said to occur from time k to m when the estimated state sequence $\hat{s}(D)$ is the same as the correct state sequence s(D) at times k and m but nowhere in between. This definition implies that a decision error has been made at that particular time and it applies to both input as well as output signal error sequences.

The notion of the error event is required in order to be able to include the effects of the errors in the calculation of the performance bounds of the receiver structure. Consider an error event ε which is defined [32] as

$$e(D) \quad e_o + e_1 D + e_2 D^2 + e_3 D^3 + ... + e_{n-1} D^{n-1} \qquad (3.25)$$

Equation 3.25 is the error sequence description, in the form of a polynomial, for both the input error sequence $e_x(D)$ and the output signal error sequence $e_a(D)$ which are associated with the error event.

The error event may also be viewed as a change from a correct to an erroneous path, when refering to the trellis diagram. To illustrate the concept, refer to Fig. 3.4.

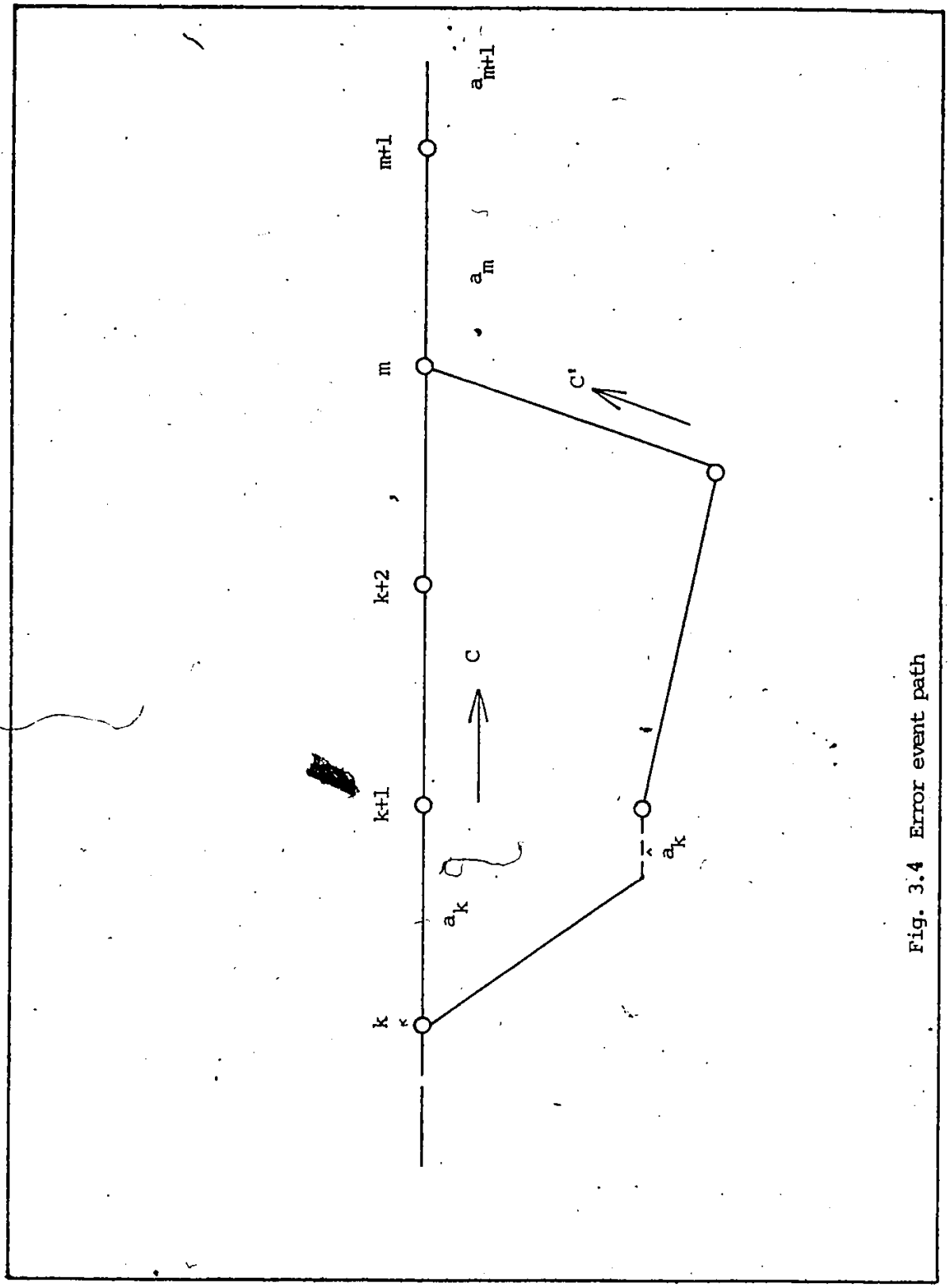

Fig. 3.4 Error event path

The assumed correct path is labelled C whereas the assumed incorrect one as C'. The two paths diverge at the node k in order to merge again at the node m. Using the state transition notation, we denote the state corresponding to the erroneous path by $\hat{s}_k$, whereas the correct one is s_k. We may subsequently write

$$s_k(i) = \hat{s}_k(i) \quad \text{for } i = k \text{ and for } i = m$$

$$s_k(i) \neq \hat{s}_k(i) \quad \text{for } k < i < m \tag{3.26}$$

At the node m, the equality

$$s_k(m) = \hat{s}_k(m) \tag{3.27}$$

allows the symbols, at that state, to be

$$a_{m-i} = \hat{a}_{m-i} \tag{3.28}$$

for $i = 1,2,3,\ldots,\nu$ and $0 \leq \nu \leq N$ with N being the signal sequence length.

The length of an error event is defined [32] as being

$$n_\varepsilon \triangleq m - k - 1 \tag{3.28a}$$

Now, considering coded sequences, for an error event to occur, the following subevents must occur:

(1) for an input sequence x(D), the associated input

error sequence will be such that

$$x(D) + e_x(D) \quad , \tag{3.29}$$

will be an allowable sequence $\hat{x}(D)$. This subevent is defined as ε_1. For uncoded sequences this subevent is the only event occuring.

(2) the contribution of the noise terms n_k, for $k_1 \leq k \leq k_1 + n$, is such that it permits the estimated sequence $\hat{x}(D)$ to survive with maximum likelihood than any other sequence. This subevent is defined as ε_2.

(3) again, the contribution of the noise terms is such, that $\hat{x}(D)$ has a greater likelihood of detection (survival) than the time sequence $x(D)$, but not necessarily the maximum likelihood. This subevent is defined as ε_3.

Considering then the subevents ε_2 and ε_3, one may also state that

$$\varepsilon_2 \in \varepsilon_3 \tag{3.30}$$

Before proceeding with the calculation of the probability that the error event might occur, we will define the concepts of the Euclidian weight and Hamming weight.

The Euclidian weight $d^2(\varepsilon)$ of an error event is defined as the energy in the associated signal-error vector sequence (defined by equation 3.25). Specifically,

$$d^2(\varepsilon) = ||e_a(D)||^2$$

$$= \sum_{k=-\infty}^{\infty} e_{ak}^2 \qquad (3.31)$$

The Hamming weight $N(\varepsilon)$ of the event is actually the number of errorsthat are associated with the input error sequence $e_x(D)$. In other words, the Hamming weight may be expressed as

$N(\varepsilon) \triangleq$ Number of non-zero coefficients associated with the $e_x(D)$. (3.31a)

3.2 Probability of error event

The probability of an error event, using the above concepts of subevents can be stated as

$$P(\varepsilon) = P(\varepsilon_1)P(\varepsilon_2|\varepsilon_1) \leq P(\varepsilon_1)P(\varepsilon_3|\varepsilon_1) \qquad (3.32)$$

i.e. the probability of a particular error event ε is weighted by the $P(\varepsilon_1)$ and upperbounded by the $P(\varepsilon_3|\varepsilon_1)$.

Assuming independent and equally likely input symbols, it can be shown [32] that

$$P(\varepsilon_1) = \prod_{i=0}^{n-\nu} \frac{L-|e_{xi}|}{L} \qquad (3.33)$$

where

L = number of states of finite state machine

e_{xi} = input error sequence

n = length of error event

ν = channel span.

Using now the log likelihood function of $\hat{s}_k(D)$ from time k_1 to $k_1 + n+1$, the term $P(\varepsilon_3|\varepsilon_1)$ in equation (3.32) is given by

$$P(\varepsilon_3|\varepsilon_1) = \left(\Gamma[\hat{s}_k(D)]_{k_1}^{k_1+n+1} > \Gamma[s(D)]_{k_1}^{k_1+n+1} \mid \varepsilon_1 \right) \qquad (3.34)$$

Using the sampled output of the whitening matched filter as well as the noise statistics (Gaussian, with variance σ_n^2), equation (3.34) may be rewritten as:

$$P(\varepsilon_3|\varepsilon_1) = [\hat{\Gamma} - \Gamma]_{k_1}^{k_1+n+1} = \frac{1}{2N_o} \sum_{k=k_1}^{k_1+n} [(x_k - r_k)^2 - (x_k - \hat{r}_k)^2]$$

$$= \frac{1}{2N_o} \left(||x(D) - r(D)||^2 - ||x(D) - \hat{r}(D)||^2 \right)_{k_1}^{k_1+n} \qquad (3.35)$$

One can see, from the last equation, that $\hat{r}(D)$ will be the more likely sequence, being closer to $x(D)$ than $r(D)$, both

with reference to the (n+1)-dimensional Euclidian space corresponding to times k_1 to k_1+n.

Using the concept of the Euclidian weight, one may express (3.35), that is the conditional probability of the subevent ε_3 as:

$$P(\varepsilon_3|\varepsilon_1) = Q\left(\frac{d(\varepsilon)}{2\sigma_n}\right) \qquad (3.36)$$

where

$$Q(x) = \frac{1}{\sqrt{2\pi}} \int_x^\infty e^{y^2/2}\, dy \quad , \text{ the error function}$$

Returning to equation (3.32), we may now express the probability of an error event, using the results of equations (3.33) and (3.36) as being

$$P(\varepsilon) \leq P(\varepsilon_1)P(\varepsilon_3|\ \varepsilon_1)$$

$$\leq \prod_{i=0}^{n-\nu} \frac{L - |\varepsilon_{xi}|}{L} \left[Q\left(\frac{d(\varepsilon)}{2\sigma_n}\right) \right] \qquad (3.37)$$

3.3 Probability of symbol error

We are now in a position to calculate the overall probability of error of the receiver structure proposed here.

Using the results obtained for the probability of error-events, we may say that the computation of the symbol error probability could be expressed in terms of weighting the error event ε with the actual number of decision errors, i.e. the Hamming weight $N(\varepsilon)$, due to ε_x (as given by 3.31a). The equation (3.37) can be rewritten as

$$P(\varepsilon) \leq \left(\prod_{i=0}^{n-\nu} \frac{L - |e_{xi}|}{L} \right) N(\varepsilon) Q\left(\frac{d(\varepsilon)}{2\sigma_n} \right) \qquad (3.38)$$

By denoting as E the set of all possible error events starting at time k_1 and by D the set of all possible distances $d(\varepsilon)$, and by using the union bound approach [32] (i.e. 'the probability of a union of events is not greater than the sum of their individual probabilities'), the probability of symbol error is given by

$$\begin{aligned} P(e) &\leq \sum_{\varepsilon \in E} P(\varepsilon) N(\varepsilon) \\ &\leq \sum_{d \in D} Q\left(\frac{d(\varepsilon)}{2\sigma_n} \right) \sum_{\varepsilon \in E} \prod_{i=0}^{n-\nu} \left(\frac{L - |e_{xi}|}{L} \right) N(\varepsilon) \end{aligned} \qquad (3.39)$$

At high signal-to-noise ratios, the minimum values of $d(\varepsilon)$, i.e. d_{min}, will dominate (exponential decrease of Q),

equation (3.39). Thus an approximation, at the same time serving as an upper bound for the symbol error probability is arrived at:

$$P(e) \simeq Q\left(\frac{d_{min}(\varepsilon)}{2\sigma_n}\right) K_a \qquad (3.40)$$

where

$$K_a = \sum_{\varepsilon \in E_{d_{min}}} \prod_{i=0}^{n-\nu} \left(\frac{L - |e_{xi}|}{L}\right) N(\varepsilon) \quad , \text{ and}$$

$E_{d_{min}}$ = set of error events having minimum distance

This upper bound, for high-signal to noise ratios, provides, in many cases, a good approximation [32] to the actual performance of the detectors, i.e. the MLD. In a similar manner, a lower bound for the error symbol probability may be derived. Thus by denoting with K_k the probability of an error event, starting at time k, as being at least

$Q(\frac{d_{min}}{2\sigma_n})$, we will have

$$P(\varepsilon) = P(e) \geq K_k Q\left(\frac{d_{min}(\varepsilon)}{2\sigma_n}\right) \qquad (3.41)$$

Clearly, the two bounds as expressed by equations (3.40) and (3.41) differ only in the parameters K_a and K_k respectively. These two bounds were computed and the results are to be found in chapter 5, Fig. 5.8.

Since the satellite channel is considered as a finite state machine, the concept of the minimum distance d_{min} applies in the case of the non-linear channel, i.e. the satellite channel as considered here. Thus, the input sequence presented to the MLD algorithm, for final decision, is the one characterized by the output sequence of the non-linear TWT transponder.

CHAPTER IV

SIMULATION OF A QPSK SATELLITE DATA LINK

1. GENERAL

In the study presented in this work, digital computer simulation was used to evaluate the system performance degradation due to Intersymbol Interference, non-linearities and Gaussian noise. The modulation scheme used is the Quaternary-Phase-Shift-Keying (QPSK).

The additive white Gaussian noise as well as the transponder non-linearities are included in the simulated system so that a realistic operational condition is obtained. In addition, operating conditions of the satellite transponder, the filter characteristics, the channel bandwidth as well as the data rate and the noise power level into the receiver may be altered and the effects are observed in the form of a probability of error P(e) vs. signal-to-noise ratio (SNR) curve. The simulation permits direct plotting of this curve. Another criterion of the quality of the transmission is the eye diagram at the receiver output. The present simulation allows for the calculation of such an "eye" diagram as well as its direct displaying on an X-Y recorder.

The description of the simulated system and the simulation

process are presented in the next section, whereas the third section presents the performance considerations of this system. The simulation was conducted using Fortran IV and APL programming languages on an IBM 360/65, model J computer, located at the Computing Centre of the University of Ottawa. Use is made of systems subroutines which are stored in bulk memory.

2. SYSTEM SIMULATION DESCRIPTION

The presentation will follow in a parallel way the block diagram of the simulated system (fig. 4.1) as well as the simulation scheme depicted in fig. 4.2: Transmitter chain, satellite transponder, receiver chain and output display.

The overall simulated system will be first described. After this, a more detailed account of the distinct system blocks will be given in the following subsections together with the underlying theoretical concepts.

The digital binary input data, from the signal source, (eqn. 4.1), are converted to baseband signal waveforms in quadrature (eqns. 4.2 and 4.3). A quaternary-phase-shift keying (QPSK modulator) signal is chosen, filtered, and converted from time to frequency domain and vice versa by the Fast Fourier Transform (FFT), for the filtering operation. The signal is expressed in complex baseband form (eqn. 4.5).

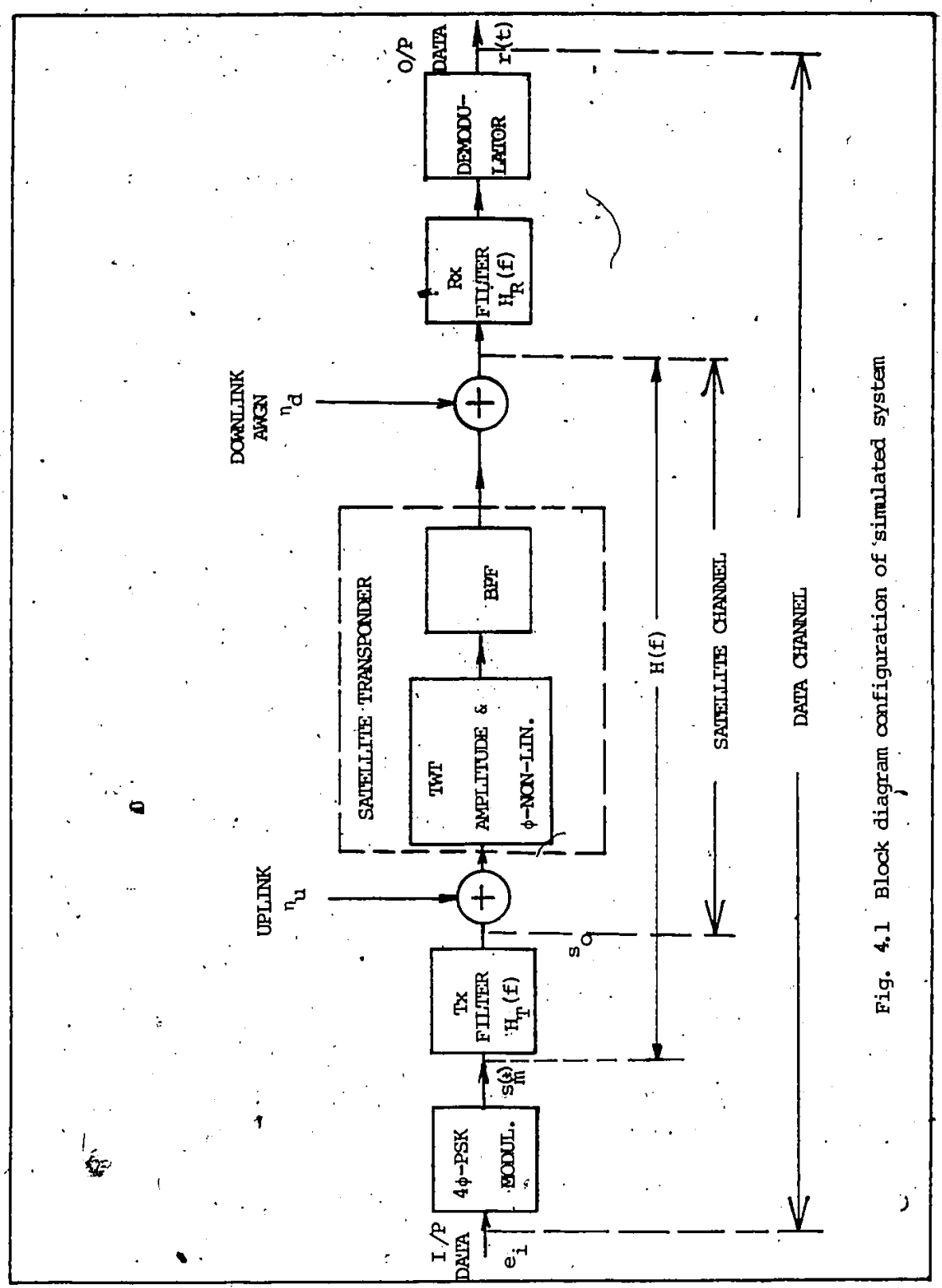

Fig. 4.1 Block diagram configuration of simulated system

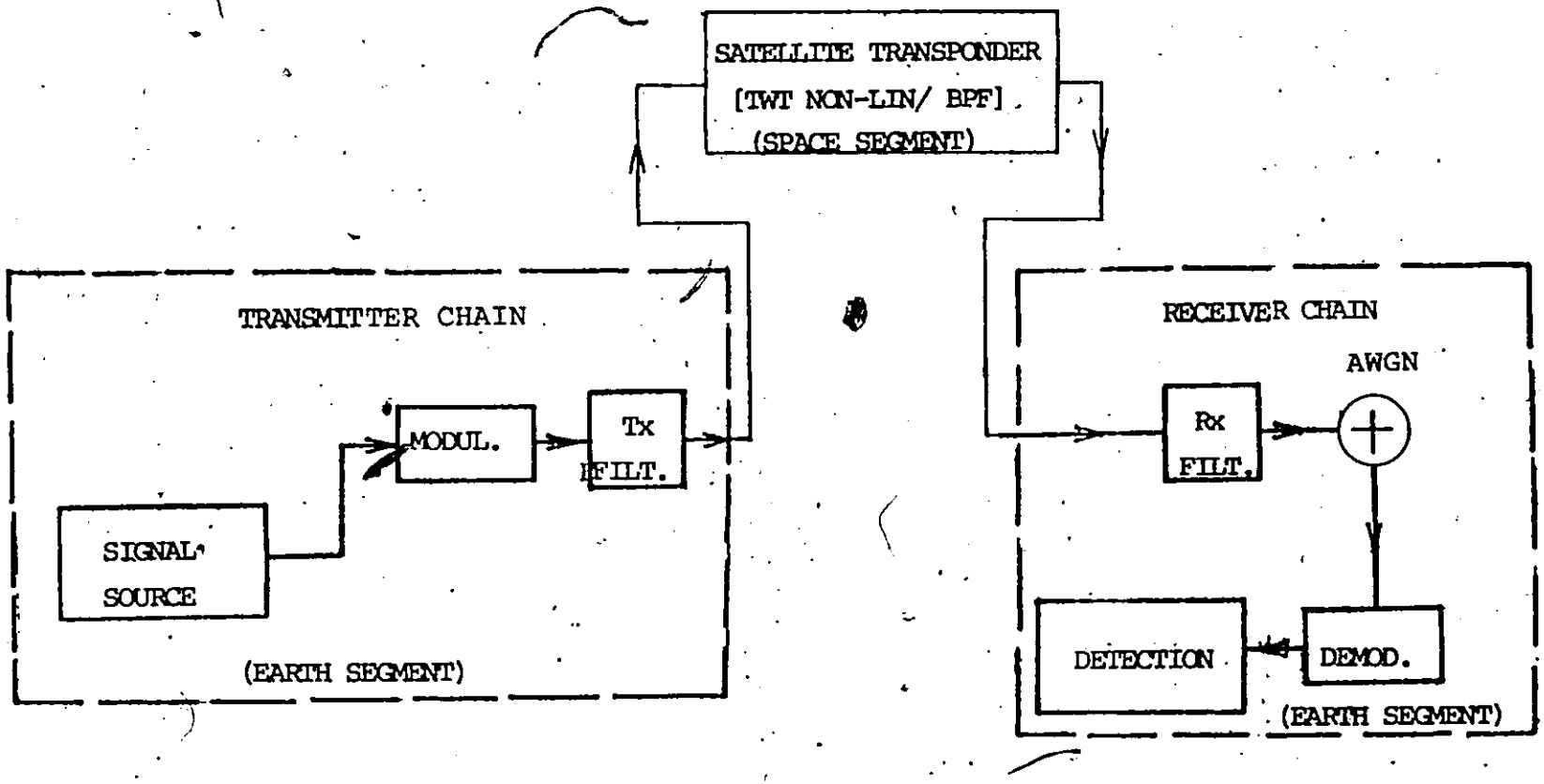

Fig. 4.2 Block diagram of simulated satellite transmission system

The filtered signal is transmitted to the satellite transponder. It is at this stage of the simulation where the non-linear elements are introduced. The TWT is first mathematically modelled and, subsequently, simulated as a bandpass non-linearity (eqn. 4.7). This form of non-linearity, in its quadrature form(eqns. 4.15 and 4.16), is the representation of the two envelope non-linearities in the TWT model: The amplitude limiting action and the amplitude-dependant output phase shift. The signal is now delivered to the receiver where the system performance will be computed.

The received signal is processed by the simulated receiver bandpass filter: This process is similar to the one at the transmitter. Both transmit and receive filters are of the same type; however, the simulation allows for interchangeability with other filters, should this be required.

Following the receiver bandpass filter, the signal is processed by the demodulator: Here, an Integrate and Dump (I&D) filter is simulated. To complete the demodulation process, the satellite down-link noise is added: It is at this stage, i.e., at the output of the integrate and dump filter that this noise is added, rather than at the input to the receiver, because this practice is preferable to introducing the noise element at the receiver input. It is to be noted that both are equivalent [48]. However, computational efficiency dictates adding of the noise at the output

of the receiver. This is further explained by considering the two known approaches [43] of noise simulation: (a) computed noise and (b) simulated noise. In (a), the signal is simulated without noise. The equivalent noise power is computed, [48,50] and the noise inserted at the output of the filter. Having specified the signal-to-noise ratio, the probability of error of each digital signal is computed, as a function of its sample value and the noise variance. The overall probability of error of the system is the average probability of error over a long signal sequence. In (b), i.e., with simulated noise, working with both signal and noise samples, the number of symbols required for processing at a P(e), of 10^{-5} to 10^{-7} would be in the order of 10^{7} to 10^{9} symbols. In addition, noise must be generated for both, the in-phase as well as the quadrature channel for each signal sample separately. This procedure requires more computing time in the order of approximately 10 hrs/single point on the output curve, whereas, the one with computed noise requires only a few seconds to accomplish the same function.

The simulation of the "eye-diagrams" has been provided as a qualitative alternative for assessing the system performance by examining the eye opening: The simulated baseband signals at the output of the receiver filter are utilized for this purpose. The superposition of the entire received sequence, whereby the samples of the individual symbols are traced, forms the required eye diagram: The

eye opening relates to the amount of Intersymbol Interference (ISI) present. The simulation includes plotting of eye patterns on either an X-Y recorder for a detailed, line drawing, or on a high-speed printer connected to a digital computer, for a 'rapid indication' assessment.

The overall description of the simulated system above is summarized in block diagram form, in Fig. 4.3. Here, the basic subroutine-based configuration is depicted along with the signal processing path (heavy solid line). The efficient use of the discrete Fourier transform requires that a finite number of symbols be processed at a time. The computer implementation of the discrete Fourier transforms is restricted to a finite number of terms N. Thus, the maximum number of locations, in this case, for the QPSK signal data array and the filter transfer function is N = 256. Since the simulation is carried out at complex baseband (B/B), two location/sample are required, for a total of 512. Consequently, the data sequence is processed in parts and at stages reconstructed as a total (dashed lines). There are 12 symbols per Fourier transformation. Thus for a signal sequence of 127 symbols 11 (Fourier Transformed) parts are required. Using 16 samples/symbol, 192 locations array, for signal samples, are required. These arrangements, allow for efficient use of the computer core storage.

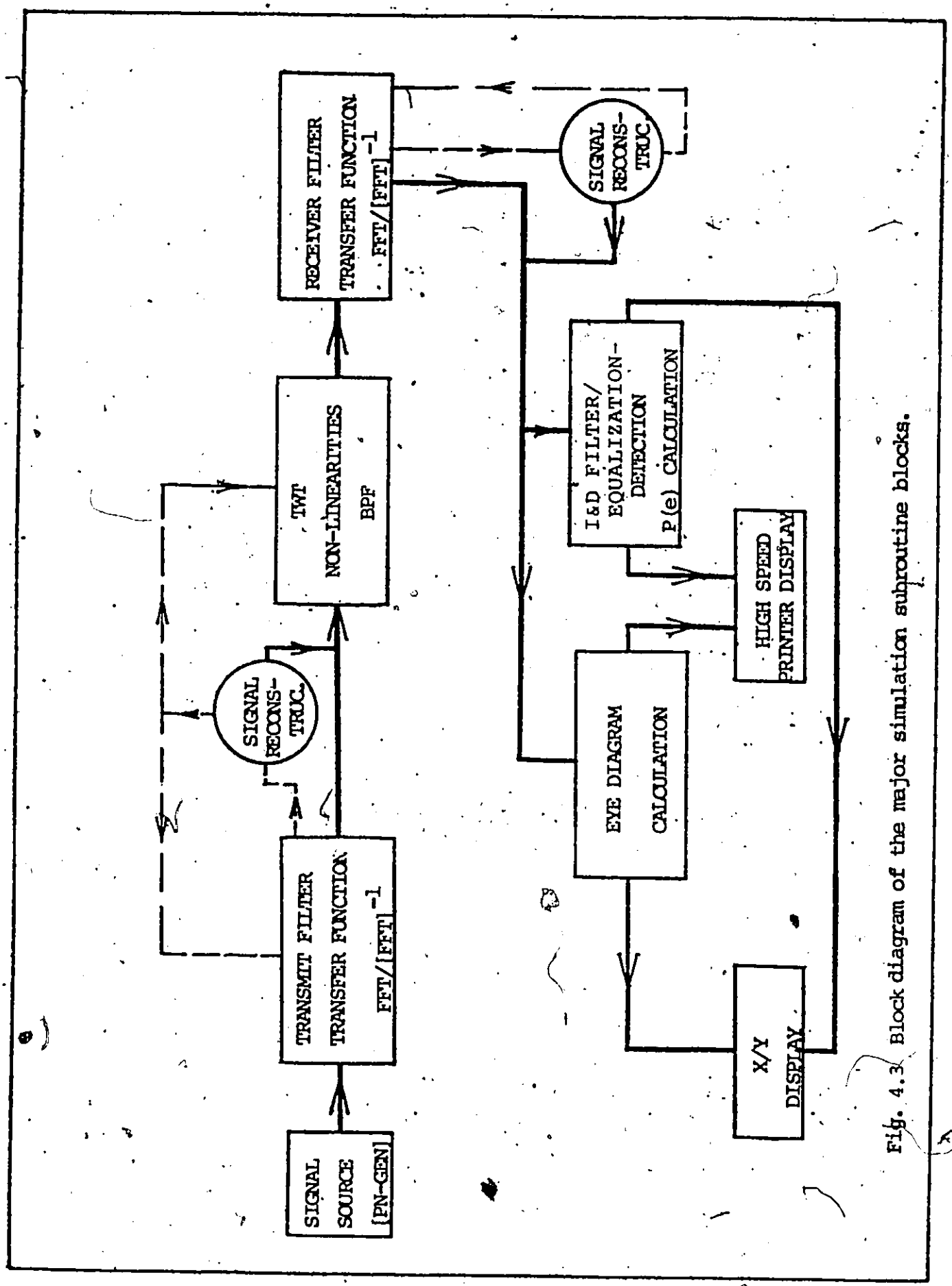

Fig. 4.3 Block diagram of the major simulation subroutine blocks.

2.1 Transmitter chain

This group of subroutine-blocks includes the signal generator, the modulator and the transmit bandpass filters, as shown in Fig. 4.4.

2.1.1 Data generator

In actual operating conditions, the input signals (data stream) to be transmitted, are of a random nature: That is, the input sequence is generated by being selected from a "sample space" in an unpredictable fashion [51]. In other words, if the obtained output signal from a generator is the result of an a priori random process, then this signal is considered as random in nature.

Such a random signal is then representative of all possible input sequence combinations. However, one may introduce statistical tests which will check whether a particular sequence was produced by a specific random process. Any sequence that passes these tests, for the appearance of randomness, is defined as pseudorandom. Specifically, one may introduce a deterministic process to generate pseudorandom sequences which pass the tests.

One of the simplest and most effective devices for generating pseudorandom (PN) sequences, is the shift register: Such a device has been simulated here. The generator consists

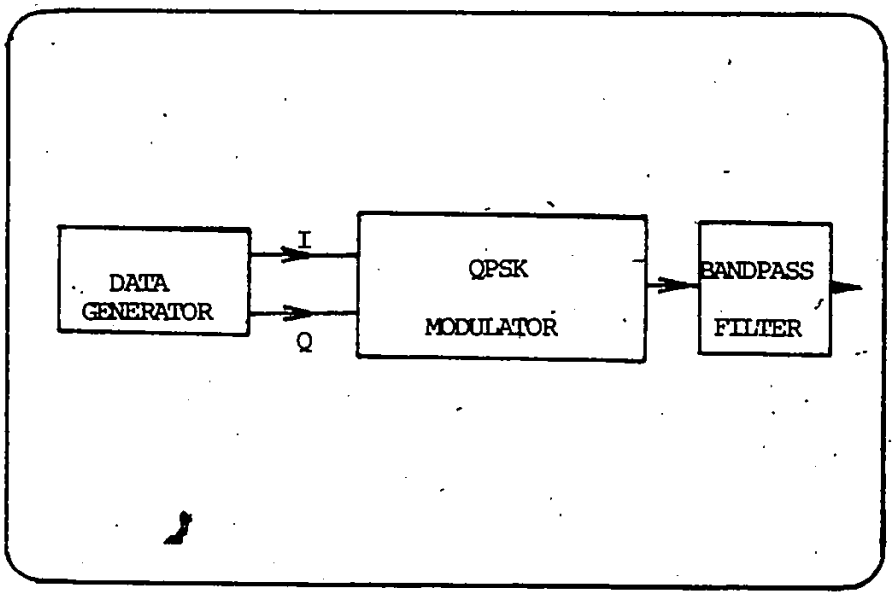

Fig. 4.4 Block diagrams of Transmitter chain simulator

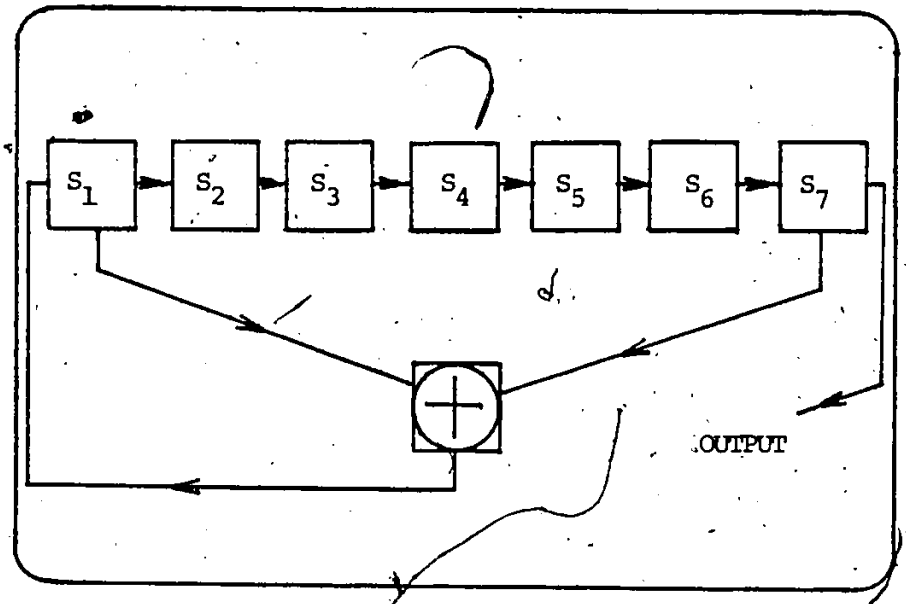

Fig. 4.5 Generator of a Pseudorandom sequence sith $p = 2^7 - 1$

then of a shift-register of degree n, i.e. consisting of n consecutive binary storage positions.

The output sequence is periodic with a maximum period 2^n-1, since, the linear shift registers have a maximum period of $2^n - 1$. Any output sequence generated by this shift register with such a period is called a maximum-length-shift-register sequence [MLSR]. The basic configuration of the generator used here is shown in Fig. 4.5, with a period $p = 2^n - 1$, where $n = 7$, or $p = 2^7 - 1 = 127$. In the simulation, two such registers are created: one for each channel of the QPSK modulator. Initial contents of the registers are set such that they are shifted relative to each other for a uniform distribution of sequence patterns. Two binary input data pulse sequences are being used and are of the form

$$e_i(t) = \sum_{k=-\infty}^{+\infty} A_k \, g(t-kT) \qquad (4.1)$$

where

A_k = amplitude of the random variable ($\pm$ 1)

$g(t)$= square pulse

T = pulse duration

The above signals carrying the information, will subsequently modulate the phase of a carrier (the carrier itself

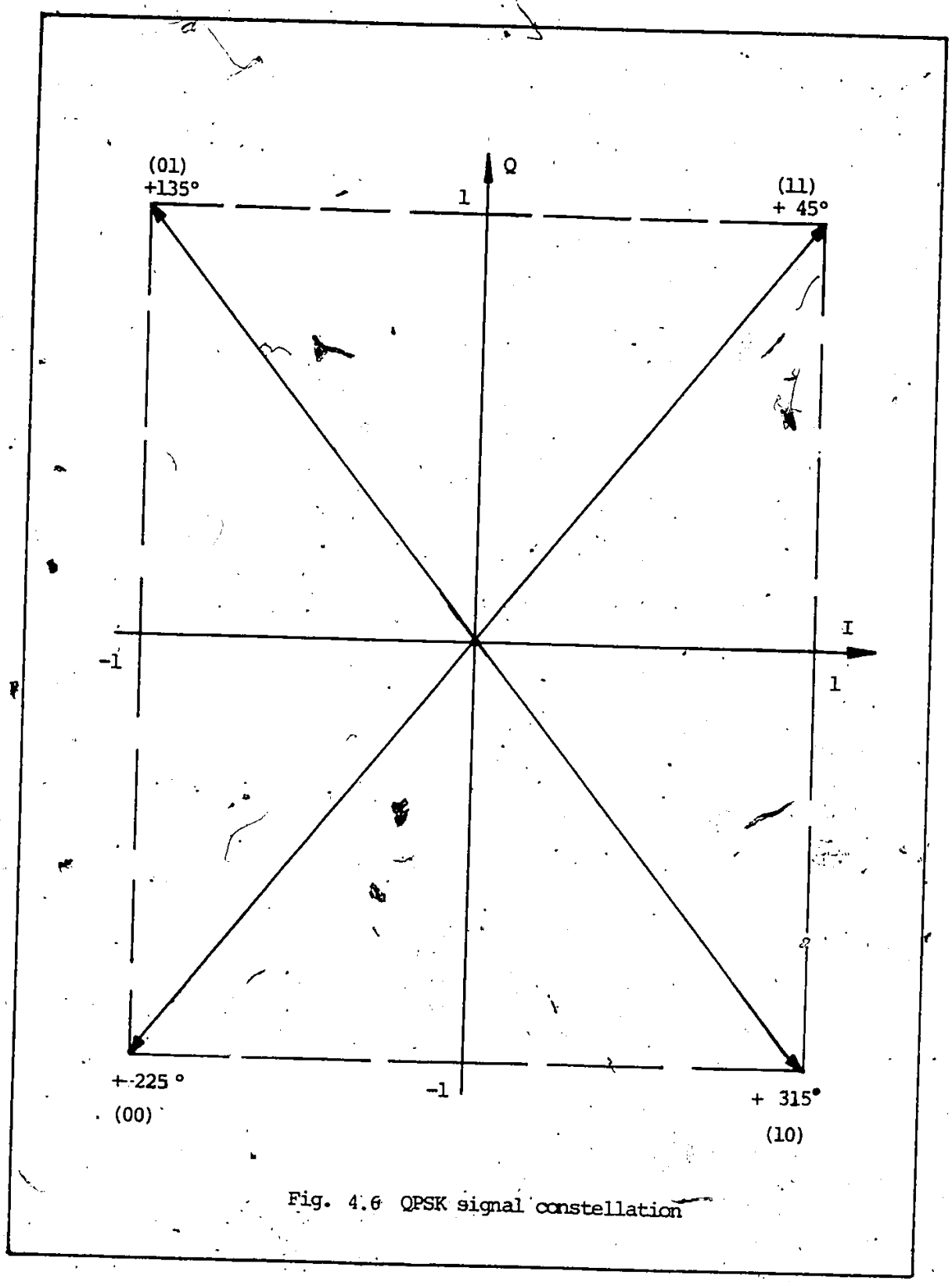

Fig. 4.6 QPSK signal constellation

carries no information), resulting in four (4), equally spaced, phases since QPSK is used, as shown in fig. 4.6.

2.1.2 Modulator and filter

The Quaternary-phase-shift-keying (QPSK) technique is here chosen primarily because of its widespread use in conjuntion with data transmission at high bit-rates [43]. In addition, an efficient bandwidth utilisation, is achieved. The signal phase diagram is shown in fig. 4.6. It is to be noted that, in the simulation of the system, the signals are considered at baseband (B/B). Consequently the complex B/B representation form will be used throughout the simulation process.

Initially, the r.f. modulated signal is given by

$$\begin{aligned} s_m(t) &= A(t)\cos[\omega_c t + \phi(t)] \qquad (4.2) \\ &= A(t)\cos\omega_c t \cos\phi(t) - A(t)\sin\omega_c t \sin\phi(t) \\ &= A(t)[\cos\omega_c t \cos\phi(t) - \sin\omega_c t \sin\phi(t)] \end{aligned}$$

Let

$A(t)\cos\phi \equiv x(t)$ represent the In-phase B/B signal

$A(t)\sin\phi \equiv y(t)$ represent the Quadrature B/B signal

Equation (4.2) above may be re-written as

$$s_m(t) = \sum_{k=-\infty}^{+\infty} A_k \cos[\ \omega_c t + \phi_k\ ] \qquad (4.3)$$

where

ϕ_k = phase samples

Equation (4.3) is further developed by introducing the complex signal function:

$$s_m(t) = \mathrm{Re}\{u(t)\exp j\omega_c t\} = \mathrm{Re}\{[\ x(t)+jy(t)\ ]\exp j\omega_c t\} \qquad (4.3a)$$

where x(t) and y(t) are the in-phase and quadrature signal envelope components, respectively, of $s_m(t)$.

As shown in fig. 4.1, the modulated signal $s_m(t)$ is the real part of (4.3a), and may be re-written as:

$$s_m(t) = \mathrm{Re}\{\ u(t)\exp j\omega_c t\ \}$$

$$= \mathrm{Re}\ \exp[j\omega_c t] \sum_{k=-\infty}^{+\infty} A_k \exp j\phi_k \qquad (4.4)$$

The signal described by (4.4) is passed through the earth station transmit filter.

The transmit, as well as the receive, filters are considered as the filters that mostly affect the performance of the system. Their effects, separately and jointly, is to

degrate the system performance due to filter distortion and the associated intersymbol interference. Use of an equalizing structure, at the receiver, is made in order to complement these filters and counteract the distorting effects. The transmit filter considered is a typical 1/2-dB ripple, 4-pole Chebyshev filter type, described by the denominator polynomial of its transmission function. The equivalent low-pass expression is given by

$$p(s) = b_o + b_1 s + b_2 s^2 + \ldots + b_{n-1} s^{n-1} + s^n \qquad (4.4a)$$

The coefficients $b_o, b_1, \ldots, b_{n-1}$ are taken from standard tables [44].

The coefficients used are: for $n = 4$, $b_o = 0.37905$, $b_1 = 1.02546$, $b_2 = 1.71687$, $b_3 = 1.19739$, $s^4 = 1$.

Finally, the transmitted signal $s_o(t)$, as described by equation (4.4) and modified by the transmit filter, will be of the form

$$\begin{aligned} s_o(t) &= \mathrm{Re}\{ [\, x_o(t) + j y_o(t)] e^{j\omega_c t} \} \\ &= x_o(t)\cos\omega_c t - y_o(t)\sin\omega_c t \end{aligned} \qquad (4.5)$$

Equation (2.5) can also be written as

$$\begin{aligned} s_o(t) &= \mathrm{Re}\{ c(t)\exp[\, j\omega_c t + \theta(t) \,] \} \\ &= c(t)\cos[\, \omega_c t + \theta(t) \,] \end{aligned} \qquad (4.6)$$

where $$c(t) = \sqrt{x_o^2(t) + y_o^2(t)}$$

$$\theta(t) = \tan^{-1} \frac{y_o(t)}{x_o(t)}$$

x_o = Real in-phase baseband signal component

y_o = Real quadrature baseband signal component

The signal after convolution with the filter impulse response function, produces the filter output. This is accomplished by multiplication of the spectra in the frequency domain. The signal is then transformed to the time domain by taking the inverse FFT. This procedure is carried out on seccessive sections of the input data stream of length 127. In the simulation, this is accomplished in such a manner as to allow for efficient use of storage, as it was shown in section 2 of this chapter.

It is to be noted that the phase $\phi(t)$, of the quadrature phase modulated signal, will take on four (4) different values, i.e. 45^o, 135^o, 225^o, 315^o, as shown in Fig. 4.6 and are related to the state of both, in-phase and quadrature signals, as determined by the incoming data. In the actual simulation, it is assumed that the signal power is normalized to unity, i.e. $\frac{A^2(t)}{2} = 1$, $A(t) = \sqrt{2}$, so that the programming parameters may be calculated (for reference, see section 4

below, system flowchart). Having generated a periodic sequence of symbols, the number of samples/symbol must now be determined: This number of samples is so chosen that the resulting bandwidth of the simulated signal is large enough with respect to the filter bandwidth to accommodate a wide range of signals. In addition, the number of samples should also be such that signal resolution, in the time domain, is satisfactory. In this case, 16 samples per symbol proved satisfactory. Having chosen a filter bandwidth of 85 MHz, and 16 samples/symbol, for a data input at, say, 140 Mb/s, the time domain sample spacing is

$$\Delta t = 1/(140 \times 10^6 \times 16) = 0.45 \text{ nsec}$$

resulting in a simulation bandwidth of

$$SB = 1/(4.5 \times 10^{-10}) = 2222 \text{ MHz}$$

For 256 samples/simulation segments, the frequency domain sampling spacing is

$$\Delta f = SB/256 = 2222 \text{ MHz}/256 = 9 \text{ MHz/sample}$$

At this point we should mention that, owing to storage limitation requirements, the generated symbol sequence, is divided into smaller blocks for processing. A block length of 12 symbols has been here chosen. Thus, the simulation process is carried out by loading sequentially these individual blocks and at some critical stage, the total signal sequence is recreated by cascading the sections. This method

is required also for the transformations from the time to the frequency domain and vice-versa, by use of the Fast Fourier Transform technique.

2.2 Satellite Transponder

The modulated signal, after filtering, is transmitted to the satellite for processing by its Travelling Wave Tube (TWT) transponder. At this stage of the satellite channel, the non-linearities are introduced. The TWT is being utilized as the main RF amplifier, in applications where both a low-noise factor as well as large bandwidth and power are operational requirements. The RF signal amplitude increases up to a maximum value whereby maximum energy transfer occurs: One speaks then of the saturation condition. At the same time, the signal output exhibits a phase-lag corresponding to and depending on the instantaneous amplitude of the input signal: this is known as AM to PM conversion.

Operation of the TWT at saturation or, near saturation will produce an amplitude limited signal due to the limiting amplifier action. If, on the other hand, the TWT is operated at some back-off point from saturation as, for example, in the case of multiple carrier access operation in high capacity satellite systems, then the effect of the AM/PM conversion is more pronounced. The effect on the AM/AM conversion is relatively negligible, when operating at or near saturation

and may, therefore, not be considered. Furthermore, when more than one modulated carrier is present (multiple access), the non-linearities mentioned above produce intermodulation noise which adds to the thermal noise encountered in the up-and down-links. To minimize the intermodulation noise the traveling wave tube is operated at a back-off quasi-linear mode.

The basic analytical model of the TWT, used in the simulation, will now be described. A development and an insight of the essentially non-linear phenomena of amplitude limiting and AM/PM conversion, has been presented in [46]. These non-linearities may also be referenced as a non-linear input-output power relationship and a non-linear output phase-input power relationship, respectively. It is assumed [46] that, these effects act simultaneously on the signal and therefore are not independent. From the theory of the TWT, it can be concluded that the amplification non-linearity originates in the end part of the electron beam-helix wave interaction rather than at the input connector. In contrast, as a first approximation, the phase non-linearity appears to exist evenly distributed over the whole helix length. Consequently, it is reasonable to connect both effects in cascade, as shown in fig. 4.7. A general expression for the TWT transfer characteristic may now be arrived at. Refering to fig. 4.7, the amplitude-amplitude non-linearity is represented by the transfer function $g_1(x)$ whereas the

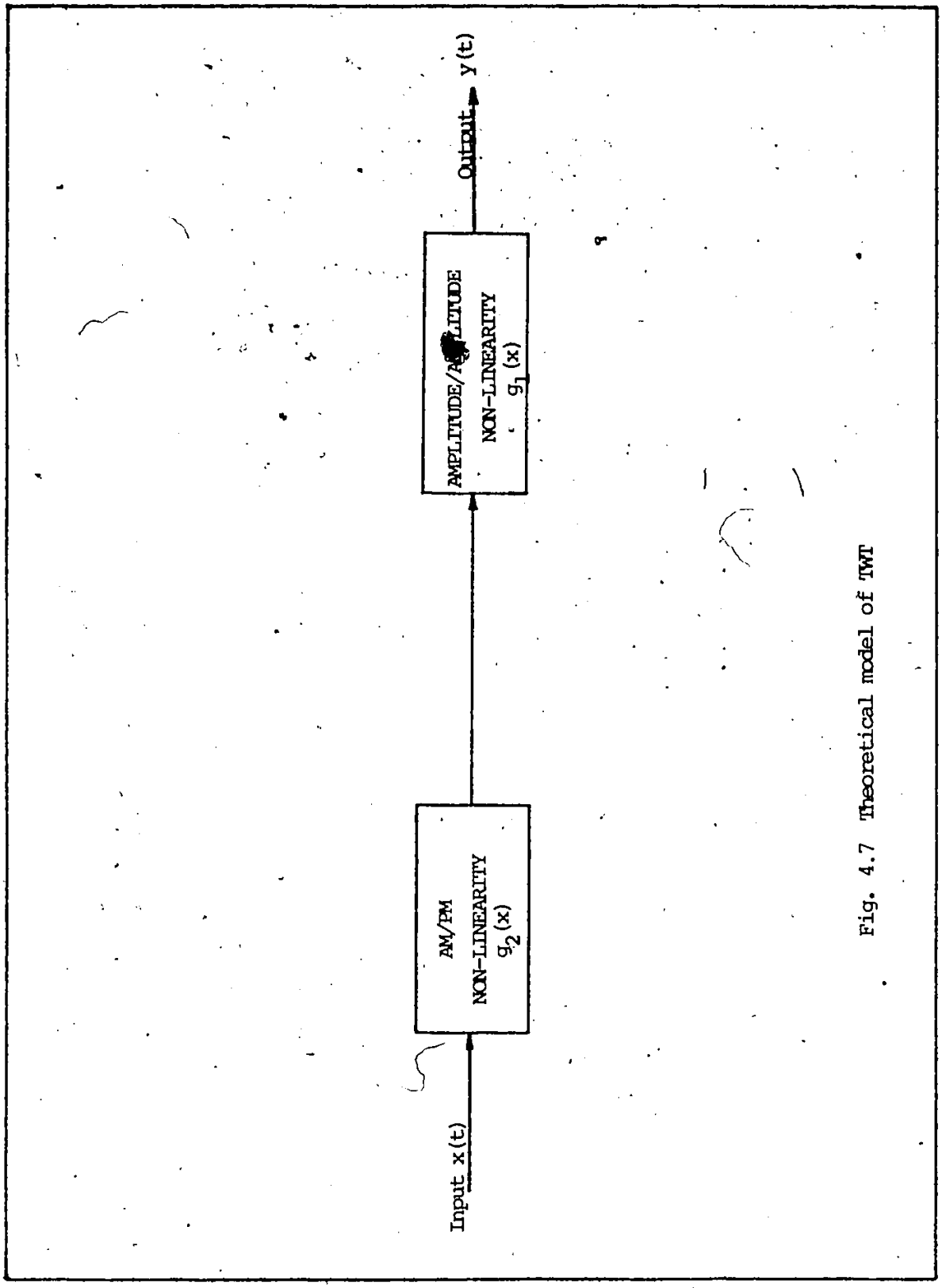

Fig. 4.7 Theoretical model of TWT

amplitude phase-shift non-linearity is given by $g_2(x)$. The overall transfer function then may be written as

$$g(x) = [g_1(x), g_2(x)] \qquad (4.7)$$

Thus, for a bandpass signal input to the essentially non-linear TWT, represented by

$$x(t) = A(t)\ \text{expj}[\omega t + \theta(t)] \qquad (4.7a)$$

the instantaneous output is expressed by

$$y(t) = \left[g_1[A(t)] \exp \left[(-j) g_2[A(t)] \right] \right] \text{expj}[\ \omega t + \theta(t)\ ] \qquad (4.8)$$

It is to be noted that this non-linear behaviour of the device is responsible for, often serious, distortion effects for pulse transmission at or near the Nyquist rate. Analytical studies regarding the non-linearity and its effects have been performed [47,48], thus only the results will be reviewed here.

2.2.1 AM/PM non-linearity

The TWT as main amplification device of the satellite transponders, is used extensively regardless as to whether the satellite system is designed as a Frequency-Division-

Multiple-Access (FDMA) or Time-Division-Multiple-Access (TDMA), and whether analog signal modulation or digital signal modulation techniques are used. For calculation purposes one uses the phase transfer characteristic which describes the relationship between small phase shifts and instantaneous input power.

The calculation of the relative phase shift can be performed by an equation of the form [46],

$$\phi = k_1[\,1 - \exp(-k_2 P_{in})\,] + k_3 P_{in} \qquad (4.9)$$

where

k_1, k_2, k_3 = tube constants

P_{in} = normalized instantaneous input power

ϕ = relative phase shift

The constants k_1, k_2, k_3 characterize the AM/PM conversion factor of the tube. Equation (4.9) has been found [46] to produce reasonably good agreement over the whole range, but best agreement is obtained for small input power. We are now in a position to more accurately define the TWT model which is adopted for simulation purposes in the course of this work.

2.2.2 TWT model

Based on the above discussion, one may deduce that, the TWT may be described by the input/output transfer characteristics. In particular, the AM/AM and AM/PM conversion factors are emphasized, as shown in equation (4.8) where the $g_1(.)$ presents the AM/AM and the $g_2(.)$ the AM/PM, conversion factors.

The approach here follows that in [49] where the overall representation of the non-linear device (the TWT in this case) is based on the analysis of a quadrature model of an equivalent bandpass device.

The main effort was directed into developing a model whereby use of an envelope transfer function is made, as opposed to the instantaneous voltage transfer function [46] used in previous analytical work[49]. The envelope transfer function approach has the advantage of encompassing a large degree of non-linearities when both, amplitude non-linearities as well as AM/PM conversion, must be considered. This envelope transfer function is then derived as a polynomial expansion which is directly produced by the quadrature model. Consider fig. 4.8. The effect that a bandpass non-linear device has upon a (narrow-band) input signal, is described [49] by the equation

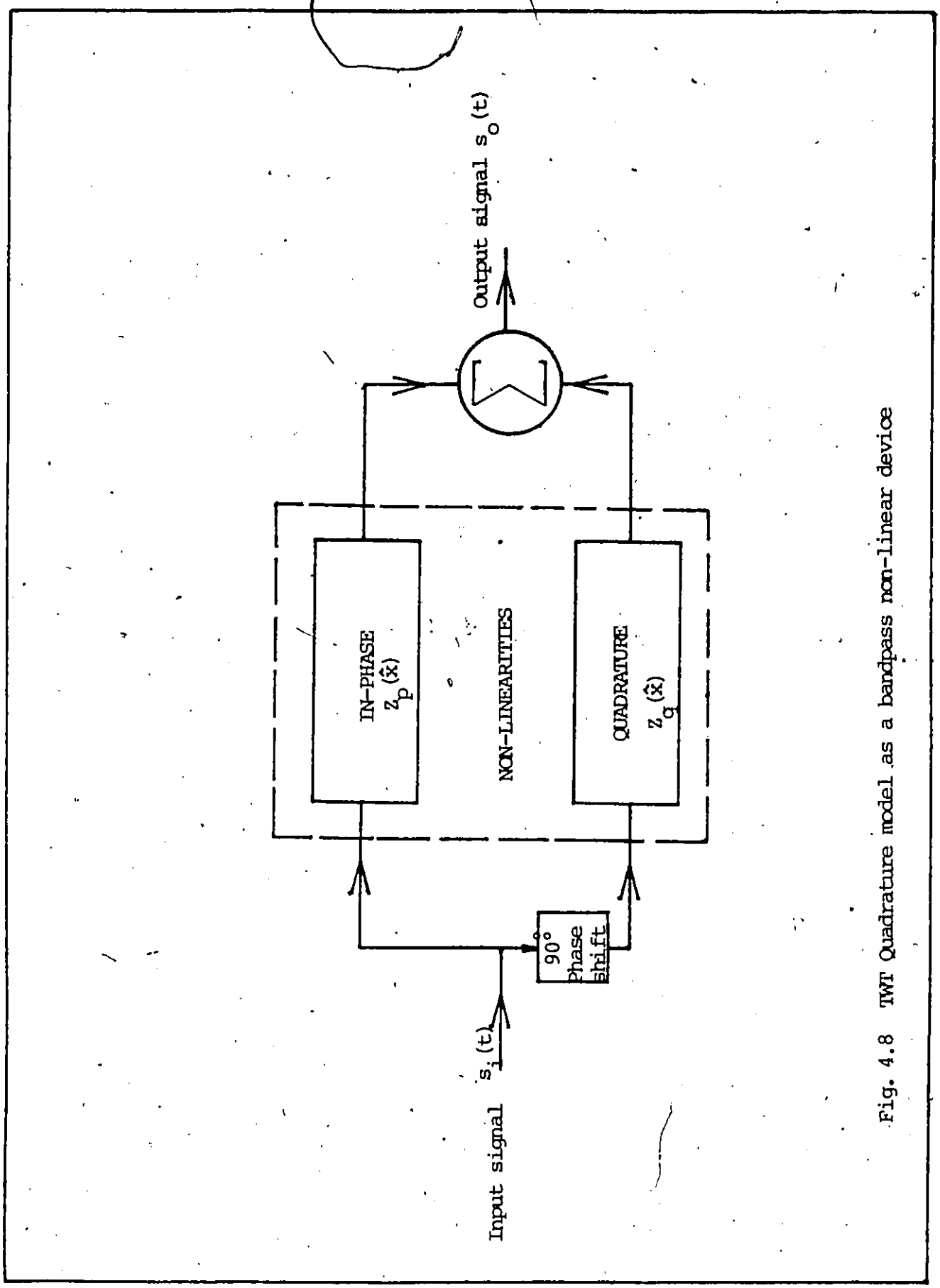

Fig. 4.8 TWT Quadrature model as a bandpass non-linear device

$$s_o(t) = \underbrace{S_o[\,\hat{S}_i(t)\,]}_{\text{output envelope}} \cos\Big[\omega_o t + \theta(t) + \underbrace{\phi[\,\hat{S}_i(t)\,]}_{\text{AM/PM conversion}}\Big] \qquad (4.10)$$

where

$\hat{S}_i(t)$ is the input envelope voltage, related to the input signal $s_i(t)$ by the following equation

$$x(t) = s_i(t) = \hat{S}_i(t)\cos[\,\omega_o t + \theta(t)\,] \qquad (4.11)$$

and ϕ is given by equation (4.9).

As it can be seen from equation (4.10), the output envelope voltage as well as the phase shift are dependent on the input envelope voltage, as it was previously indicated in the general expression of the TWT output signal given by equation (4.8). Having a narrow-band bandpass signal being described by equation (4.11), the output of the non-linear device will be given by equation (4.10). Re-writing (4.10) one obtains

$$s_o(t) = \hat{S}_o(t)\cos[\,\omega_o t + \theta(t) + \hat{\phi}(t)\,] \qquad (4.12)$$

where

$\hat{S}_o(t) = S_o[\,\hat{S}_i(t)\,]$ represents the output envelope distortion,

and

$\hat{\phi}(t) = \phi[\,\hat{S}_i(t)\,]$ represents the AM/PM conversion.

Using trigonometric identities, development of equation (4.12) will result in

$$s_o(t) = S_o[\,\hat{S}_i(t)\,]\cos\phi[\,\hat{S}_i(t)\,]\cos[\,\omega_o t + \theta(t)\,] -$$

$$- S_o[\,\tilde{S}_i(t)\,]\sin\phi[\,\hat{S}_i(t)\,]\sin[\omega_o t + \theta(t)\,]$$

$$= S_o^I[\,\hat{S}_i(t)\,]\cos[\,\omega_o t + \theta(t)\,] -$$

$$- S_o^Q[\,\hat{S}_i(t)\,]\sin[\,\omega_o t + \theta(t)\,] \qquad (4.13)$$

where

$S_o^I = S_o[\,.\,]\cos\phi[\,.\,]$ represents the In-phase non-linearity envelope component

$S_o^Q = S_o[\,.\,]\sin\phi[\,.\,]$ represents the Quadrature non-linearity envelope component

It is evident, from equation (4.13) that the power spectra of the two separate components (see fig. 4.8) will be added at the output of the device to form the final output signal spectrum.

Since the signal processing is carried out at baseband, in the simulation, the complex baseband equivalent representation of the signal described by equation (4.13), will be given by

$$s_o^*(t) = \left[S_o[\hat{S}_i(t)]\cos\phi[\hat{S}_i(t)]\cos\theta(t) - S_o[\hat{S}_i(t)]\sin\phi[\hat{S}_i(t)]\sin\theta(t)\right] + j\left[S_o[\hat{S}_i(t)]\sin\phi[\hat{S}_i(t)]\cos\theta(t) + S_o[\hat{S}_i(t)]\cos\phi[\hat{S}_i(t)]\sin\theta(t)\right] \quad (4.14)$$

To simplify the model for computational purposes, the non-linearities are presented in the form of series instead of analytical functions. The method developed in [49], which we use in the simulation, arrives at a polynomial representation for each of the non-linear envelope components. It has been determined then that, the instantaneous envelope voltage transfer function $S[\hat{S}_i(t)]$ is an odd function of the input voltage S_i whereas the phase characteristic $\phi[\hat{S}_i(t)]$ is an even function of S_i. Algebraic manipulation of the respective expressions, results in odd-order polynomials. It has been found [49] that, the in-phase envelope component may be represented as

$$\begin{aligned} S_o^I &= S_o[\hat{S}_i(t)]\cos\phi[\hat{S}_i(t)] \\ &= a_1\hat{S}_i(t) + a_3[\hat{S}_i(t)]^3 + a_5[\hat{S}_i(t)]^5 + \ldots + a_{2i+1}[\hat{S}_i(t)]^{2i+1} \\ &= \sum_{i=0}^{N} a_{2i+1}[\hat{S}_i(t)]^{2i+1} \end{aligned} \quad (4.15)$$

whereas the quadrature envelope component may be represented as

$$S_o^Q = S_o[\hat{S}_i(t)]\sin\phi[\hat{S}_i(t)]$$

$$= b_3[\hat{S}_i(t)]^3 + b_5[\hat{S}_i(t)]^5 + b_7[\hat{S}_i(t)]^7 + \ldots + b_{2i+1}[\hat{S}_i(t)]^{2i+1}$$

$$= \sum_{i=1}^{N} b_{2i+1}[\hat{S}_i(t)]^{2i+1} \qquad (4.16)$$

The coefficients a and b in equations (4.15) and (4.16) are determined from numerical data for a given TWT. Curve fitting techniques are then used to produce the typical characteristics, as shown in fig. 4.9.
For a value of N = 17, i.e. an 8-term series, the values of the coefficients a and b in the above equations are determined from numerical data and are given [49] in Table I.

The simulation model is as shown in fig. 4.10. In this simulation, a separate subroutine performs the TWT operation, whereby a predetermined number of sampled symbols (see section 2), is processed to produce the required output signal. The characteristics of the non-linear amplifier chosen are those of a typical INTELSAT-IV transponder. Provision has been made for substitution of other similar data, namely the coefficients of the polynomial representing the in-phase and quadrature non-linearities, saturated values of the in-phase and quadrature non-linearity and the maximum input envelope voltage.

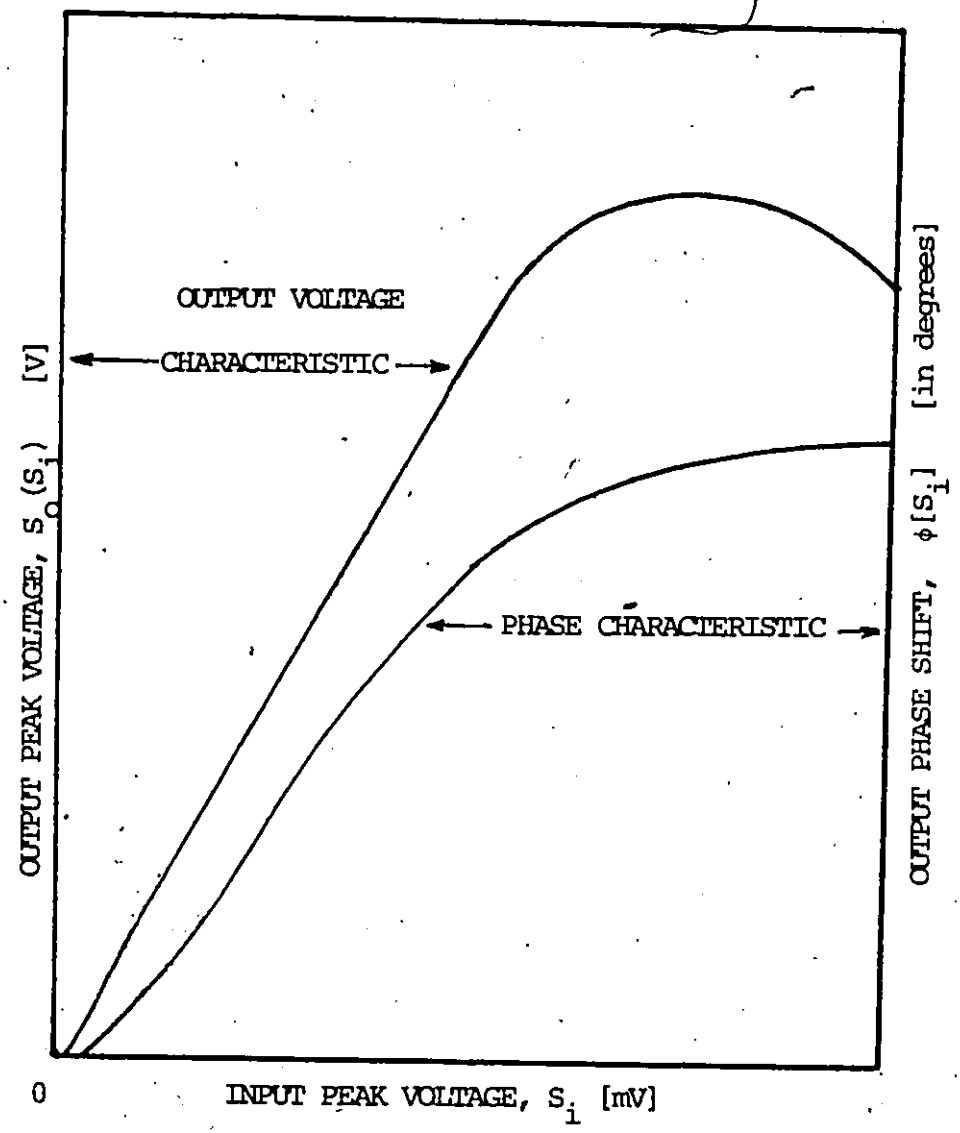

Fig. 4.9 TWT Envelope characteristics

TABLE I

Values of the in-phase (a)
and quadrature (b) envelope component coefficients

i	a_{2i+1} (volts/(mV)^i	b_{2i+1} (volts/(mV)^i
0	1.76245	-1.99286×10^{-3}
1	-1.53871×10^{-1}	1.81398×10^{-1}
2	1.35508×10^{-2}	-3.43698×10^{-2}
3	-9.07704×10^{-4}	3.37647×10^{-3}
4	4.20410×10^{-5}	-1.93769×10^{-4}
5	-1.28062×10^{-6}	6.67438×10^{-6}
6	2.41983×10^{-8}	-1.35523×10^{-7}
7	-2.55080×10^{-10}	1.49262×10^{-9}
8	1.14074×10^{-12}	-6.86914×10^{-12}

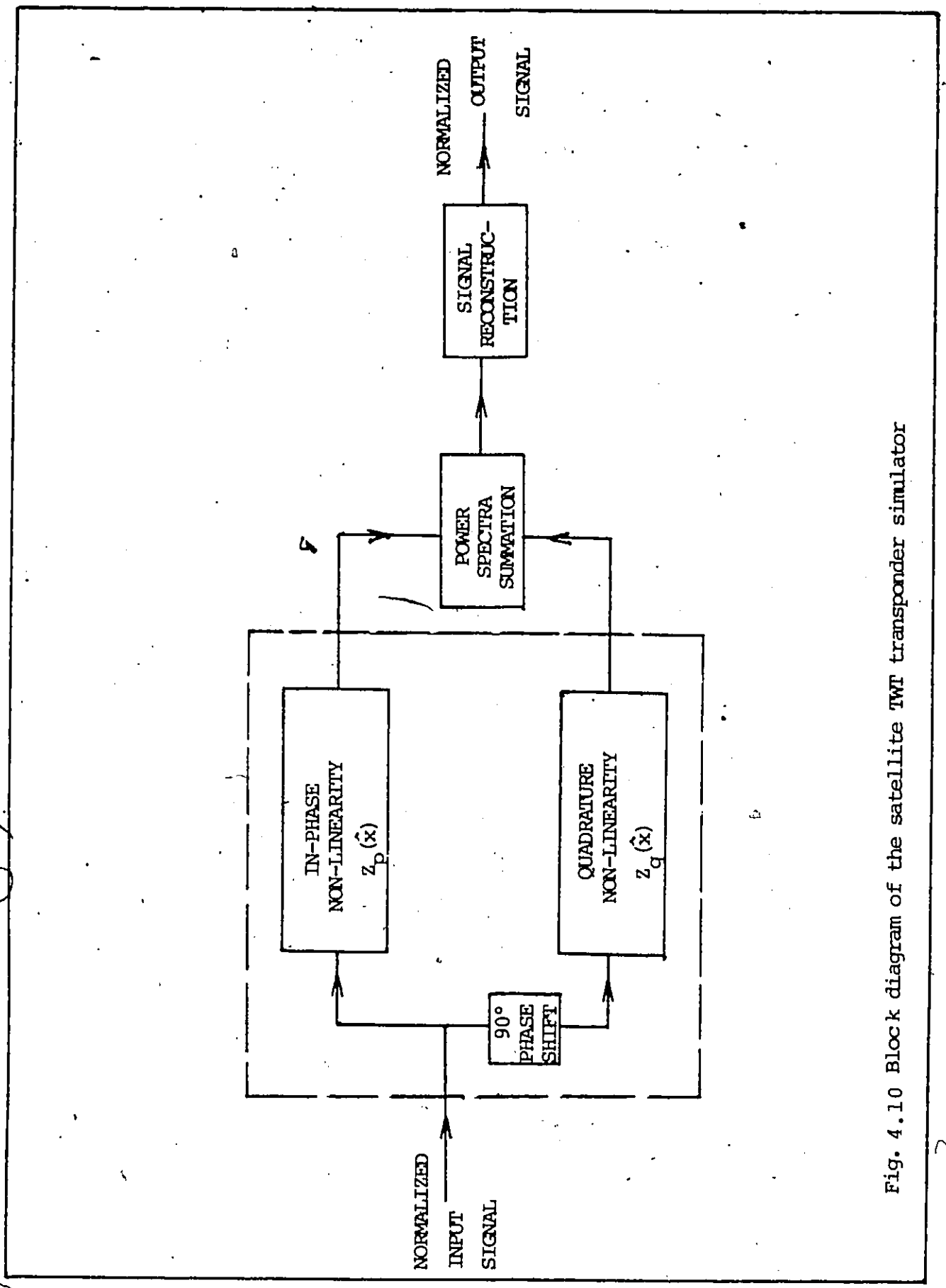

Fig. 4.10 Block diagram of the satellite TWT transponder simulator

The data stream is processed through the TWT in sections. At the output, the entire stream is reconstructed before it is further processed by the receiver filter. It is to be noted that care must be taken to normalize, to unit power, the input as well as the output signal to the TWT so that, it may be brought up to the normalized operating point. This is accomplished by dividing, both signals by $\sqrt{2}$. The output signal of the TWT will consist of a first spectral component centered on the higher frequency ω_c together with components centered on harmonics of ω_c. In communications usually [48], only the first spectral component is of interest, whereas the higher harmonics are effectively filtered and, consequently, one may neglect them.

The simulated TWT model preserves the quadrature characteristics of the signal after it is passed through it. Consequently, it is considered as a suitable one.

2.3 Receiver chain

The transmitted signal, after processing and translation at the satellite transponder, is retransmitted, usually at a lower frequency, to a receiving ground terminal. After demodulation and equalization, it is decided whether or not the received bits are correct. We assume that the carrier frequency conversion does not distort the signal. Similarly, correct synchronization is also assumed.

The in-phase and quadrature signal components, (see eqn. 4.2), in complex baseband (B/B) representation are obtained

after low-pass filtering in a similar manner as described for the transmit chain. The received signal is distorted by the additive down-link noise and ISI. This signal is band-limited by the BPF and further processed by the demodulator. Here, it will be determined as to which symbol was originally transmitted. To facilitate this process additional filtering is required whereby one attempts to maximize the signal-to-noise ratio. In the simulated receiver this filter is of the Integrate-and-Dump type (I&D) and there is no equalizer present. Use of the equalizer will be made later on, replacing the I&D (see ch. 3). The test receiver model considered is as shown in fig. 4.11.

The down-link noise power is computed [50] according to

$$\sigma_{n_o}^2 = \int_0^{+\infty} N_o |H(f)|^2 |G(f)|^2 \, df \qquad (4.17)$$

where

$H(f)$ = Receiver filter transfer function

$G(f)$ = I & D filter transfer function

N_o = one-sided noise power spectral density

The receiver bandpass filter is here also approximated by its low-pass equivalent, in much the same way as at the transmitter: A 1/2-dB ripple, 4-pole Chebyshev typical earth station

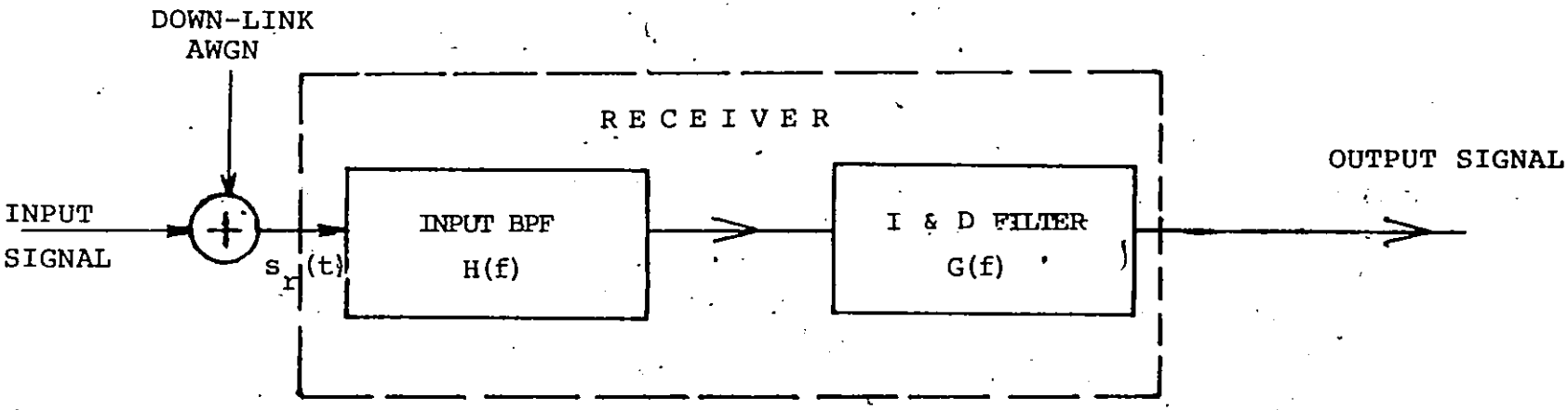

Fig. 4.11 Receiver model (front end)

filter is used [44].

The processing of the simulated signal is performed in a similar way to that in the transmitter chain: Individual signal sections are processed through the receive filter and finally the total data stream is reconstructed. The decisions are performed for each signal segment separately and on a bit-by-bit basis. Filtering introduces some delay in the sampled signals. Depending on filter memory, this amounts to several sample positions. Thus, the optimum sampling position for each segment must be determined. This is accomplished in the simulation by forming test sums. By selecting the largest sum, the starting (sample) locations, at the transmitter as well as the receiver filter outputs, are determined. In this manner, decoding of the corresponding samples is ensured.

In simulating the equalizer structure proposed in chapter 3, the received discrete sequence, distorted by the presence of the transponder non-linearities as well as the down-link noise, is presented to the decision feedback equalizer portion, of the proposed receiver, for partial equalization and a first, tentative, decision on a particular transmitted symbol. The simulated signal, as the input signal to the TWT is that of the unit pulse response of the channel. It was found that, this response contained terms that are of extremely small magnitude after 10 symbol samples. Therefore, in

the numerical computations these, small terms, were neglected. The normalized sampled input sequences to the equalizer are as shown in Fig. 4.12.

The optimum operating point of the TWT is backed-off from saturation to reduce the level of intermodulation products. As the operating point of the TWT is backed-off from saturation, the effects of non-linear phase-shift, i.e. the AM/PM conversion factor, become more pronounced. Consequently, one may say that the non-linear behaviour of the TWT is characterized mainly by these effects. To examine the effectiveness of the proposed equalisation scheme, an operating condition is established such that a significant amount of ISI will be introduced. This condition was achieved by backing-off the operating point of the TWT by 1 dB.

In simulating the hybrid equalizer, one decides first on the number of terms in the sampled response at the input to the equalizer (here, $\nu = 10$) and on the number of those terms that will be operated upon by the MLD (here, $C = 3$). The remaining intersymbol interference terms will be equalized by the feedback section, in the usual manner (see chapter II). To achieve this, i.e. the first step, one has to consider the cost implications of implementing the MLD: It was previously shown that the number of computations and storage locations, as a function of channel memory, increases in an exponential manner: With an increased number of terms,

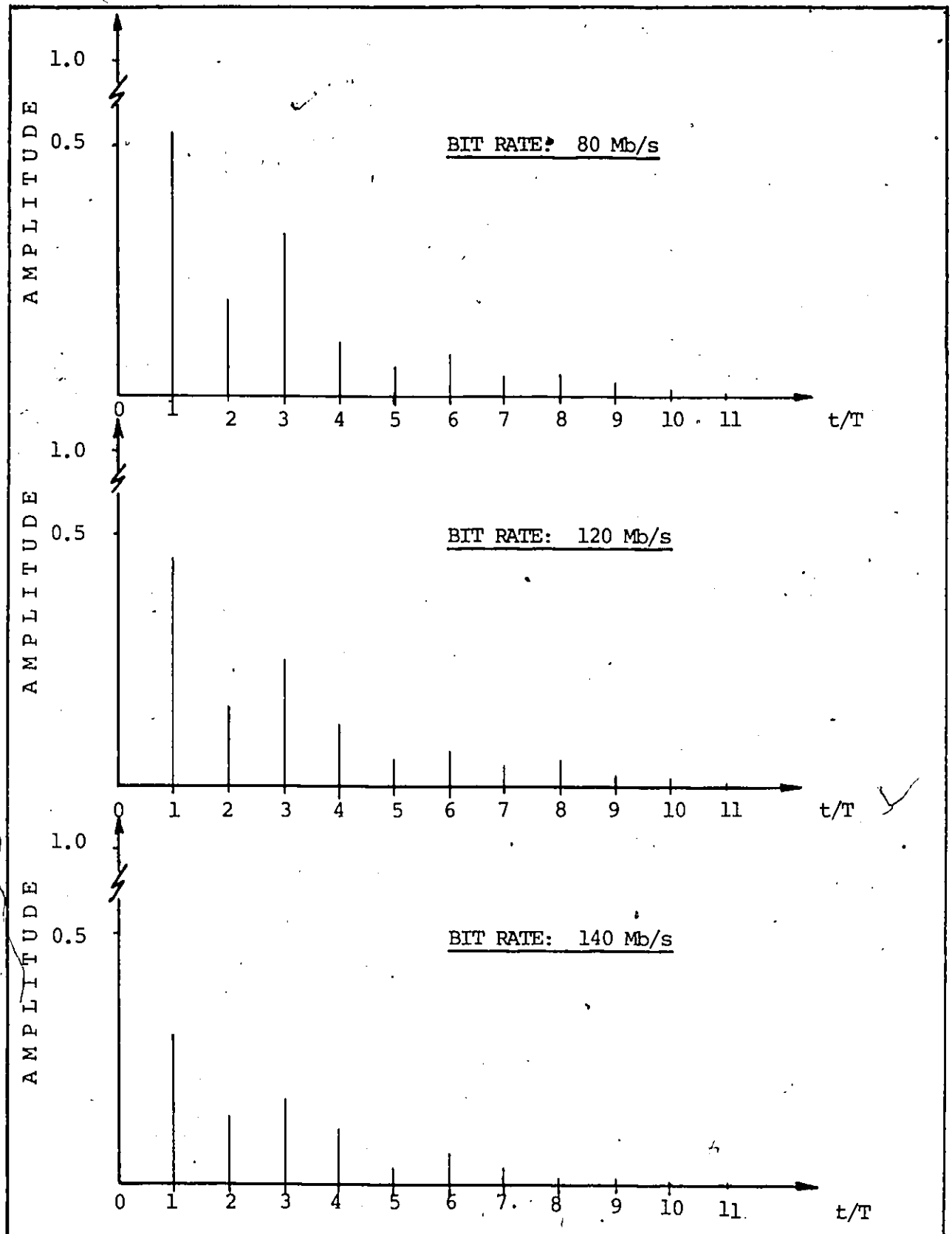

Fig. 4.12 Normalised sampled input sequences to the equalizer.

for the MLD, the implementation complexity and cost become extreme.

The way this problem was approached was by examining the performance obtained with increased complexity, identified by C. Thus, having simulated the DFE and MLD, based on the analysis, the C was varied between o and ν. The response of the channel was approximated by retaining the first 10 terms (i.e. $\nu = 10$). It must be noted that the remaining sampling terms are insignificantly small ($<0.001^2$) and therefore the truncated version represents an acceptable approximation to the original channel.

For pure DFE operation, i.e. complexity C = 0 or, no input samples to MLD, the calculated performance (for comparison purposes only) is as shown in Fig. 5.9. However, by gradually increasing the value of C, i.e. allowing the MLD to operate upon the response samples (=C) we observed that there was very little to be gained, in terms of performance, by increasing from C = 2, to C = 3. Translating this value in terms of complexity constraint, we had a 4-state (C = 2) or 8-state (C = 3) Viterbi algorithm to deal with. We decided that a 4-state algorithm, i.e. C = 2, is a reasonable compromise between complexity and performance, with a more complex equalizer being of little interest.

In summary then, from the 10 samples of the signal response, seven (7) terms are being operated upon by the DFE section i.e. $M_1 + M_2 = 7$) and the remaining three (3) including

the reference tap (i.e. C = 3), by the MLD section. The channel response terms are shown in Table II.

It is emphasized that, the performance of the DFE section alone ("DFE" curve in fig. 5.9) has been here calculated as an indication only that this simulated section is indeed functioning correctly. Of interest here is the performance of the combined simulated (hybrid) section, i.e. DFE/MLSE. System performance calculations are based upon the performance of the hybrid section ("DFE/MLSE" curve in fig. 5.9).

The operation of the MLD, as simulated here, follows the analytical development of the dynamic programming arguments, as presented in chapter 3. To effect a final decision on a particular transmitted symbol, a "merging of states" procedure was implemented, whereby the states are examined, within the allowed symbol storage limitation, as to whether they merge or not. It may happen, though, that despite the reasonable survivor length allowed here, there will be no such merging of states. In this case, the simulation allows for re-examination of the first half of the stored symbols. The final decision now will be made on the basis of this half by choosing as the detected sequence, the one with the maximum log likelihood.

3. System performance

The evaluation of a communication system usually con-

TABLE II

Channel response terms

Sample No.	Input x_i (Normalized) for Data rate		
	80Mb/s	120 Mb/s	140 Mb/s
0	1.0000	1.0000	1.0000
1	0.5323	0.4722	0.2985
2	0.1950	0.1664	0.1458
3	0.3336	0.2986	0.2241
4	0.1230	0.1120	0.1007
5	0.0250	0.0184	0.0152
6	0.0330	0.0292	0.0226
7	0.0198	0.0177	0.0143
8	0.0200	0.0181	0.0098
9	0.0150	0.0095	0.0054
10	0.0023	0.0018	0.0012

sists of calculations and measurements of its performance in terms of Probability of Error P(e) vs. Bit-energy-to-noise ratio, E_b/N_o .

In the system under study, the modulated received signal plus noise can be represented by

$$s_r(t) = s_I(t)\cos\omega_c t - s_q(t)\sin\omega_c t + n_I(t)\cos\omega_c t - n_q(t)\sin\omega_c t$$

$$= [\, s_I(t) + n_I(t) \,]\cos\omega_c t - [\, s_q(t) + n_q(t) \,]\sin\omega_c t \qquad (4.18)$$

where $s_I = S_o^I$ and $s_q = S_o^Q$ denote the in-phase and quadrature components respectively. This signal is pre-amplified, down-converted, to the IF frequency of 70 MHZ, amplified by the IF amplifier and is detected. The combined vector of the detected signal plus noise, will be in one of the four (4) decision regions (for QPSK modulation) of the phasor plane. Now, if this combined signal or, received symbol, is located outside the (correct) decision region, then, this signal is in error: The probability that this composite signal vector will be lying outside the given region, is the probability that the received symbol is in effect in error.

It has been shown [3] that in coherent detection of a four phase modulation signal, the probability of error for the signal and Gaussian noise only is given by

$$P(e) = 1 - [\, 1 - Q\sqrt{\rho} \,]^2 \qquad (4.19)$$

where

$$Q(\nu) = \frac{1}{\sqrt{2\pi}} \int_{\nu}^{+\infty} e^{-t^2/2}\, dt \quad , \quad \text{the error function}$$

and

$$\rho = \frac{A^2}{2\sigma^2} \quad , \quad \text{the signal-to-noise ratio.}$$

Most of the results regarding system performance are given in terms of either the average symbol energy or, the signal-to-noise ratio. The relationship between signal-to-noise ratio (S/N) and bit energy-to-noise ratio (E_b / N_o), for a 4ϕ-CPSK system, can be stated as

$$\frac{E_b}{N_o} = \frac{S}{N} - 3 \quad [dB] \qquad (4.20)$$

It is to be noted that equation 4.20 is valid only when the theoretical case is considered, i.e. the noise bandwidth of the receiver equals the double sided Nyquist bandwidth [45].

The performance characteristics have been evaluated following the analysis presented in the previous section. The operation is repeated on a segment-by-segment basis until the entire signal has been processed. The simulation facilitates the display of the results in two forms: (a) the probability of error vs. signal-to-noise ratio performance curve and, (b) the eye-diagram. The produced characteristic

curves as well as the eye diagrams have been plotted with the aid of a CALCOMP plotter, available at the University of Ottawa computing centre.

4. System flowchart

The previously described simulation procedure will now be presented in the form of a flowchart. Although specific programming statements are not included, the logic of the complete simulation is presented, as shown in fig. 4.13.

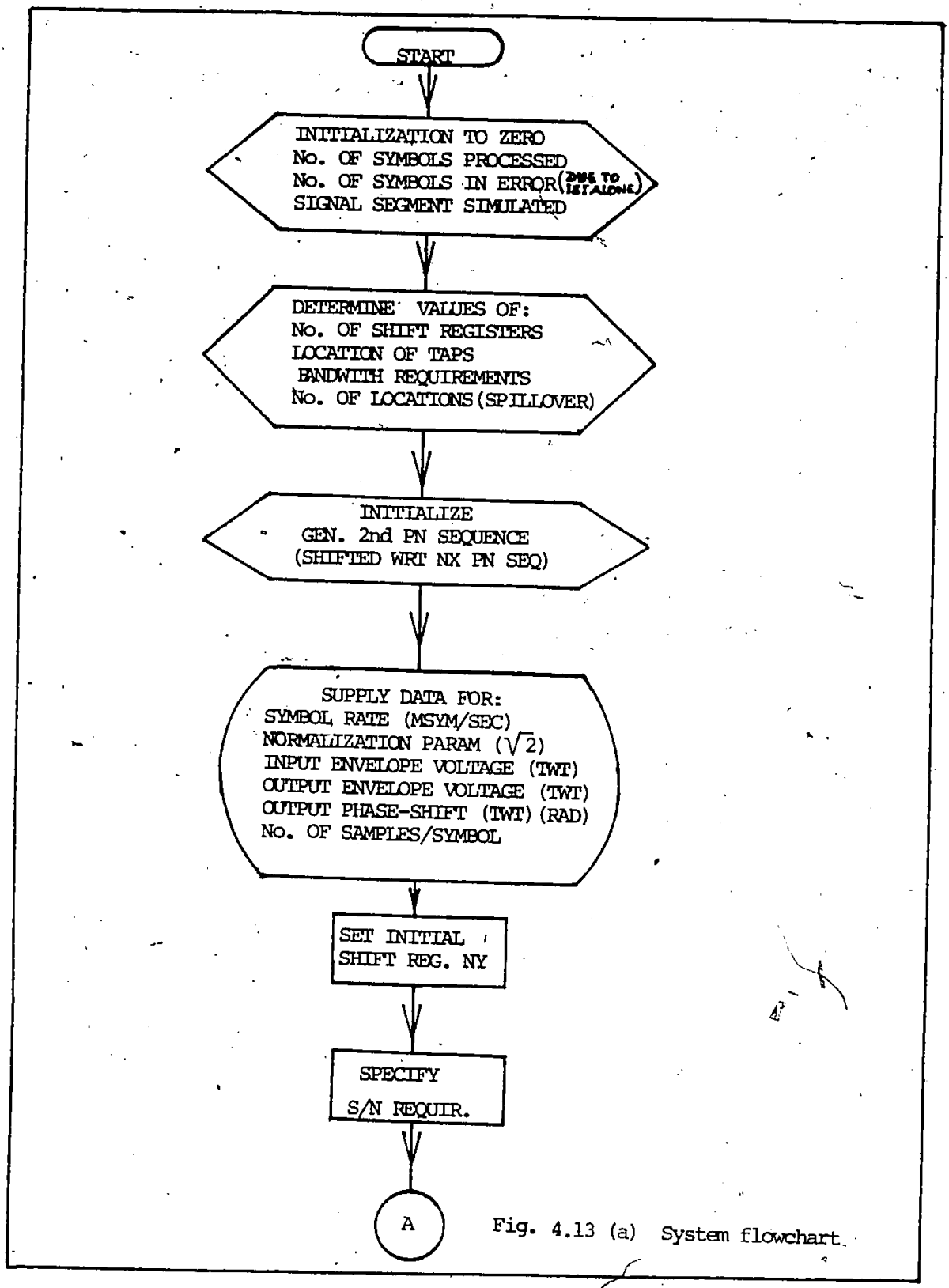

Fig. 4.13 (a) System flowchart

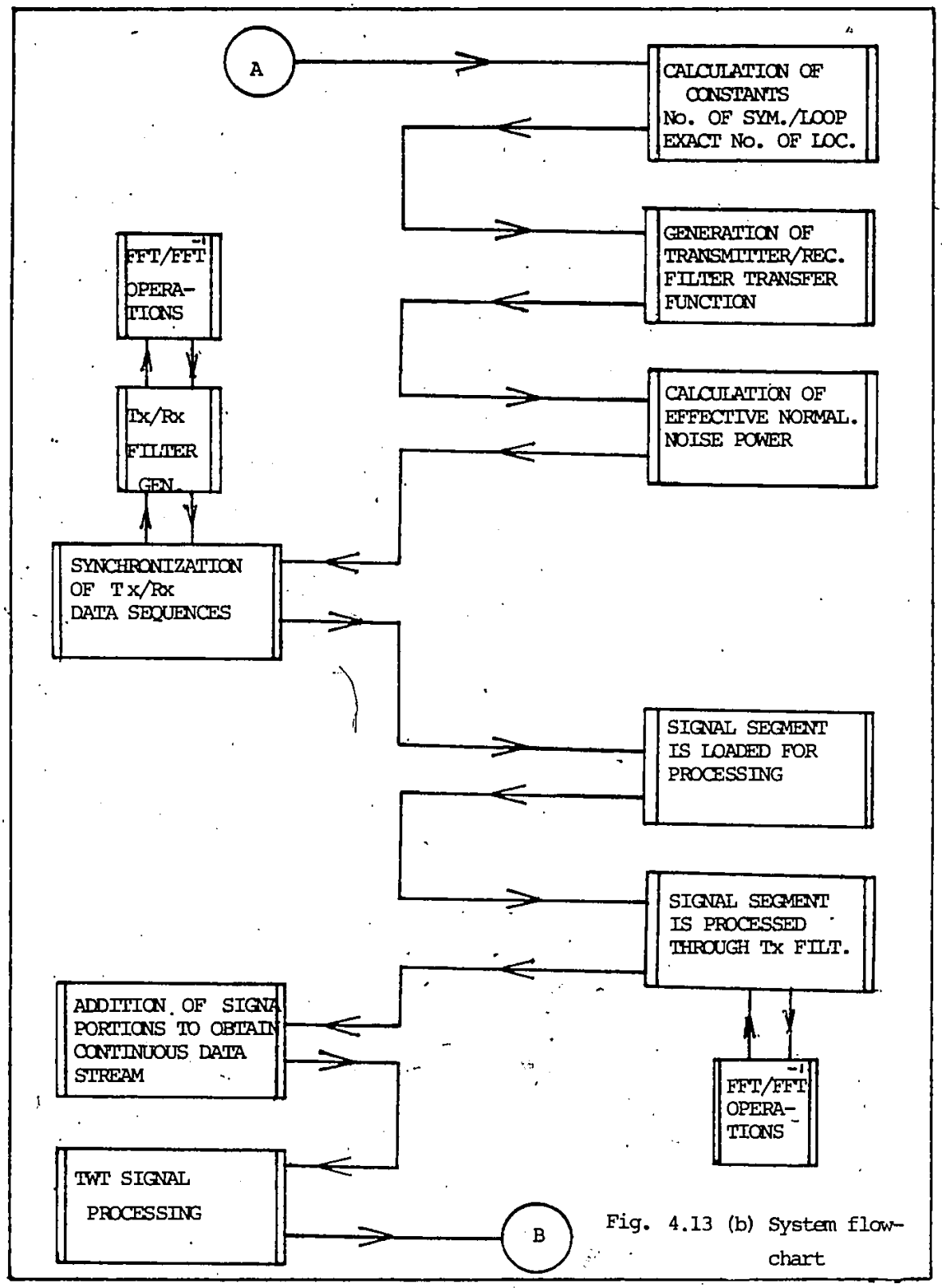

Fig. 4.13 (b) System flow-chart

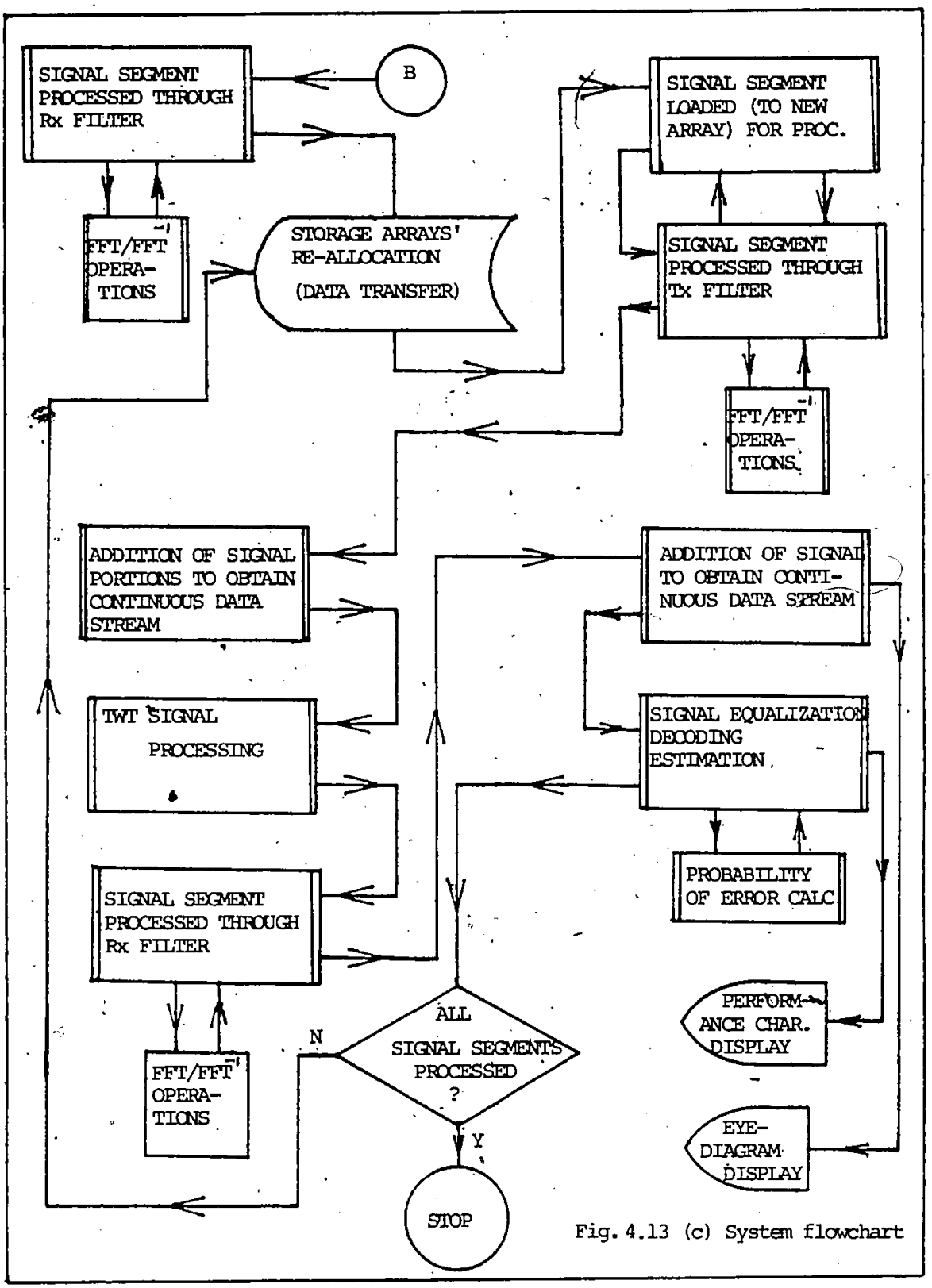

Fig. 4.13 (c) System flowchart

CHAPTER V

SIMULATION RESULTS

1. SUMMARY OF RESULTS

The simulation described in the previous chapter has been successfully implemented. There were two TWT operating conditions considered:

(a) Operation close to the saturation point, i.e. operation at 1 db input power backoff, and

(b) Operation at a linear region of the TWT, i.e. operation at 12 db input power backoff.

Simulation runs were performed at various data speeds for each of the above conditions. The results of these computer simulation runs are presented in this chapter under two separate sub-headings:

(1) Bit-by-Bit decision results, and

(2) Hybrid equalization/decision results.

1.1 Bit-by-Bit decision results

The performance of the satellite transmission system, using QPSK modulation format, has been calculated in terms of the probability of error vs. signal-to-noise ratio or, vs.

bit-energy-to-noise ratio, at various bit-rates.

The obtained performance characteristics are shown in figures 5.1 to 5.4. The satellite system was, at first, simulated without any filters and without the presence of the non-linear TWT, i.e. without any pulse constraints: the resulting performance characteristic is as shown in Fig. 5.1. By adding the filters and the bit detector, the performance characteristics of Fig. 5.2 were obtained: the degradation of performance, with increasing bit rate, is evident from that figure. Subsequently, by adding the non-linearity of the TWT, operating at 1 dB input backoff, i.e. near saturation, while retaining the filters and the bit detector, the performance characteristics of Fig. 5.3 were obtained: Comparing these last two figures one observes that, for bit rates up to 100 Mb/s there is a system performance degradation (fig. 5.3), i.e. increased probability of error with the non-linear system element present, as expected. However, for higher bit-rates, i.e. above 100Mb/s and for the same signal-to-noise ratio, there is some relatively small system performance degradation (fig. 5.2) even though the non-linearities are not included in the system configuration. At these high bit rates there is, of course, higher ISI created due to the transmit filters. Now, the paradox of the system performance degradation, at these high bit rates (fig. 5.2) might be attributed to this very absence of the non-linearity which, essentially, acts (when present) as a limiter-amplifier

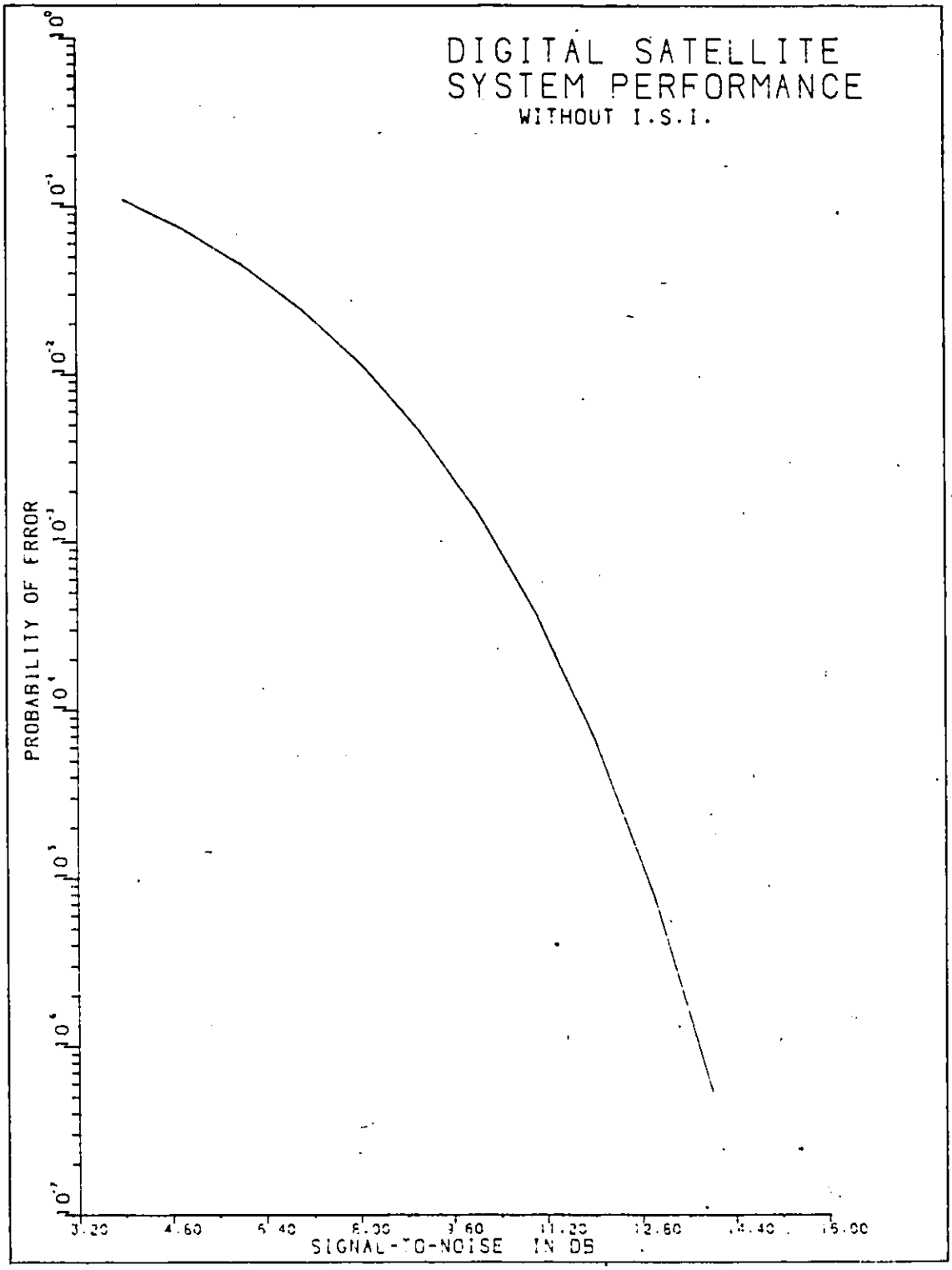

Fig. 5.1 . Probability of error vs. signal-to-noise ratio (No ISI present - QPSK modulation format, in theoretical minimum bandwidth)

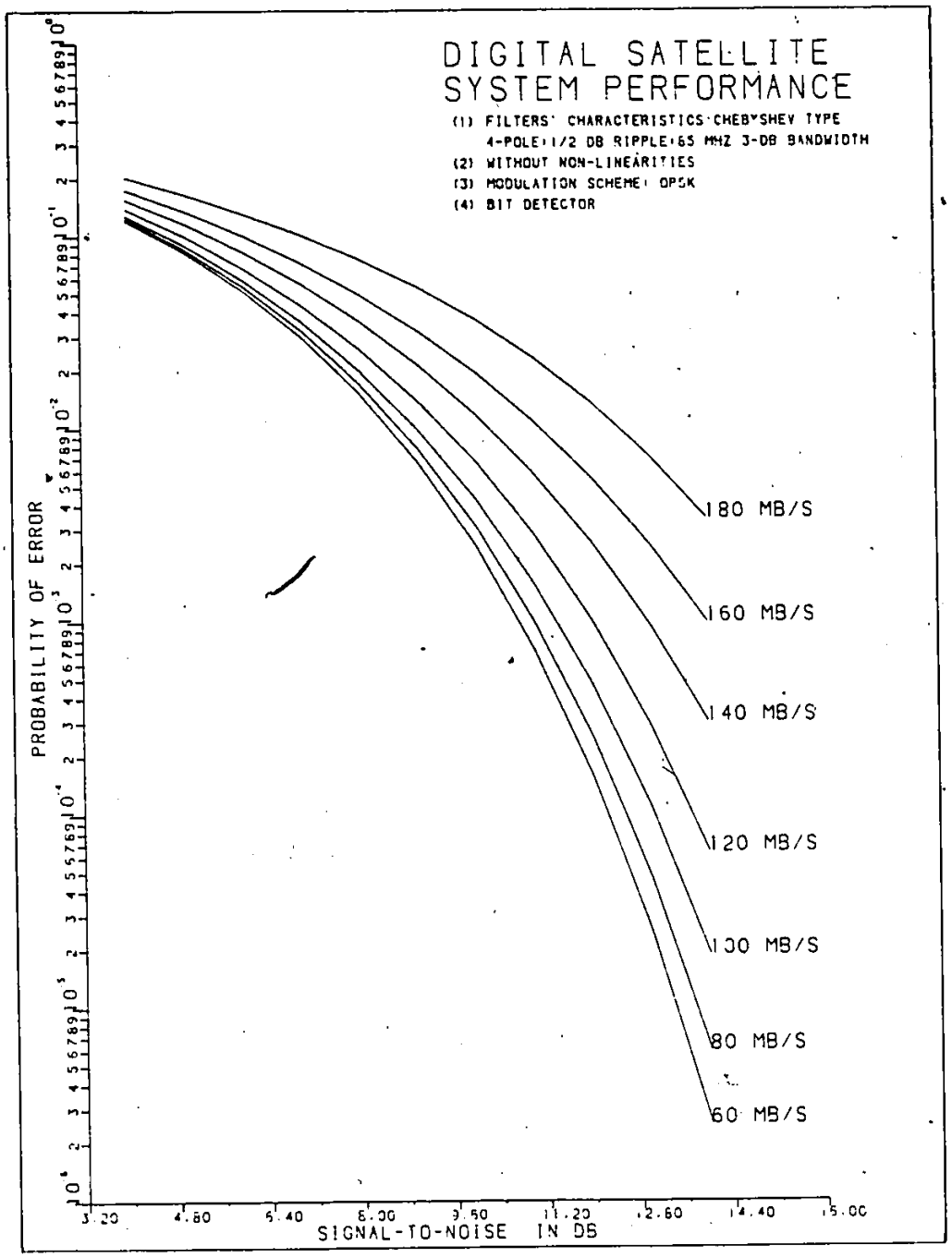

Fig. 5.2. Probability of error vs. signal-to-noise ratio

(see legend above, noise power computed in the Nyquist bandwidth corresponding to each bit rate)
(the same comment applies to figs. 5.3 - 5.12)

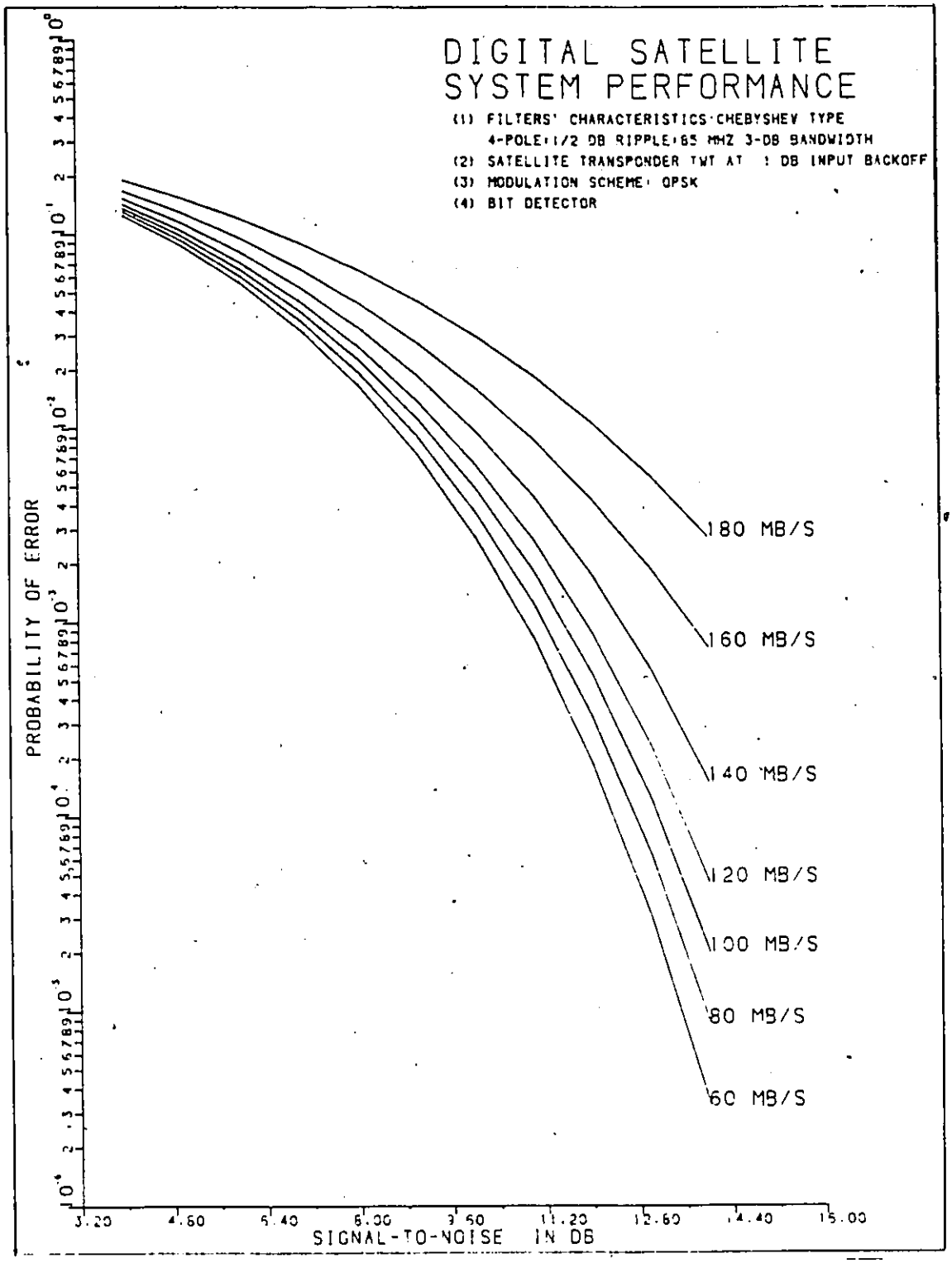

Fig. 5.3. Probability of error vs. signal-to-noise ratio
(see legend above)

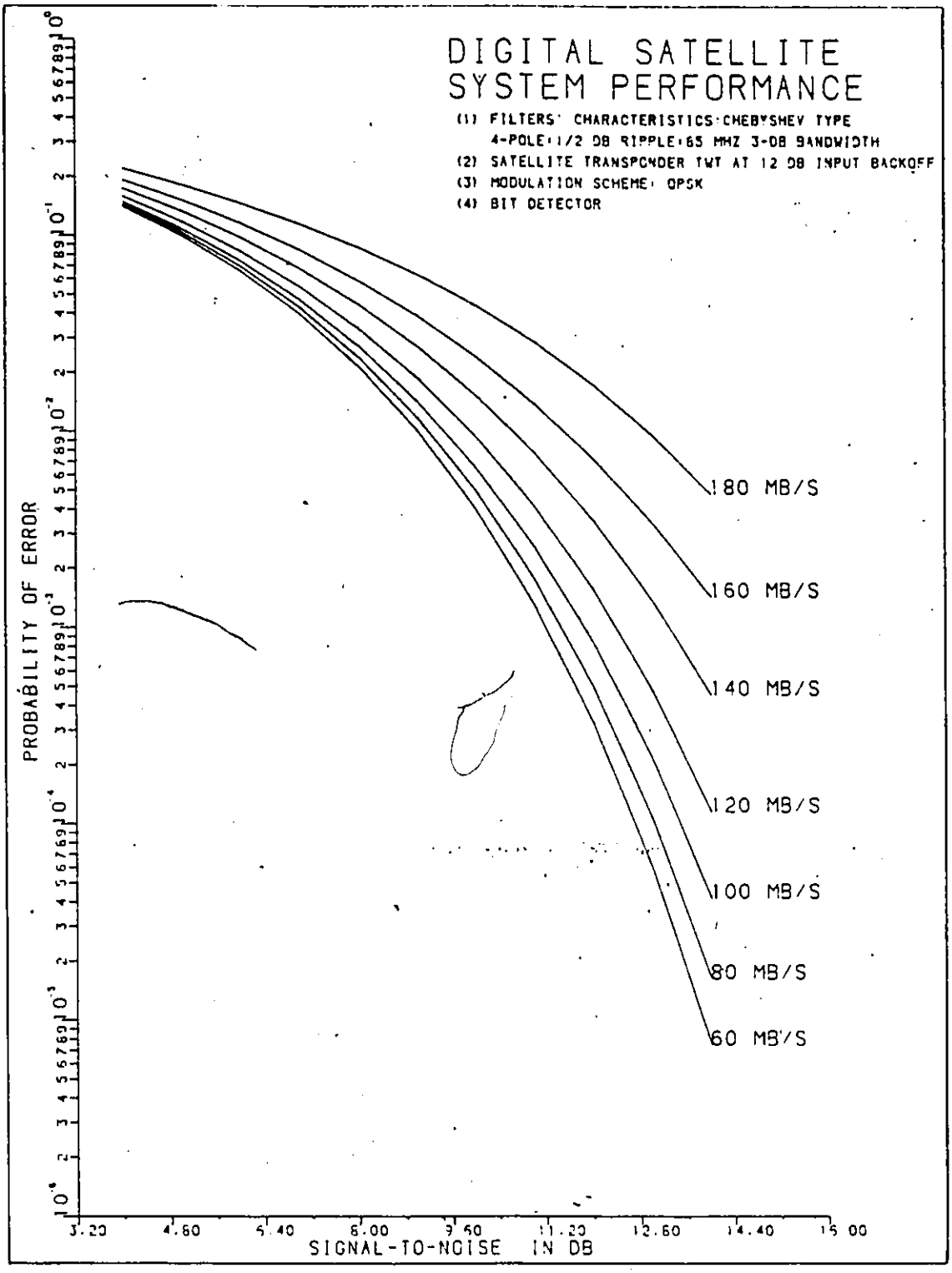

Fig. 5.4. Probability of error vs. signal-to-noise ratio (see legend above)

thereby mitigating (to some extent) the effects of the transmit filters. In a simulated operating condition of TWT in its linear region, i.e. at 12 dB input backoff, the resulting characteristics are as shown in Fig. 5.4. Comparing now figures 5.3 and 5.4, one observes that, there is a higher probability of error when the input signal to the non-linear amplifier (TWT) is reduced well below saturation (fig.5.4). This degradation in performance is due to the distortion created mainly by the AM/PM conversion effects. It has been shown [68] that these AM/PM effects often dominate the amplitude non-linearity (AM/AM) effect when the non-linear amplifier system element is operated in the linear region of its characteristic. In contrast, operation close to saturation (hard-limiting) results (fig. 5.3) in an AM/PM distortion effect which increases with input power at a relatively slower rate. Here, the hard-limiting amplifier action is compensating, in a sense, the more pronounced non-linear amplitude variations [43, 49]. Furthermore, under both TWT operating conditions, there is a degradation in performance with increasing bit rate, as expected.

Using the baseband signal of the in-phase channel, the eye diagrams, for each of the above operating conditions, were plotted on an X-Y recorder, The results are as shown in Figures 5.5 through 5.7. Here, one can see clearly the degradation of the P(e) performance due to increasing intersymbol interference and down-link noise, as the bit-rate

increases. This is done by inspecting the eye-opening (at the middle of the diagram) which becomes narrower as the bit-rate increases. As it can be seen, quite satisfactory system performance is obtained even at very high bit rates (fig. 5.7). Namely, at 180 Mb/s, the eye is still open although with a quite reduced noise margin. Similar remarks apply here, as in the case of the performance characteristics regarding the differences between TWT operating conditions.

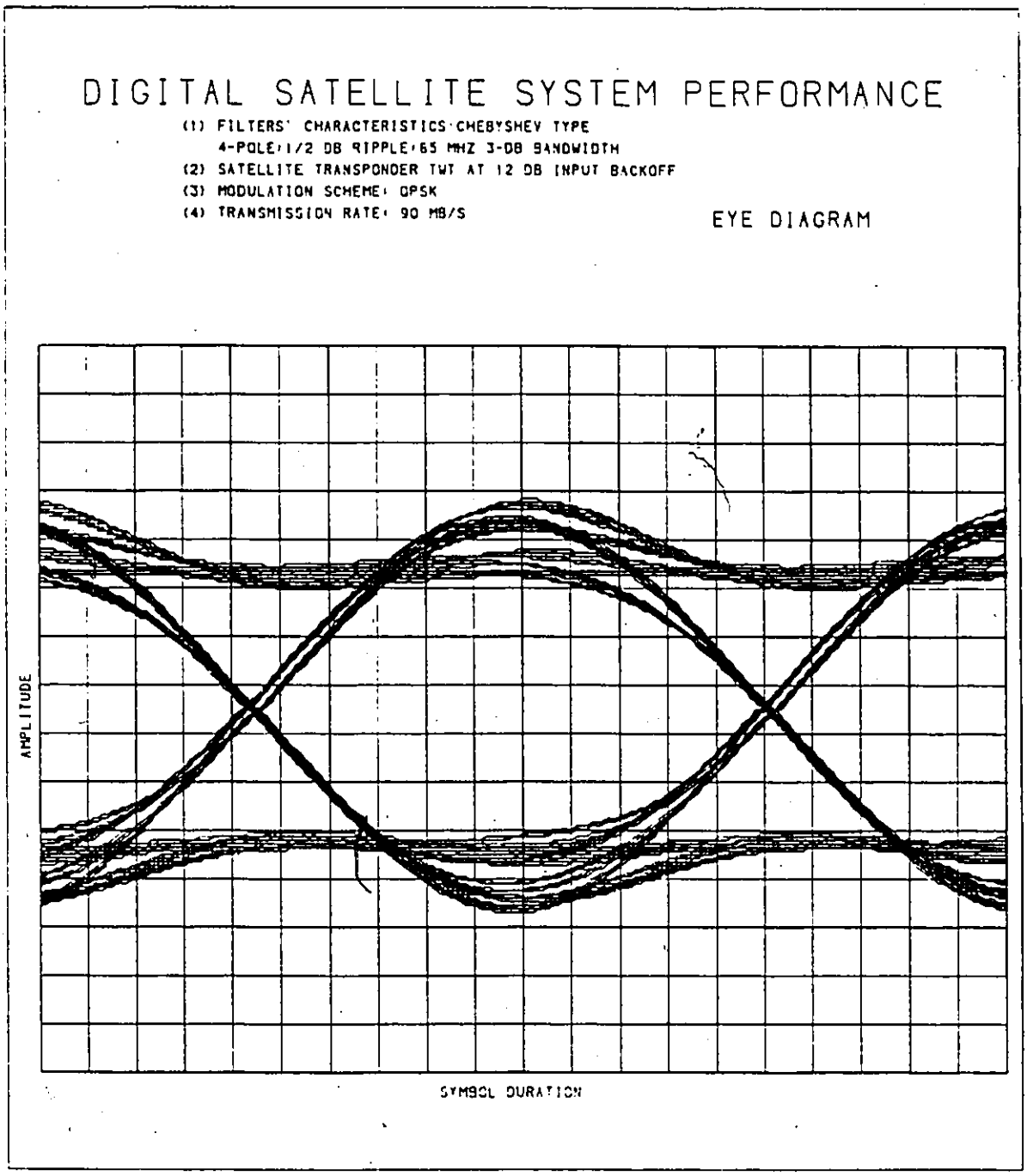

Fig. 5.5 Eye diagram - 90 Mb/s (see legend above)

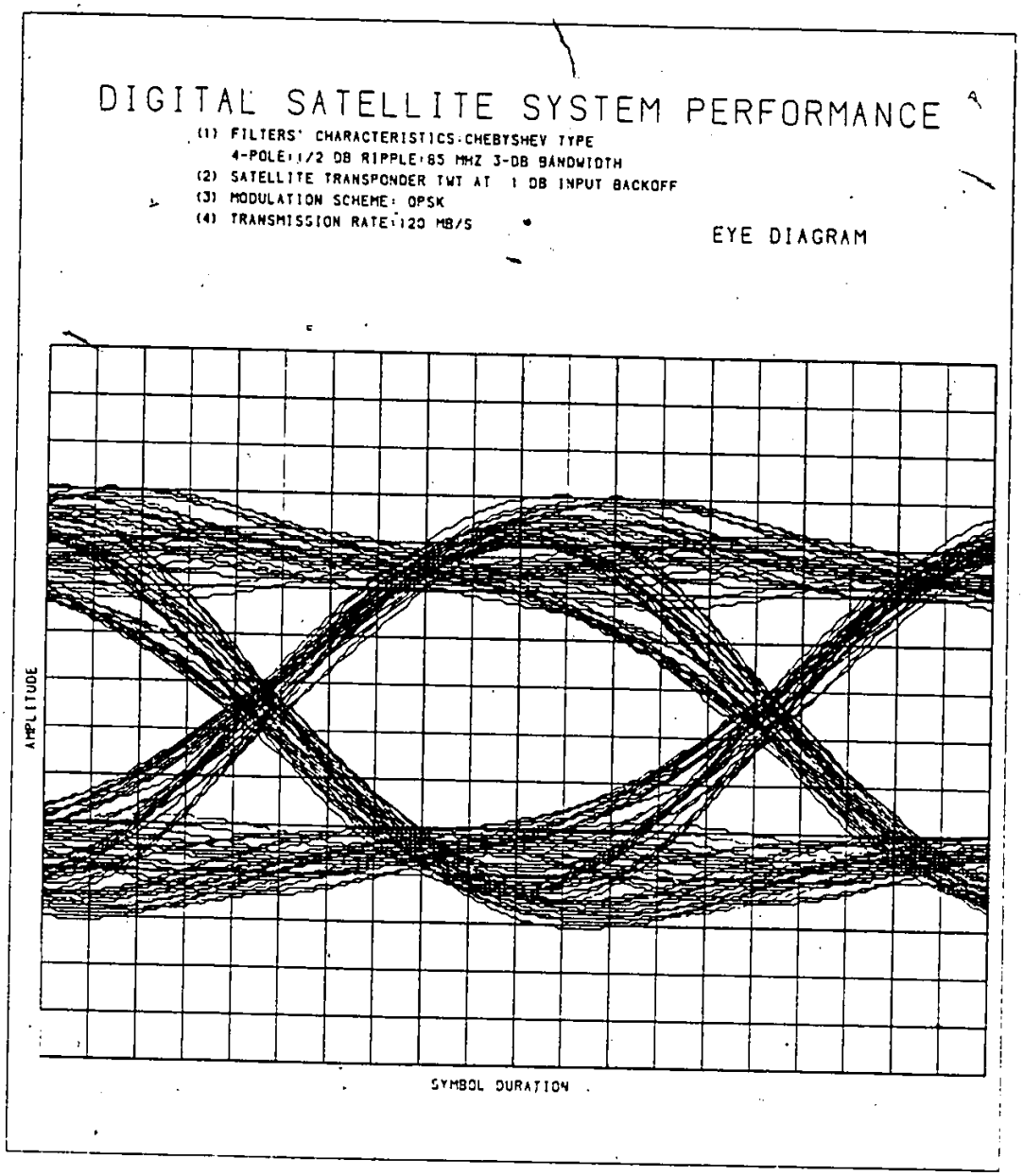

Fig. 5.6 Eye diagram - 120 Mb/s (see legend above)

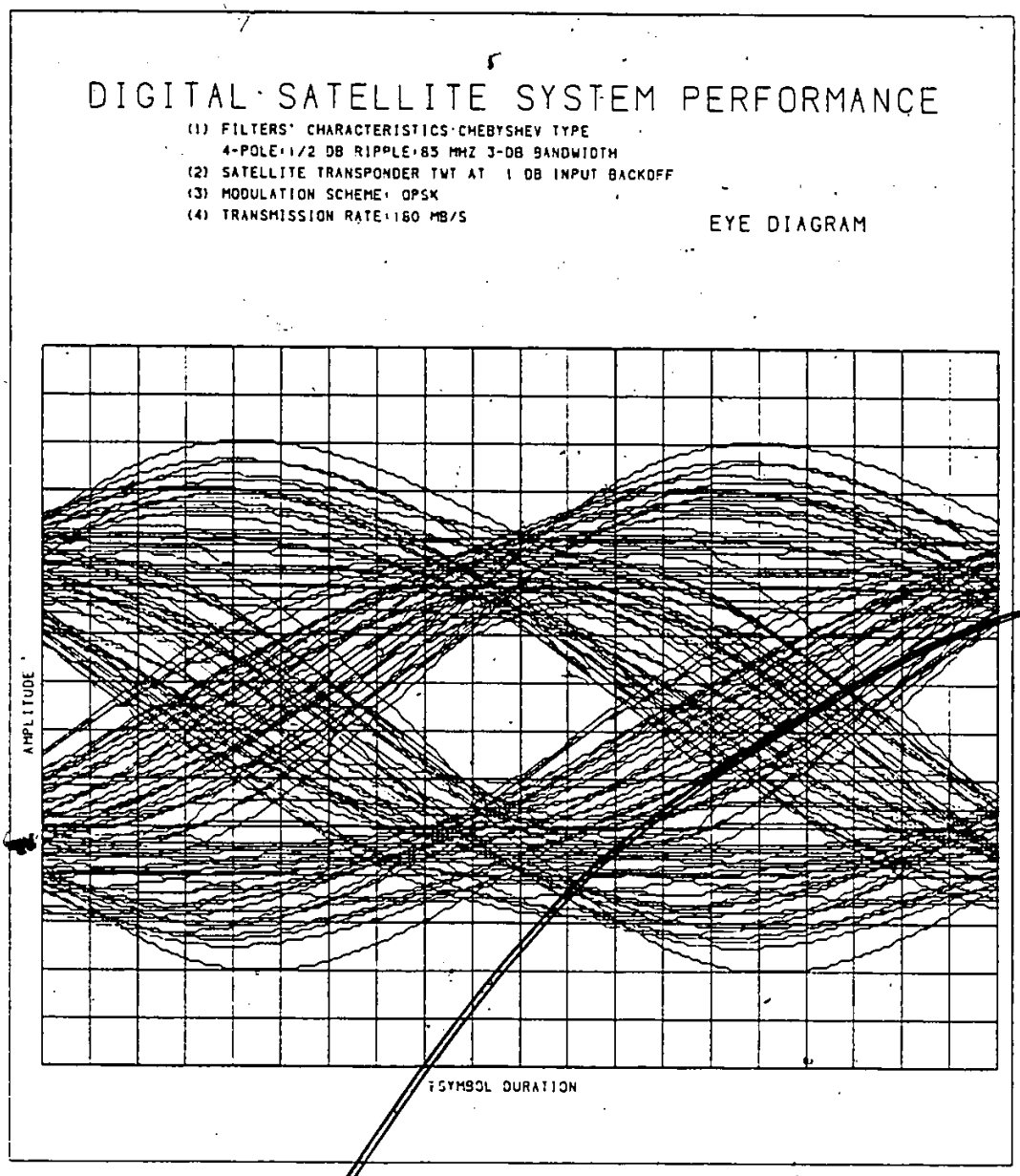

Fig. 5.7 Eye diagram - 180 Mb/s (see legend above)

1.2 Hybrid equalization/decision results

The introduction of the hybrid equalizer, into the receive chain, has been effected by incorporating its simulated structure into the basic satellite communication system. The performance of this system configuration has been calculated anew, using the same criteria as before.

The operation of the basic equalizer stages was first examined. The resulting performance characteristics, for a system transmitting at 80 Mb/s, chosen as an initial example only, and with a TWT operating at 1 db input power backoff, are as shown in fig. 5.8. These characteristics demonstrate the noticeable improvement one may obtain when the hybrid equalizer configuration is used. Thus, for the sake of comparison, the simulated equalizer was first configured in decision feedback form, without the benefit of the VA section. The resulting performance curve is identified as 'DFE'. Subsequently, the structure was configured as proposed, i.e. in its hybrid form. The resulting performance curve is identified as 'DFE-MLSE'. One clearly distinguishes, by comparing the two curves that, pure 'DFE' operation, in the non-linear satellite channel environment, is not beneficial. Whereas, use of the combined configuration, results in improved operation.

Performance bounds calculations, as indicated in chapter 3, resulted in the characteristic curves shown in fig. 5.9. Here, the lower bound is the same as that of the Viterbi

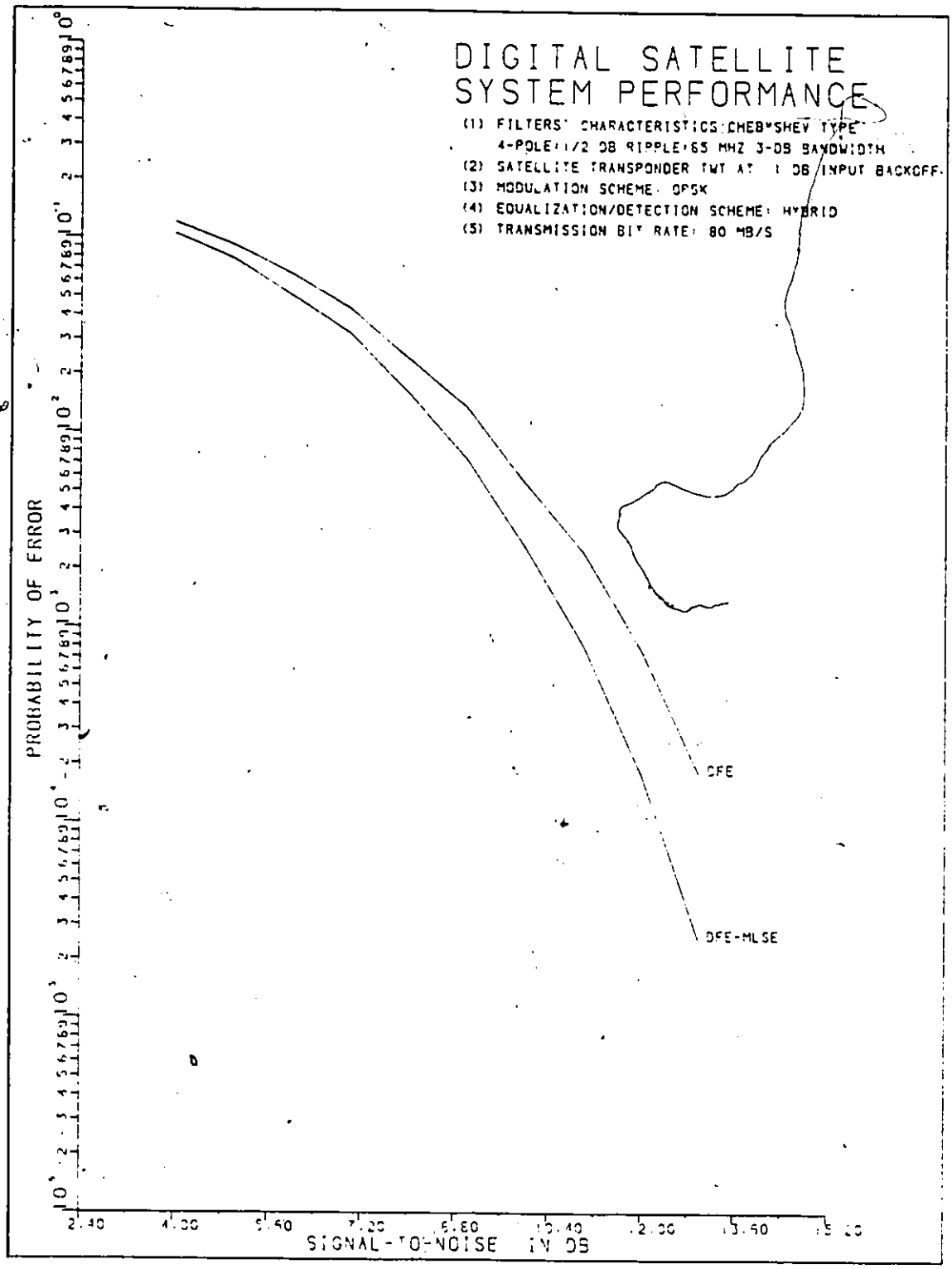

Fig. 5.8 Probability of error vs. signal-to-noise ratio
(see legend above)

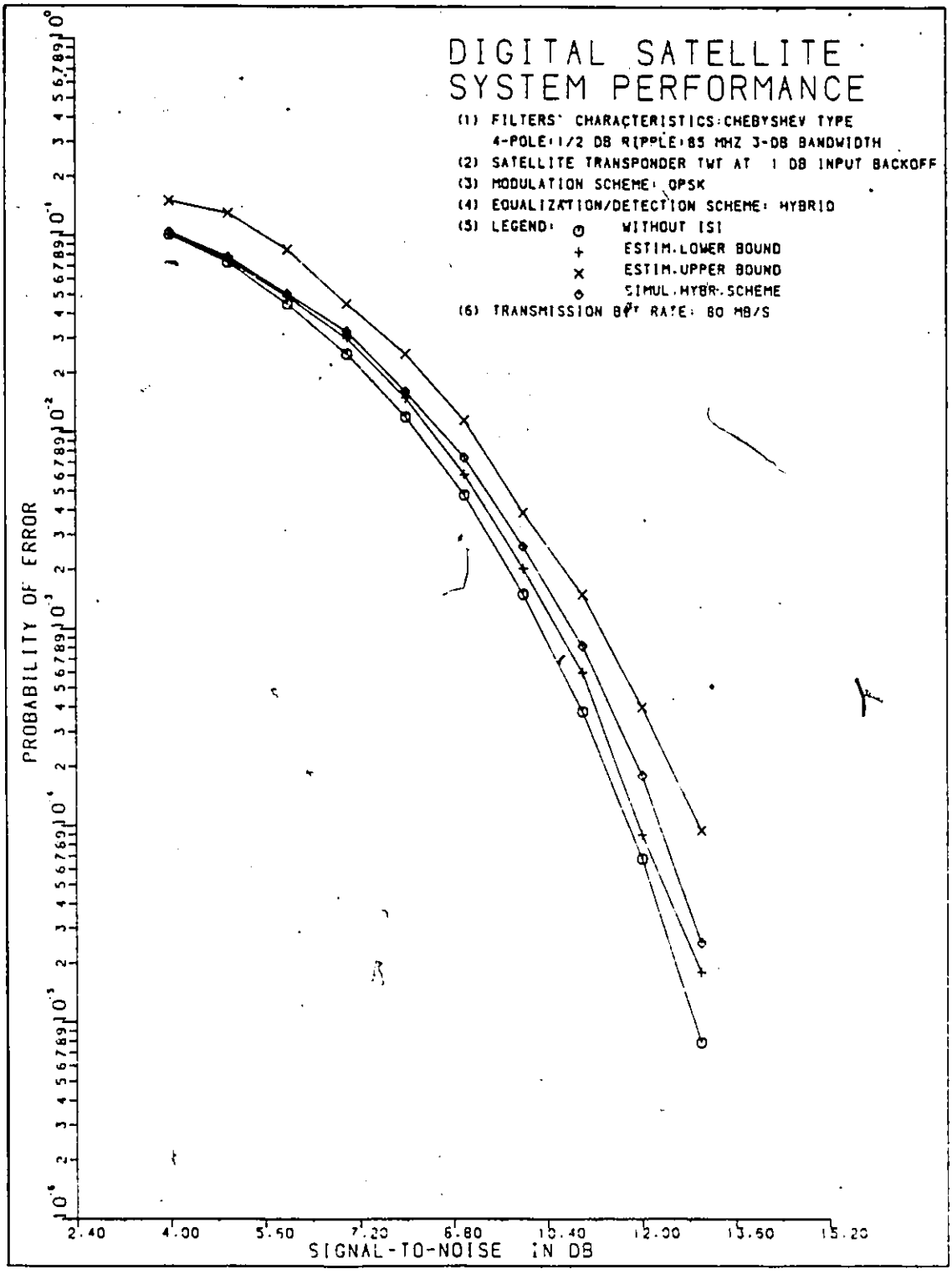

Fig. 5.9 Probability of error vs. signal-to-noise ratio (see legend above)

algorithm since, in essence, we consider the hybrid structure as being a maximum likelihood estimator for an equalized channel. In addition, this bound is considered [32] as the lower bound for any receiver for the particular channel.

To facilitate further comparisons using the previous system configuration as an example, a composite figure is provided. Thus, by superimposing the simulation results of the bit-by-bit decision as well as the estimated and simulated results obtained by using the proposed structure, fig. 5.10 is obtained. Again, the improvement in performance, when using the proposed structure, is readily identified.

To achieve the same order of probability of error, e.g. 10^{-4}, a smaller signal-to-noise ratio is required when the (simulated) hybrid equalizer scheme is used than with the bit detector. Further comparison of these performance characteristics, in Fig. 5.10, indicate a tendency of the hybrid equalization scheme to perform with reduced probability of error, at the higher signal-to-noise ratios, than the bit detector. This observation agrees well with the analytical results expressed in the form of bounds, as shown in Fig. 5.8.

To demonstrate the effectiveness of the hybrid equalization scheme at higher bit rates, further simulation runs were performed. Thus, operating the (simulated) TWT in its nonlinear region and at high transmitting bit-rates, i.e. 120 Mb/s and 140 Mb/s the performance characteristics of fig. 5.11 were

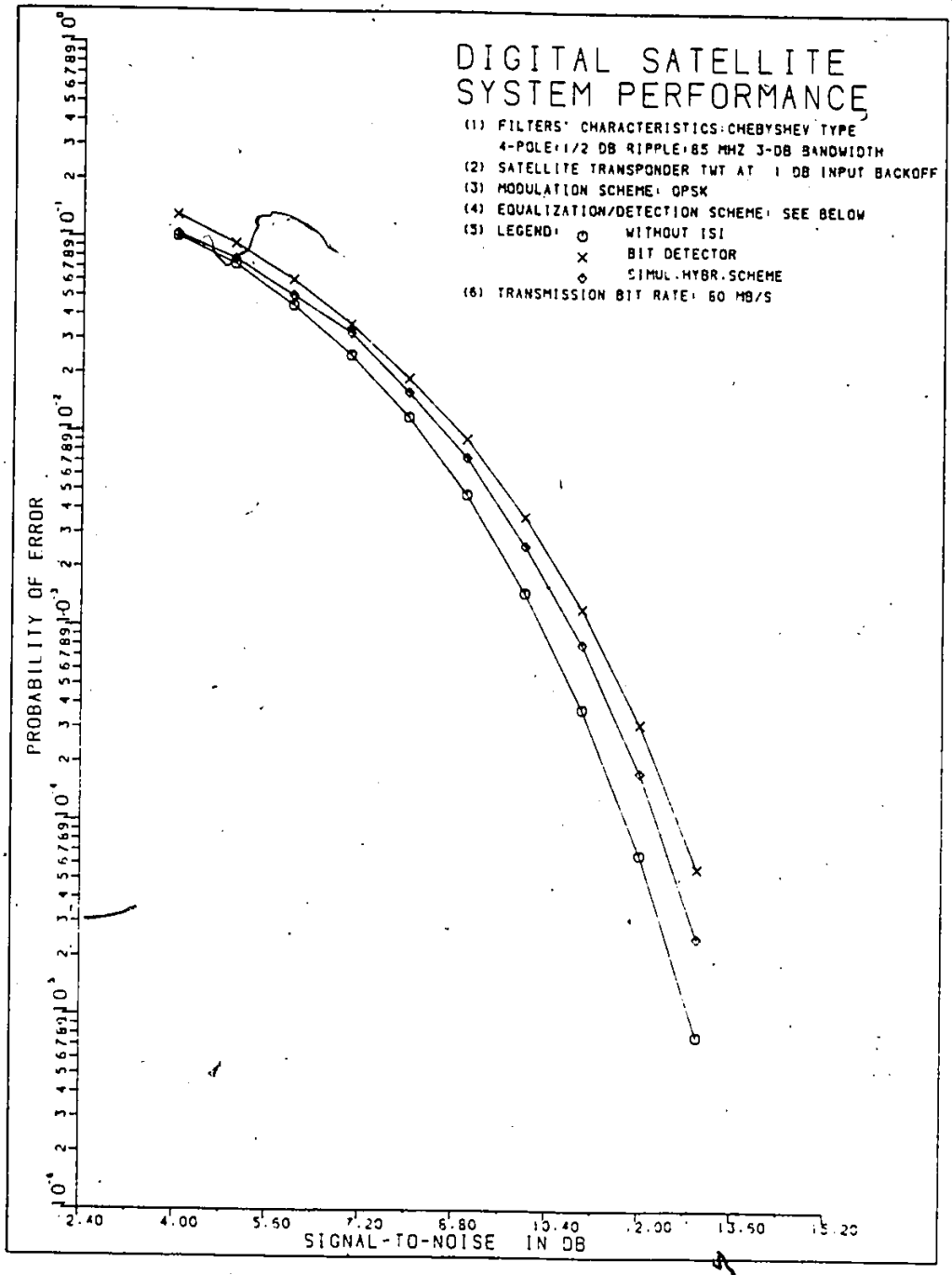

Fig. 5.10 Probability of error vs. signal-to-noise ratio
(see legend above)

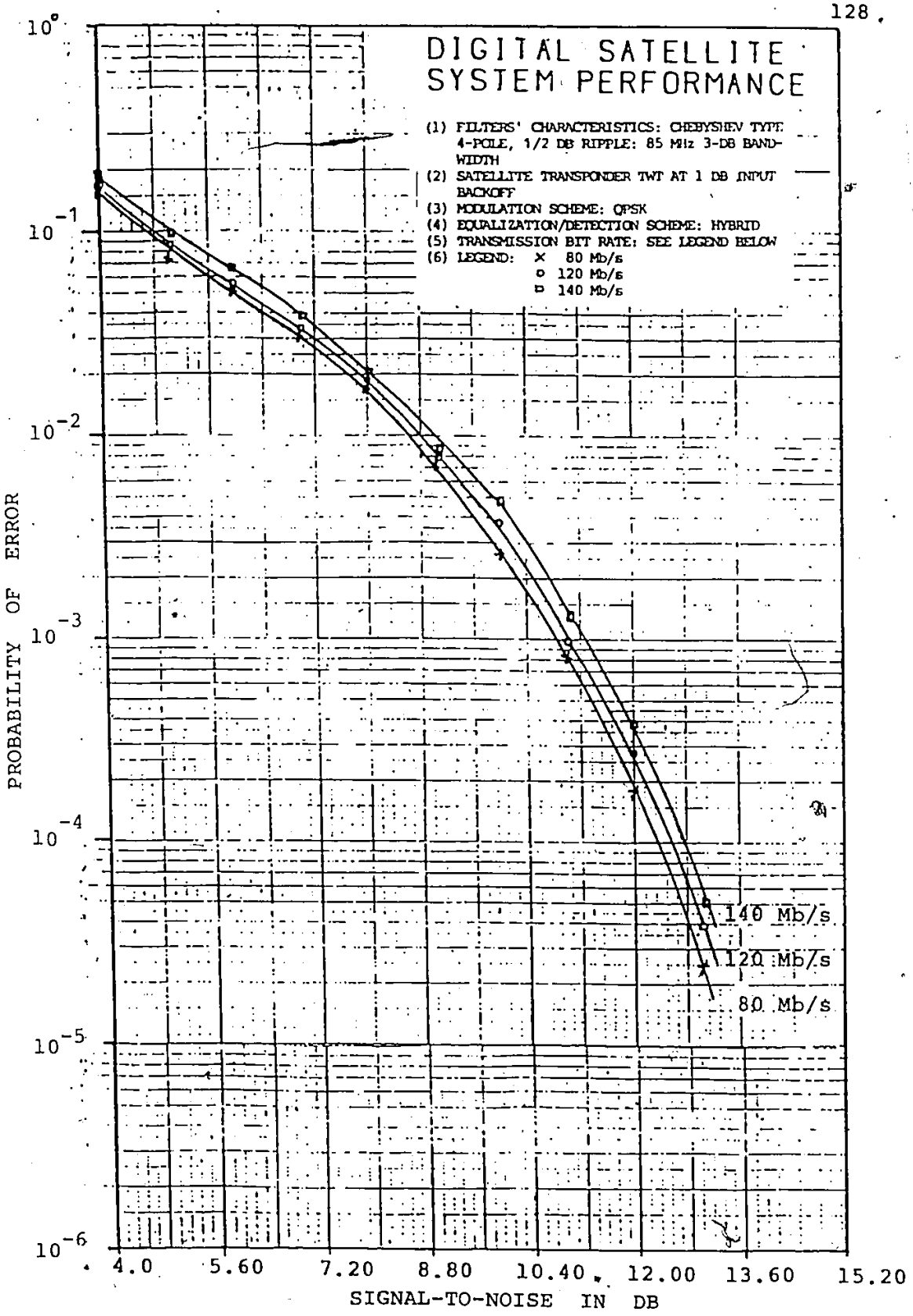

Fig. 5.11 Probability of error vs. signal-to-noise ratio

(see legend above)

obtained: One observes that there is a (slight) increase in the probability of error, with increasing bit rate, as expected. However, one also observes that there is an improvement of the probability of error, when compared with the "bit-detector" results, at the same bit rates. (fig. 5.3).

A typical qualitative indication of the performance of the simulated hybrid equalizer is provided by means of an eye diagram, as shown in Fig. 5.12: In this example, the left-hand side indicates the signal condition when a bit detector is used whereas the right-hand side of the same figure indicates the condition of the same signal when the proposed hybrid equalizer structure is used instead of the bit detector. The improvement, in terms of eye-opening, is evident.

2. DISCUSSION

Data transmission through non-linear satellite channels is affected by intersymbol interference. The nature and causes of this interference have been reviewed. In the case of linear channels, well established equalization methods have been developed to counteract such a phenomenon. However, when non-linear elements are introduced in the signal path, additional intersymbol interference, due to these elements, is introduced, thereby adversely affecting the overall system performance.

The existing equalization methods, as it can be seen from the literature review, have largely been categorized as linear

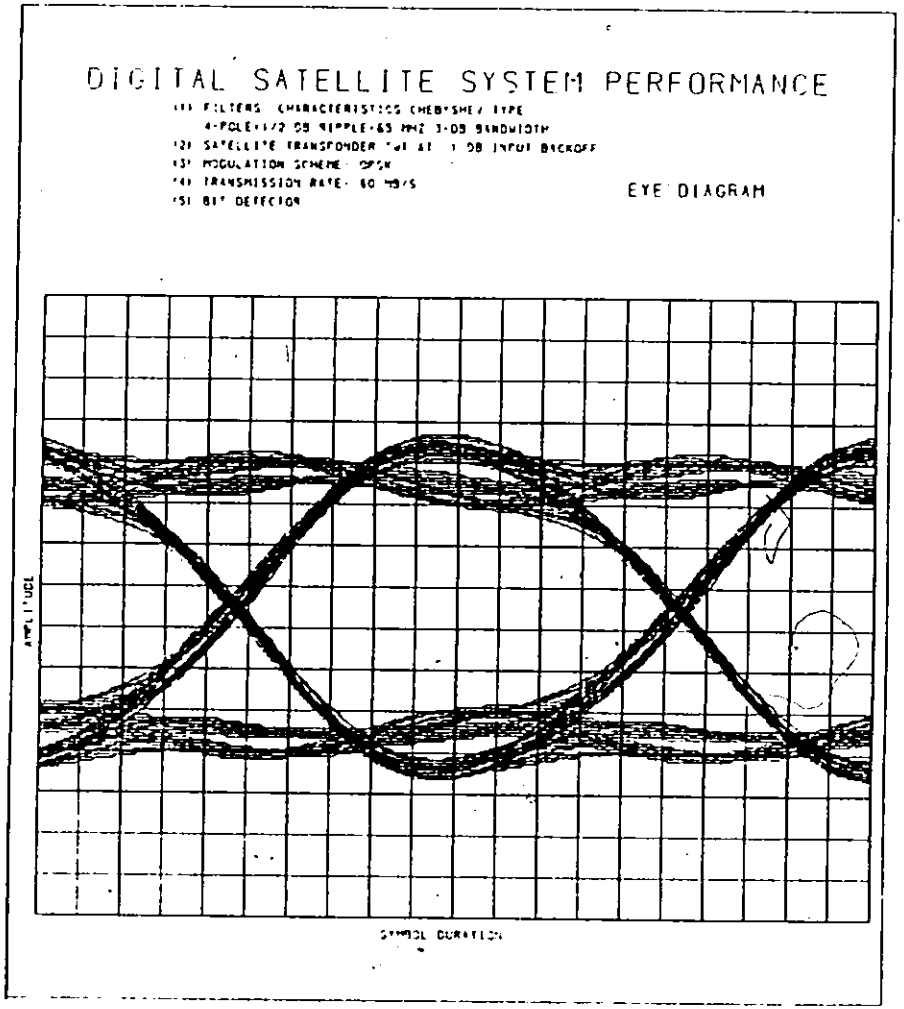

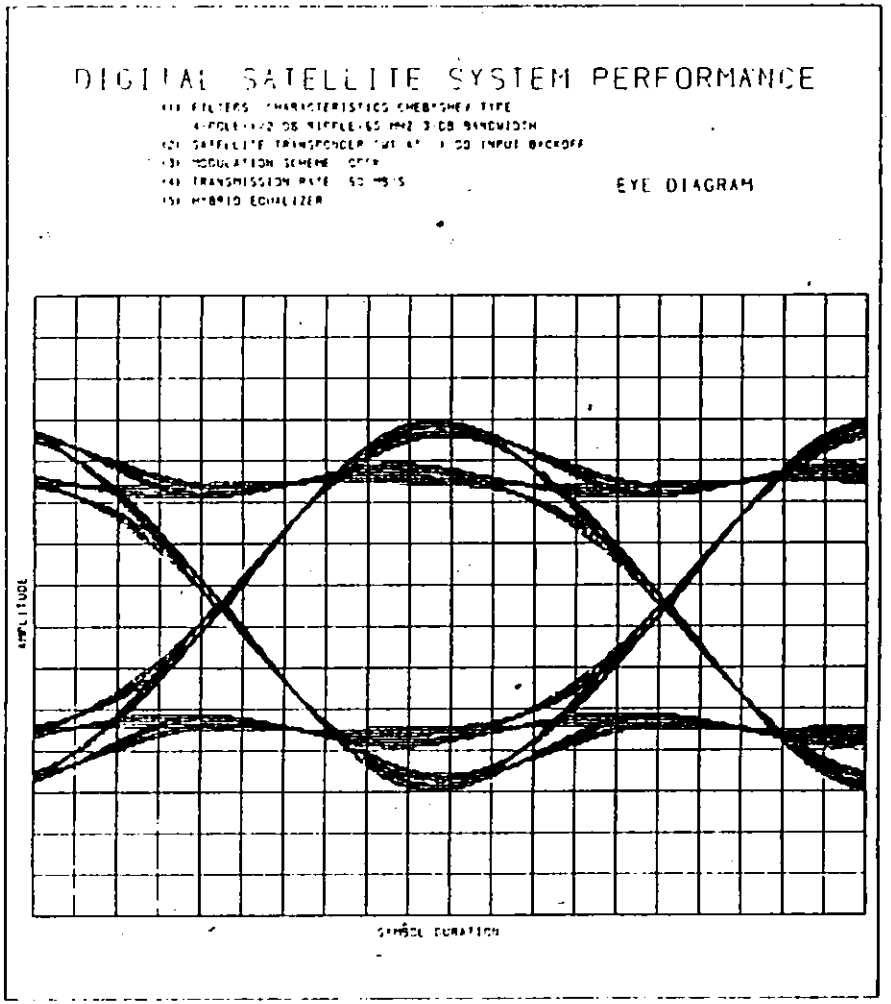

Fig. 5.12 Eye diagrams - 80 Mb/s (see legend above)

and non-linear, depending on the circuit elements they utilize. The effectiveness of some non-linear approaches, such as the decision feedback and maximum likelihood detection, make them quite attractive for consideration as potential solutions to the ISI problem, in the presence of non-linearities, such as those encountered in a satellite channel. These methods have been here, in a relatively detailed manner, presented. Their advantages and disadvantages have also been remarked upon.

It has been shown that, although the maximum likelihood detector, in its complete form, i.e. as presented by Viterbi, is the optimum receiver structure one may aim at. However, due to its complexity, it is practically not feasible, with present time technology. Consequently, efforts towards minimizing this complexity seem to be justified. In such an attempt, a hybrid equalizer structure has been here proposed which consists of two sections: the first one is configured as a decision feedback equalizer; the second one as a maximum likelihood detector. Thus, the received signal sequence is "pre-equalized", with the aid of the decision feedback equalizer section, by removing part of the intersymbol interference. In this manner, a sequence with ISI over a reduced range is presented to the second section, i.e. the maximum likelihood detector. The advantage of this method is that such a signal requires only a reduced state Viterbi algorithm. This, in turn, leads to a reduced complexity equalizer structure.

To study the validity of the proposed concept, a basic transmission system was simulated in a digital computer. A non-linear satellite repeater was also included in the transmission path. The initial detection scheme chosen was of the well-known bit-by-bit approach. In this manner a reference is established which is utilized later-on for comparison purposes. The results obtained agree well, indeed, with those in the literature thus confirming the validity of the simulated system model. In an effort to make the simulated system more versatile and useful, a performance display flexibility, in addition to the filter and TWT characteristics changing capability, has been developed and built-in. Thus, one may choose either a quantitative or a qualitative display.

The performance of the proposed hybrid equalisation scheme has been, first analytically, evaluated by computing approximate upper and lower bounds. The equalizer has been subsequently simulated and integrated in the (also simulated) basic satellite transmission system, and its performance, numerically, evaluated. It is shown that, a good agreement between the analytical and simulated results is achieved. Furthermore, by studying the (hybrid equalizer) performance curves, one may observe a trend towards reduced probability of error, particularly at the higher signal-to-noise ratios. The improvement achieved is readily identified by comparing these results (fig. 5.11) with those of the bit detector (fig. 5.3).

It may then be concluded that, such hybrid schemes are quite feasible as well as effective, in reducing the effects of intersymbol interference in the presence of non-linearities and at, relatively, high bit-rates. Furthermore, the original complexity of the optimal receiver structures, may be reduced, by considering such hybrid structures. In this manner, a near-optimal configuration is feasible, while retaining most of the performance advantages of the, more complicated, optimal one, i.e. the Viterbi algorithm alone [32, 39, 41, 42, 63, 65]

3. SUGGESTIONS FOR FURTHER RESEARCH

The proliferation of satellite communications systems and the advances made by technology, seem to be a good justification for further examining the concepts presented in this work. One immediate area that comes to mind and which requires investigation, is the detailed study of the ISI problem in the context of the new, higher frequency range TWTs: it would be interesting to investigate the behaviour of the ISI, by considering the non-linearities' effect in the higher frequency band and, of course, at high bit rates. As a logical sequel, further examination of hybrid equalization schemes, such as the proposed one here or, similar with necessary modifications, would also be of interest.

We believe that, careful and parallel study and consider-

ation of various information theoretic and communications concepts, particularly in the area of "equalization" and parameter estimation/detection, as applied to the satellite communications environment, would produce interesting results and solutions to related problems.

The applicability of such hybrid equalization schemes, as here proposed, to other modulation formats (e.g. OPSK, MSK) would also be of some interest. In another attempt, the consideration of an optimizing algorithm for the channel parameter identification, and its incorporation to the proposed hybrid equalizer structure, could be investigated: it would be interesting to see whether any substantial improvement may be achieved, particularly in view of its ensuing implementation complexity. In a similar manner, it would be worthwhile, notwithstanding the difficulties, to study the possibility of some sort of "pre-equalization" of the high bit rate data sequences, on the transponder, with the remaining, "final" equalization, on the earth segment: it might be possible that, for a proper combination of such a scheme, a more economical overall system design will be the end result. In another attempt, the hardware aspects and economics of implementation of the proposed scheme could provide adequate motivation for further work.

REFERENCES

[1] H. Nyquist, "Certain topics in Telegraph Transmission Theory", AIEE, vol. 47, Feb. 1928, pp. 617-644.

[2] W. Bennett and H. Davey, "Data Transmission", McGraw-Hill, 1965.

[3] R. Lucky et al, "Principles of Data Communication", McGraw-Hill, 1968.

[4] J. Wozencraft & I. Jacobs, "Principles of Communications Engineering", J. Wiley, 1965.

[5] J.Jones,"Distortion & Interference Effects on PSK Signals", IEEE Trans.on Comm.Tech.,vol.COM-19,No.2,April 1971,pp.120-132.

[6] D.G. Messerschmitt, "A Geometric Theory of Intersymbol Interference, Part I: Zeroforcing and Decision Feedback Equalization", BSTJ, vol. 52, no. 9, Nov. 73, pp. 1483-1519.

[7] _____, "A Geometric Theory of Intersymbol Interference, Part II:Performance of the Maximum Likelihood Detector", BSTJ, vol. 52, no. 9, Nov. 73, pp. 1521-1539.

[8] M.E. Austin, "Decision-Feedback Equalization for Digital Communication over Dispersive Channels", MIT, Tech. Rep. No. 437, August 1967.

[9] H.E. Kallmann, "Transversal Filters", Proc. IRE, vol. 28, July 1940, pp.302-310.

[10] R.W. Lucky," Automatic Equlization for Digital Communication", BSTJ, vol. 44, no. 4, April 1965.

[11] _____, "Techniques for Adaptive Equalization of Digital Communications Systems", BSTJ, vol. 45, No. 2, Feb. 1966.

[12] R. Gitlin et al, "On the Design of Gradient Algorithms for Digitally Implemented Adaptive Filters," IEEE Trans. on Circuit Theory, vol. CT-20, No. 2, March 1973.

[13] A. Gersho, "Adaptive Equalization of Highly Dispersive Channels for Data Transmission", BSTJ, vol. 18, Jan. 1969.

[14] W. Steenaart, R. Ramachandran, "Optimal Equalization of Discrete Signals Passed Through a Random Channel", IEEE Trans. on Communications, vol. COM-20, N . 5, Oct. 1972.

[15] J.G. Proakis, "Advances in Equalization for Intersymbol Interference", Advances in Communications, Academic Press, 1978, pp. 123-198.

[16] K.H. Mueller, "A New, Fast Converging Mean-Square Algorithm for Adaptive Equalizers with Partial Response Signalling", BSTJ, vol. 54, no. 1, pp. 143-153, Jan. 1975.

[17] K.H. Mueller and D.A. Spaulding, "Cycle Equalization a New Rapidly Converging Equalization Technique for Synchronous Data Communications", BSTJ, vol. 54, No. 2, pp. 369-406, Feb. 1975.

[18] F.R. Magee, Jr., "A Comparison of Compromise Viterbi Algorithm and Standard Equalization Techniques Over Band-Limited Channels", IEEE Trans. on Communications, Vol. COM-23, No. 3, pp. 361-367, March 1975.

[19] M.J. Di Toro, "Communication-in-Time-Frequency Spread Media Using Adaptive Equalization", Proc. of IEEE, Vol. 56, No. 10, Oct. 1968.

[20] P.A. Bello,"Characterization of Randomly Time Variant Linear Channels", IEEE Trans. Commun. Syst., Vol. CS-11, pp. 360-393, Dec. 1963.

[21] F. Assal, "Approach to a Near Optimum Transmitter-Receiver Filter Design for Data Transmission Pulse Shaping Networks", Comsat. Tech. Review, vol. 13, No. 2, Fall 1973.

[22] P. Monsen, "Feedback Equalization for Fading Dispersive Channels", IEEE Transactions on Info. Theory, pp. 56-64, Jan. 1971.

[23] K. Abend and B. Fritchman, "Statistical Detection for Communication Channels with Intersymbol Interference", Proc. of IEEE, Vol. 58, No. 5, May 1970.

[24] R. Price, "Non-Linearly Feedback Equalized PAM vs Capacity for Noisy Filter Channels", Conf. Rec. (IEEE) ICC 72, pp. 22-12 to 22-17.

[25] R.D. Gitlin and E.Y. Ho, "A Null-Zone Decision Feedback equalizer Incorporating Maximum Likelihood Bit Detection", IEEE Trans. on Communications, Vol. COM-23, No. 11, pp. 1243-1250, Nov. 1975.

[26] H.L. Berger and H.B. Poza, "Performance Characterization of High-Data Rate QPSK Channels with Adaptive Equalization", Canad. Con. on Commun. (IEEE), Montreal, Oct. 1976.

[27] D. Falconer et al.,"Echo Cancellation Techniques for Full-Duplex Data Transmission on Two-Wire Lines", Conf. Rec. NTC 75, pp. 8.3-1 to 8.3-7, Dec. 1976.

[28] B. Widrow, J. McCool and M. Ball, "The Complex LMS Algorithm", Proc. of the IEEE, Vol. 63, No. 4, pp. 719-720, April 1974.

[29] Y. Sato, "A Method of Self-Recovering Equalization for Multilevel Amplitude-Modulation Systems", IEEE Trans. on Communications, Vol. COM-23, No. 6, pp. 679-682, June 1975.

[30] D.G. Messerschmitt, "Generalized Partial Response for Equalized Channels with Rational Spectra", IEEE Trans. on Communications, vol. COM-23, No. 11, pp. 1251-1258, Nov. 1975.

[31] P. Butler and A. Cantoni, "Noniterative Automatic Equalization", IEEE Trans. on Communications, vol. COM-23, No. 6, pp. 621-633, June 1975.

[32] G.D. Forney,"Maximum Likelihood Sequence Estimation of Digital Sequences in the Presence of Intersymbol Interference", IEEE Trans. Perform. Theory, vol. IT-18, May 1972, pp. 363-378.

[33] A.J. Viterbi," Error Bounds for Convolutional Codes and an Asymptotically Optimum Decoding Algorithm", IEEE Trans. Inform., Theory, vol. IT-13, Apr. 1967, pp. 260-269.

[34] M. Goutmann," Intersymbol Interference as Natural Code", IEEE Trans. on Comm., Oct. 1972, pp. 1033-1037.

[35] T.J. Klein & J.K. Wolf," On the Use of Channel Introduced Redundancy for Error Correction", IEEE Trans. on Comm. Tech., Vol. COM-19, August 1971, pp. 396-402.

[36] R. Bellman, Dynamic Programming. Princeton Univ. Press, 1957.

[37] H. Kobayashi," Correlative Level Coding and Maximum Likelihood Decoding", IEEE Trans. on Inform. Theory, vol. IT-17, Sept. 1971, pp. 486-594.

[38] _____,"Application of Probabilistic Decoding to Digital Magnetic Recording Systems", IBM J. Res. Develop., vol. 15, Jan. 1971, pp. 64-74.

[39] G. Ungerboeck,"Adaptive Maximum Likelihood Receiver for Carrier-Modulated Data Transmission Systems", IEEE Trans. on Comm., vol. COM-22, No. 5, May 1974, pp. 624-636.

[40] S.H.Qureshi,"An adaptive Decision-feedback receiver using maximum-likelihood sequence estimation",Intern. Conf. on Comms., 1973,pp.14-10 to 14-16

[41] M.Mesiya et al.,"Maximum likelihood sequence estimation of binary sequences transmitted over bandlimited non-linear channels",IEEE Trans. on Comm.,vol. COM-25 No.7, July 1977,pp.633-643

[42] G.Herrmann,"Performance of maximum-likelihood receiver in the non-linear satellite channel", IEEE Trans. on Comm.,vol.COM-26,No.3, March 1978, pp.373-378.

[43] H.Chan et al.,"Comparative evaluation of digital modulation techniques", Mc Master Univ., Report No. CRL-18, 1974.

[44] L.Weinberg,"Network analysis and synthesis", Mc Graw Hill Book Co. Inc., 1962.

[45] K.Feher,"Digital modulation techniques in an interference environment", Don White Consultants, Inc., 1977.

[46] A.Berman and C.Mahle,"Non-linear phase shift in Travelling Wave Tubes as applied to multiple-access communications satellites", IEEE Trans. on Comm.Tech., vol. COM-18, No.1, Feb.1970.

[47] D.Middleton,"Introduction to statistical communication theory", Mc Graw Hill Book Co., New York 1960.

[48] N.Blachman,"Noise and its effect on communication", Mc Graw Hill Book Co., New York 1966.

[49] M.Eric,"Intermodulation analysis of non-linear devices for multiple carrier inputs", CRC Report No.1234,Nov.1972.

[50] A.Papoulis,"Probability,Random variables and stochastic processes", Mc Graw Hill Book Co., 1965.

[51] S.Golomb,"Digital communications with space applications", Prentice Hall, 1964.

[52] J.Salz,"Optimum mean-square Decision feedback equalization", BSTJ, vol.52, No.8, October 1973, pp.1341-1373.

[53] E.Shamash and K.Yao,"On the structure of a linear decision feedback equalizer based on the minimum error probability criterion", Conf. Rec. ICC 74, June 1974,pp.25F-1 to 25F-5.

[54] R.Pulleybank,"A comparison of receivers designed on the basis of minimum mean-squre error and probability of error for channels with Intersymbol Interference and noise", IEEE Trans. on Comm., vol. COM-21, No.12, Dec. 1973, pp. 1434-1438.

[55] D.Duttweiler et al.,"An upper bound on the error probability in Decision feedback equalization", IEEE Trans. on Info. Theory, vol.IT-20, No.4, July 1974, pp.490-497.

[56] C.Helstrom,"Statistical theory of signal detection", Pergamon Press, 1960.

[57] G.D.Forney,"The Viterbi algorithm", Proc. of the IEEE, vol.61, No.3, Mar.1973, pp.268-278.

[58] J.Omura,"On the Viterbi decoding algorithm", IEEE Trans. on Info. Theory, Jan.1969, pp.177-179.

[59] D.Messerschmitt,"Design of a finite impulse response for the Viterbi algorithm and decision feedback equalizer", Conf. Rec. ICC 74, June 1974, pp.37d-1 to 37D-5.

[60] S.Fredricson,"Joint optimization of transmitter and receiver filters in digital PAM-systems with a Viterbi detector", Conf. Rec. ICC 74, June 1974, pp.37C-1 to 37C-5.

[61] _____,"Optimum transmitting filter in digital PAM systems with a Viterbi detector", IEEE Trans. on Info. Theory, vol.IT-20, No.4, July 1974, pp.479-489.

[62] W.Lee and F.S.Hill,Jr.,"A maximum-likelihood sequence estimator with decision-feedback equalization", IEEE Trans. on Comm., vol.COM-25, No.9, Sept.1977,pp. 971- 979.

[63] D.Kazakos,"Computational savings and implementation of maximum likelihood detectors", IEEE Trans. on Info. Theory, vol.IT-24, No.1, Jan.1978, pp.124-126.

[64] G.Ungerboeck,"Nonlinear equalization of binary signals in Gaussian noise", IEEE Trans. on Comm.Tech., vol. COM-19, No.6, Dec. 1971, pp.1128-1137.

[65] A.Viterbi,"Convolutional codes and their performance in communications systems", IEEE Trans. on Comm.Tech., vol. COM-19, October 1971, pp.751-772.

[66] M.G.Stringis,"A solution to the matrix factorization problem", IEEE Trans. on Info.Theory, March 1972, pp.225

[67] J.Fuenzalida et al.,"Time-domain analysis of intermodulation effects caused by non-linear amplifiers", Comsat Tech. Review, vol.3, No.1, Spring 1973, pp.89-141.

[68] J.J. Spilker, Jr., "Digital Communications by Satellite", Prentice Hall, Inc., 1977

APPENDIX I

PROBABILISTIC DEVELOPMENT OF LIKELIHOOD RATIO

The decision statistic for the likelihood ratio Λ_i will be here developed. We have that

$$\Lambda_i = \frac{p[\, z_i | \hat{s}_i = 1 \,]}{p[\, z_i | \hat{s}_i = -1]} \qquad (A\text{-}1)$$

We will analyze the nominator and denominator separately. Using Baye's rule, one may express the a posteriori probability density function as follows:

$$p[\, z_i | \hat{s}_i = 1 \,] = \frac{p[\, z_i, \hat{s}_i = 1 \,]}{p(\, \hat{s}_i = 1)} \qquad (A\text{-}1a)$$

Let the previous symbol transmitted be identified as s_{i-1} . This symbol can either be +1 or -1 . Then, equation (A-1) can be written as

$$p[z_i | \hat{s}_i = 1 \,] = \frac{p[\, z_i, \hat{s}_i = 1, \hat{s}_{i-1} = 1 \,] + p[\, z_i, \hat{s}_i = 1, \hat{s}_{i-1} = -1 \,]}{p(\, \hat{s}_i = 1)} \qquad (A\text{-}2)$$

Consider the first term of the RHS of equation (A-2) . It can be written as follows

$$p[z_i, \hat{s}_i = 1, \hat{s}_{i-1} = 1] = p[z_i | z_{i-1}, \hat{s}_i = 1, \hat{s}_{i-1} = 1]\; p[z_{i-1}, \hat{s}_i = 1, \hat{s}_{i-1} = 1] \qquad (A\text{-}3)$$

We stipulated, however, that the signals are independent. Therefore, considering the first factor of equation (A-3), z_i would also be independent from z_{i-1} . This fact simplifies this equation which now may be written as

$$p[\, z_i | z_{i-1},\ \hat{s}_i=1,\ \hat{s}_{i-1}=1\,] = p[\, z_i | \hat{s}_i=1,\ \hat{s}_{i-1}=1\,] \qquad (A\text{-}4)$$

Similarly, the second term of equation (A-3), based on the independence of z_{i-1} from s_i , may be written as

$$p[\, z_{i-1},\ \hat{s}_i=1,\ \hat{s}_{i-1}=1\,] = \frac{p[\, z_{i-1},\ \hat{s}_{i-1}=1\,]}{2}$$

$$= \frac{p[\, z_{i-1} | \hat{s}_{i-1}=1\,] P[\, \hat{s}_{i-1}=1\,]}{2} \qquad (A\text{-}5)$$

Substituting, we get

$$p[\, z_i,\ \hat{s}_i=1,\ \hat{s}_{i-1}=1\,] = \frac{1}{4} p[\, z_i | \hat{s}_i=1\ ,\ \hat{s}_{i-1}=1\,] p[\, z_{i-1} | \hat{s}_{i-1}=1\,] \qquad (A\text{-}6)$$

In analogous manner, we develop the second term of the RHS of equation (A-2) and obtain

$$p[\, z_i,\ \hat{s}_i=1,\ \hat{s}_{i-1}=-1\,] = \frac{1}{4} p[\, z_i | \hat{s}_i=1,\ \hat{s}_{i-1}=-1] p[\, z_{i-1} | \hat{s}_{i-1}=-1\,] \qquad (A\text{-}7)$$

By direct substitution of equations (A-6) avd (A-7) into equation

(A-2), we get

$$p[\, z_i|\hat{s}_i=1 \,] = \frac{p[\, z_i|\hat{s}_i=1,\hat{s}_{i-1}=1\,]p[\, z_{i-1}|\hat{s}_{i-1}=1\,]}{2} +$$

$$+ \frac{p[\, z_i|\hat{s}_i=1,\hat{s}_{i-1}=-1\,]p[\, z_{i-1}|\hat{s}_{i-1}=-1\,]}{2} \qquad \text{(A-8)}$$

The analysis of the denominator of equation (A-1) is performed in a similar way to that of nominator. The final denominator expression will then be written as

$$p[\, z_i|\hat{s}_i=-1\,] = \frac{p[\, z_i|\hat{s}_i=-1,\ \hat{s}_{i-1}=1\,]p[\, z_{i-1}|\hat{s}_{i-1}=1\,]}{2} +$$

$$+ \frac{p[\, z_i|\hat{s}_i=-1,\ \hat{s}_{i-1}=-1]p[\, z_{i-1}|\hat{s}_{i-1}=-1\,]}{2} \qquad \text{(A-9)}$$

The likelihood ratio may, consequently, be obtained by dividing the two final expressions. Thus,

$$\Lambda_i = \frac{p[\, z_i|\hat{s}_i=1,\ \hat{s}_{i-1}=1\,]p[\, z_{i-1}|\hat{s}_{i-1}=1\,]}{p[\, z_i|\hat{s}_i=-1,\ \hat{s}_{i-1}=1\,]p[\, z_{i-1}|\hat{s}_{i-1}=1\,]} +$$

$$+ \frac{p[\, z_i|\hat{s}_i=1,\hat{s}_{i-1}=-1\,]p[\, z_{i-1}|\hat{s}_{i-1}=-1\,]}{p[\, z_i|\hat{s}_i=-1,\hat{s}_{i-1}=-1\,]p[\, z_{i-1}|\hat{s}_{i-1}=-1\,]} \qquad \text{(A-10)}$$

By further using notation and derivations developed in chapter 2, one may evaluate equation (A-10) in terms of probability density function over the entire signal sequence for the given basis q. Thus, considering the output sequence vector Z_k and the fact that the noise samples N_k are also assumed to be independent and of normal distribution, in the general case, equation (A-10) may be written in the following form

$$P[\, z_i | \hat{s}_i \,] = \frac{1}{\sqrt{2\pi\sigma}} \exp\left\{ - \frac{1}{2\sigma^2} \sum_{k=1}^{i} \left|\left| z_k - \sum_{q=0}^{n} G_q^T S_{k-q} \right|\right|^2 \right\} \quad (A\text{-}11)$$

where

$$\frac{1}{\sqrt{2\pi\sigma}} = K \text{ is a normalizing constant}$$

APPENDIX II

SIMULATION PROGRAMS

The listings of the computer programs used in this study are included in this appendix.

The programs are written in FORTRAN IV language. To facilitate the use of these programs, additional information is to be found in chapter 4. It must be noted that, where applicable for standard operations, such as the Fast-Fourier transforms and the random number generator, the already available at the computing centre, IMSL subroutine package was used.

To further facilitate the understanding of the logical process of the main simulation program, reference to the system flowchart (chapter 4) is recommended.

```
C       PROGRAM QPSK(INPUT,OUTPUT)
        DIMENSION NX(11),NY(11),NRX(11),NRY(11),DATA(512),DATA1(512)
        DIMENSION TATA1(512)
        DIMENSION C(15)
        DIMENSION TF(512),TFTX(512),TFR(512),PE(25),PEI(25),SNRDB(25)
        LDIM=512
        NN=LDIM/2
        DATA NTOTAL,NERROR,LOOP,II,IK/0,0,0,0,0/
        DATA NY(1),NY(2),NY(3),NY(4),NY(5),NY(6),NY(7)/-1,-1,1,1,1,1,-1/
        DATA JLAST,JTAP,LLTNOM,FBANDW/7,1,50,85./
C
        PRINT 1
      1 FORMAT(1H1,29H SIMULATION OF COHERENT 4-PSK)
        PRINT 2
      2 FORMAT(49H REQUEST(BIRATE,AVAMP,TWTIN,TWTOUT,PSHIFT,LSAMPL)/,
     *31H FORMAT(F6.2,1X,F9.6,1X,F6.3,1X,F6.3,1X,F9.6,1X,I2)/)
        READ 33,BIRATE,AVAMP,TWTIN,TWTOUT,PSHIFT,LSAMPL
     33     FORMAT(F6.2,1X,F9.6,1X,F6.3,1X,F6.3,1X,F8.6,1X,I2)
        READ 34,FBW1,FBW2,KNK,KC
     34 FORMAT(F6.2,1X,F6.2,1X,I2,1X,I2)
        READ 35,(C(IK),IK=1,KC)
     35 FORMAT(5(F8.5,1X))
        DO 306 IK=1,KC
        PRINT 305,C(IK)
    305 FORMAT(5X,F10.4)
    306 CONTINUE
        AVAMP=SQRT(2.)
        FNORMI=TWTIN/AVAMP
        FNORMO=TWTOUT/AVAMP
C       PSHIFT=0.
        QFBW=5.
        QBRATE=10.
        II=0
        IK=0
        DO 107 KM=1,KNK
        VAL=60.
        PRINT 20,BIRATE,AVAMP,TWTIN,TWTOUT,PSHIFT,LSAMPL
     20 FORMAT(1X,F6.2,5X,F9.6,5X,F6.3,5X,F6.3,5X,F8.6,7X,I2,/)
C
        DO 4 I=1,JLAST
        NX(I)=-1
        NRY(I)=NY(I)
      4 NRX(I)=-1
C
C
        NSNR=11
        QSNR=1.
        QSNRDB=0.
        DO 5 I=1,NSNR
        PE(I)=0.
        PEI(I)=0.
        SNRDB(I)=4.+QSNRDB
        QSNRDB=QSNRDB+QSNR
      5 CONTINUE
C
        CALL CALCON(LSAMPL,LLTNOM,KKK,LLT,NSYMB,JLAST,LOOPM,LDIM,BIRATE,
     *SBANDW)
        CALL QF4PS(SBANDW,FBW1,TFTX,LDIM,KC,C)
        CALL QF4PS(SBANDW,FBW2,TFR,LDIM,KC,C)
        CALL HHGG(TFR,FNOISE,LSAMPL,LDIM)

        CALL BISINC(DATA,TFTX,TFR,LSAMPL,NSTART,LSTART,LDIM)
        CALL LOAD4(DATA,KKK,LSAMPL,NX,NY,II,JLAST,JTAP,LDIM)
        CALL FILTER(DATA,TFTX,NN,LDIM)
        CALL LOAD4(DATA1,KKK,LSAMPL,NX,NY,II,JLAST,JTAP,LDIM)
        CALL FILTER(DATA1,TFTX,NN,LDIM)
        CALL ADTAIL(DATA,DATA1,LLT,LDIM)
        CALL TWTI(DATA,LSAMPL,NSTART,KKK,FNORMI,FNORMO,LDIM)
        CALL FILTER(DATA,TFR,NN,LDIM)
C
   50   CONTINUE
C
        DO 12 I=1,LDIM
        TATA1(I)=DATA(I)
   12   DATA(I)=DATA1(I)
```

```
C
      CALL LOAD4(DATA1,KKK,LSAMPL,NX,NY,II,JLAST,JTAP,LDIM)
      CALL FILTER(DATA1,TFTX,NN,LDIM)
      CALL ADTAIL(DATA,DATA1,LLT,LDIM)
      CALL TWT1(DATA,LSAMPL,NSTART,KKK,FNORMI,FNORMQ,LDIM)
      CALL FILTER(DATA,TFR,NN,LDIM)
      CALL ADTAIL(TATA1,DATA,LLT,LDIM)
      CALL DECOD4(TATA1,NRX,NRY,PE,PEI,KKK,LSAMPL,LSTART,NSNR,NERRCR,
     *SNRDB,IK,NTOTAL,FNOISE,LOOP,JLAST,JTAP,NSYME,FSHIFT)
      IF (LOOP.GT.LOOPM)GO TO 100
      GO TO 50
  100 CONTINUE
      WRITE(11,99)(SNRDB(I),I=1,14),(PEI(J),J=1,14)
   99 FORMAT(25A4)
      IF(KM.NE.1)GO TO 250
      CALL PLOTS(25.0,27.0)
      CALL PECT(4.5,0.0,20.7,20.0,0.0,3)
      CALL PLOT(6.0,1.0,-3)
      CALL SCALE(SNRDB,16.0,11,1)
      CALL AXIS(0.0,0.0,22HSIGNAL-TO-NOISE  IN DB,-22,16.0,
     10.0,SNRDB(12),SNRDB(13))
      CALL SCALG(PEI,25.0,11,1)
      CALL LGAXS(0.0,0.0,20HPROBABILITY OF ERROR,20,25.,90.0,
     1PEI(12),PEI(13))
  250 CALL PLOT(0.0,25.0,3)
      CALL LGLIN(SNRDB,PEI,11,1,0,0,1)
      VAL=VAL+(KM-1)*20.
      CALL WHERE(RXPAGE,RYPAGE,RFACT)
      CALL NUMBER(RXPAGE,RYPAGE,0.3,VAL,0.0,-1)
      CALL SYMBOL(999.,999.,0.3,5H MB/S,0.0,5)
      BIRATE=BIRATE+DERATE
      NTOTAL=0
      NERROR=0
      LOOP=0
      II=0
      IK=0
  107 CONTINUE
      CALL SYMBOL(8.0,24.5,0.5,17HDIGITAL SATELLITE,0.0,17)
      CALL SYMBOL(8.0,23.75,0.5,18HSYSTEM PERFORMANCE,0.0,18)
      CALL SYMBOL(8.1,23.20,0.2,
     143H(1) FILTERS' CHARACTERISTICS:CHEBYSHEV TYPE,0.0,43)
      CALL SYMBOL(8.1,22.75,0.2,
     146H    4-POLE;1/2 DB RIPPLE;65 MHZ 3-DB BANDWIDTH,0.0,46)
      CALL SYMBOL(8.1,22.30,0.2,
     152H(2) SATELLITE TRANSPONDER TWT AT  1 DB INPUT BACKOFF,0.0,52)
C     CALL SYMBOL(8.1,22.30,0.2,
C    127H(2) WITHOUT NON-LINEARITIES,0.0,27)
      CALL SYMBOL(8.1,21.85,0.2,27H(3) MODULATION SCHEME: QPSK,
     10.0,27)
      CALL SYMBOL(8.1,21.40,0.2,16H(4) BIT DETECTOR,0.0,16)
      CALL PLOT(0.0,0.0,999)
      STOP
      END
```

```
C EYE DIAGRAM OF 4  CPSK
      DIMENSION ANIX(512),BNIY(512)
      DIMENSION NX(11),NY(11),NRX(11),NRY(11),DATA(512),DATA1(512)
      DIMENSION TATA1(512)
      DIMENSION C(15)
      DIMENSION TF(512),TFTX(512),TFR(512),PE(25),PEI(25),SNRDB(25)
      KL=1
      LDIM=512
      NN=LDIM/2
      DATA NTOTAL,NERROR,LOOP,II,IK/0,0,0,0,0/
      DATA NY(1),NY(2),NY(3),NY(4),NY(5),NY(6),NY(7)/-1,-1,1,1,1,1,-1/
      DATA JLAST,JTAP,LLTNOM,FBANDW/7,1,50,85./
      PRINT 22
   22 FORMAT (1H1)
      PRINT 1
    1 FORMAT(22H EYE DIAGRAM OF 4-CPSK)
      READ 3,BIRATE,AVAMP,TWTIN,TWTOUT,PSHIFT,LSAMPL
    3 FORMAT(F6.2,1X,F9.6,1X,F6.3,1X,F6.3,1X,F8.6,1X,I2)
      READ 34,FBW1,FBW2,KNK,KO
   34 FORMAT(F6.2,1X,F6.2,1X,I2,1X,I2)
      READ 35,(C(IK),IK=1,KO)
   35 FORMAT(5(F8.5,1X))
      READ 31,INDEXC,IOPT,SCALA
   31 FORMAT (I1,1X,I1,1X,F5.2)
      PRINT 30,INDEXC,IOPT,SCALA
   30 FORMAT(/5X,'INDEXC=',I1,3X,'IOPT=',I1,3X,'SCALA=',F5.2/)
      DO 4 I=1,JLAST
      NX(I)=-1
      NRY(I)=NY(I)
    4 NRX(I)=-1
      FNORMI=TWTIN/AVAMP
      FNORMO=TWTOUT/SQRT(2.)
      PRINT3,BIRATE,AVAMP,TWTIN,TWTOUT,PSHIFT,LSAMPL
      CALL CALCON(LSAMPL,LLTNOM,KKK,LLT,NSYMB,JLAST,LOOPM,LDIM,BIRATE,
     *SBANDW)
      CALL CF4PS(SBANDW,FBW1,TFTX,LDIM,KO,C)
      CALL CF4PS(SBANDW,FBW2,TFR,LDIM,KO,C)
      CALL HHGG(TFR,PNOISE,LSAMPL,LDIM)
      CALL BISINC(DATA,TFTX,TFR,LSAMPL,NSTART,LSTART,LDIM)
      CALL LOAD4(DATA,KKK,LSAMPL,NX,NY,II,JLAST,JTAP,LDIM)
      CALL FILTER(DATA,TFTX,NN,LDIM)
      CALL LOAD4(DATA1,KKK,LSAMPL,NX,NY,II,JLAST,JTAP,LDIM)
      CALL FILTER(DATA1,TFTX,NN,LDIM)
      CALL ADTAIL(DATA,DATA1,LLT,LDIM)
      CALL TWT1(DATA,LSAMPL,NSTART,KKK,FNORMI,FNORMO,LDIM)
      CALL FILTER(DATA,TFR,NN,LDIM)
   50 CONTINUE
      DO 12 I=1,LDIM
      TATA1(I)=DATA(I)
   12 DATA(I)=DATA1(I)
      CALL LOAD4(DATA1,KKK,LSAMPL,NX,NY,II,JLAST,JTAP,LDIM)
      CALL FILTER(DATA1,TFTX,NN,LDIM)
      CALL ADTAIL(DATA,DATA1,LLT,LDIM)
      CALL TWT1(DATA,LSAMPL,NSTART,KKK,FNORMI,FNORMO,LDIM)
      CALL FILTER(DATA,TFR,NN,LDIM)
      CALL ADTAIL(TATA1,DATA,LLT,LDIM)
      IF (LOOP.EQ.0) GO TO 33
      COSPS=COS(PSHIFT)
      SINPS=SIN(PSHIFT)
      DO 80 M=1,LDIM,2
      XB=TATA1(M)*COSPS+TATA1(M+1)*SINPS
      YB=TATA1(M+1)*COSPS-TATA1(M)*SINPS
      TATA1(M)=XB
   80 TATA1(M+1)=YB
      CALL DWEYE1(SCALA,TATA1,KKK,LSTART,LSAMPL,INDEXC,IOPT,KL)
   33 LOOP=LOOP+1
      IF(LOOP.GT.LOOPM) GO TO 100
      GO TO 50
  100 CALL PLOT(0.0,0.0,999)
      STOP
      END
```

```
      SUBROUTINE CFW(FBW,SEANCW,FBANCW,LCDIM,KC)
      DIMENSION C(15),WW(17),TF(512)
      JJ=KC
      NH=LCDIM/2
      NO=LCDIM/4
      CW=SEANCW/FLOAT(NH)/FBANCW**2.
      DO 1 I=2,NO
      W=DW*FLOAT(I-1)
      WS=-W*W
      SW=1.
      DO 2 J=1,JJ,2
      J1=J+1
      WW(J)=SW
      WW(J1)=SW*W
    2 SW=SW*WS
      SX=0.
      DO 3 J=1,JJ,2
    3 SX=SX+C(J)*WW(J)
      SY=0.
      DO 4 J=2,JJ,2
    4 SY=SY+C(J)*WW(J)
      SS=SX*SX+SY*SY
      SS=SS/C(1)
      X=SX/SS
      Y=SY/SS
      I2=I*2
      I1=I2-1
      TF(I1)=X
      TF(I2)=-Y
      I2=2*(NH-I+2)
      I1=I2-1
      TF(I1)=X
      TF(I2)=Y
    1 CONTINUE
      TF(1)=1.
      TF(2)=0.
      TF(NH+1)=0.
      TF(NH+2)=0.
      RETURN
      END
      SUBROUTINE SLOPE(X,Y,SLOPES,N)
C
C     THIS ROUTINE CALCULATES THE SLOPES AS THE AVERAGE OF THE POINTS
C     EITHER SIDE
C
      DIMENSION SLOPES(512),X(512),Y(512)
      N1=N-1
      DO 10 J=2,N1
      I=J-1
      K=J+1
      SLOPES(J)=(Y(K)-Y(I))/(X(K)-X(I))
   10 CONTINUE
      RETURN
      END

      SUBROUTINE QUAD(A,B,C,X1,Y1,X2,Y2,S2)
      DELX=X1-X2
      A=(Y1-Y2-S2*DELX)/(DELX**2)
      B=S2-2*A*X2
      C=Y1-B*X1-A*X1**2
      RETURN
      END

      SUBROUTINE CALCCN(LSAMPL,LLTNCM,KKK,LLT,NSYMB,JLAST,
     1LCCPM,LCDIM,BIRATE,SEANCW)
      SEANCW=BIRATE*LSAMPL
      LL=LCDIM/2
      AKK=(LL-LLTNCM)/LSAMPL
      KKK=IFIX(AKK)
      LLT=LL-(KKK*LSAMPL)
      NSYMB=2**JLAST-1
      SYMB=NSYMB
      SKK=KKK
      PCCL=SYMB/SKK
      LCCPM=IFIX(PCCL)
      X=LCCPM
      IF(X.LT.PCCL)LCCPM=LCCPM+1
      RETURN
      END
```

```
      SUBROUTINE TWTI(DATA,LSAMPL,NSTART,KKK,FNORMI,FNORMC,LDIM)
      DIMENSION DATA(512),ZP(9),ZQ(9)
      DATA ZP(1),ZP(2),ZP(3),ZP(4),ZP(5),ZP(6),ZP(7),ZP(8),ZP(9)
     1/1.76245,-1.53871E-1,1.35508E-2,-9.07704E-4,4.2041E-5,
     2-1.28062E-6,2.41583E-8,-2.5508E-10,1.14074E-12/
      DATA ZQ(1),ZQ(2),ZQ(3),ZQ(4),ZQ(5),ZQ(6),ZQ(7),ZQ(8),ZQ(9)
     1/-1.99286E-3,1.81398E-1,-3.43698E-2,3.37647E-3,-1.93769E-4,
     26.67438E-6,-1.35523E-7,1.49262E-9,-6.86514E-12/
      DATA ZPMAX,ZQMAX,VMAX/3.09,1.31,6./
      J2=9
      I1=2*KKK*LSAMPL
C     GO TO 5
C 6   CONTINUE
      DO 120 II=1,I1,2
      I2=II+NSTART-1
      X=DATA(I2)*FNORMI
      Y=DATA(I2+1)*FNORMI
      RR=X*X+Y*Y
      R=SQRT(RR)
      IF(R.GT.VMAX)GO TO 1
      P=ZP(1)
      Q=ZQ(1)
      DO 121 JJ=2,J2
      Q=Q+ZQ(JJ)*RR**(JJ-1)
      P=P+ZP(JJ)*RR**(JJ-1)
  121 CONTINUE
      DATA(II)=(P*X-Q*Y)/FNORMC
      DATA(II+1)=(Q*X+P*Y)/FNORMC
      GO TO 120
    1 DATA(II)=(ZPMAX*X-ZQMAX*Y)/FNORMC/R
      DATA(II+1)=(ZQMAX*X+ZPMAX*Y)/FNORMC/R
  120 CONTINUE
C   5 CONTINUE
C     DO 22 II=1,I1
C     I2=II+NSTART-1
C     DATA(II)=DATA(I2)
C 22  CONTINUE
      I3=I1+1
      DO 122 II=I3,LDIM
      DATA(II)=0.
  122 CONTINUE
      RETURN
      END

      SUBROUTINE ACTAIL(ARRAYA,ARRAYB,LLT,LDIM)
      DIMENSION ARRAYA(512),ARRAYB(512)
      I2=2*LLT
      DO 1 II=1,I2
      IJ=LDIM-I2+II
      ARRAYB(II)=ARRAYB(II)+ARRAYA(IJ)
    1 ARRAYA(IJ)=ARRAYB(II)
      RETURN
      END
```

```
      SUBROUTINE HHGG(TF,FNOISE,LSAMPL,LDIM)
      DIMENSION TF(512)
      LL=LDIM/2
      SAMPLE=LSAMPL
      SUM=SAMPLE**2
      ANG=3.141593/LL
      DO 1 L=2,LL
      LX=2*L-1
      LY=2*L
      HH=TF(LX)**2+TF(LY)**2
      ANGLE=ANG*FLOAT(L-1)
      ANGLES=ANGLE*SAMPLE
      GG=(SIN(ANGLES)/SIN(ANGLE))**2
      SUM=SUM+HH*GG
    1 CONTINUE
      SHHGG=SUM/SAMPLE**2
      FNOISE=SHHGG*SAMPLE/LL
      RETURN
      END

      SUBROUTINE FILTER(SIGNAL,TF,N,LDIM)
C
C     THIS SUBROUTINE PERFORMS THE OPERATION OF FOURIER TRANSFORMING
C     THE SIGNAL ARRAY SIGNAL INTO FREQUENCY DOMAIN AND MULTIPLYING IT
C     WITH THE FILTER TRANSFER FUNCTION TF. THE RESULT IS STORED
C     IN THE ARRAY SIGNAL.
C
      DIMENSION SIGNAL(1024),TF(1024)
      DIMENSION IWK(9)
      COMPLEX A(512)
C
      CALL CONJUG(A,SIGNAL,N,1.)
C
      CALL BITREV(A,N)
C
      CALL FFT2RV(A,E,IWK)
C
      CALL NONCOM(A,SIGNAL,N)
      CALL CONJUG(A,SIGNAL,N,-1.)
      CALL NONCOM(A,SIGNAL,N)
C
      DO 1 II=1,LDIM,2
           X=SIGNAL(II)
           Y=SIGNAL(II+1)
           SIGNAL(II)=TF(II)*X - TF(II+1)*Y
           SIGNAL(II+1)=TF(II+1)*X + TF(II)*Y
    1 CONTINUE
C
      CALL CONJUG(A,SIGNAL,N,1.)
C
      CALL BITREV(A,N)
C
      CALL FFT2RV(A,E,IWK)
C
      CALL NONCOM(A,SIGNAL,N)
C
      CALL CONJUG(A,SIGNAL,N,-1.)
      CALL NONCOM(A,SIGNAL,N)
C
      DO 11 I=1,LDIM
           SIGNAL(I)=SIGNAL(I)/FLOAT(N)
   11 CONTINUE
C
      RETURN
      END


      SUBROUTINE CONJUG(A,SIGNAL,N,R)
      DIMENSION SIGNAL(1024),XR(512),XI(512)
      COMPLEX A(512)
      DO 11 I=1,N
           II=I*2
           IR=II-1
           XR(I)=SIGNAL(IR)
           XI(I)=SIGNAL(II)*R
           A(I)=CMPLX(XR(I),XI(I))
   11 CONTINUE
      RETURN
      END
```

```
      SUBROUTINE ACNCON(A,SIGNAL,N)
      DIMENSION A(1024),SIGNAL(1024)
      COMPLEX A
      DO 11 I=1,N
           II=I*2
           IR=II-1
           SIGNAL(IR)=REAL(A(I))
           SIGNAL(II)=AIMAG(A(I))
11    CONTINUE
      RETURN
      END
```

```
      SUBROUTINE BITREV(SIGNAL,LDIM)
      DIMENSION SIGNAL(1024),INDEX(512),Y(512)
      COMPLEX SIGNAL,Y
      INDEX(1)=1
      INDEX(2)=1+LDIM/2
      J=2
      IDIV=1
20    CONTINUE
      IDIV=IDIV*2
      INCR=LDIM/IDIV
      IF(INCR .EQ. 1) GO TO 50
      K=1
      DO 10 I=1,LDIM,INCR
           J=J+1
           INDEX(J)=INDEX(K)+INCR/2
           K=K+1
10    CONTINUE
      GO TO 20
50    CONTINUE
      DO 100 I=1,LDIM
           Y(I)=SIGNAL(I)
100   CONTINUE
      DO 1000 I=1,LDIM
           K=INDEX(I)
           SIGNAL(I)=Y(K)
1000  CONTINUE
      RETURN
      END
```

```
      SUBROUTINE CUBIC(A,B,C,D,X1,Y1,S1,X2,Y2,S2)
C
C     FITS A CUBIC TO 2 POINTS WHICH HAVE THEIR SLOPES SPECIFIED
C
      H=X2-X1
      T1=((Y2-Y1)/H-S1)/H
      T2=(S2-S1)/H
      A=(T2-2*T1)/H
      B=3.*T1-T2
      C=S1
      D=Y1
      RETURN
      END
```

```
      SUBROUTINE DECOD4(DATA,NRX,NRY,PE,PEI,KKK,LSAMPL,LSTART,NSNR,
     *NERROR,SNRDB,I,NTOTAL,ENOISE,LOOP,JLAST,JTAP,NSYMB,PSHIFT)
      DIMENSION DATA(512),NRX(11),NRY(11),PE(25),PEI(25),SNRDB(25)
      COSPS=COS(PSHIFT)
      SINPS=SIN(PSHIFT)
      RT2=1.
C
      DO 1 K=1,KKK
C
C     REGENERATING THE TRANSMITTED SYMBOLS
C
      IF(I.EQ.JLAST) I=0
      I=I+1
      J=I-JTAP
      IF(I.LE.JTAP) J=J+JLAST
      IX=NRX(J)*NRX(I)
      IY=NRY(J)*NRY(I)
      NRX(I)=IX
      NRY(I)=IY
C
C     FIRST LOOP SYMBOLS ARE NOT PROCESSED
C
      IF(LOOP.EQ.0) GO TO 1
C
C     DECODING
C
      J1=LSTART+2*LSAMPL*(K-1)
      J2=LSTART+2*(LSAMPL*K-1)
      AMPLIX=0.
      AMPLIY=0.
C
C     AVERAGED SYMBOL AMPLITUDE
C
      DO 2 J3=J1,J2,2
      AMPLIX=AMPLIX+DATA(J3)
    2 AMPLIY=AMPLIY+DATA(J3+1)
      AMPLIX=AMPLIX/FLOAT(LSAMPL)
      AMPLIY=AMPLIY/FLOAT(LSAMPL)
      AXBAR=AMPLIX*COSPS+AMPLIY*SINPS
      AYBAR=AMPLIY*COSPS-AMPLIX*SINPS
C
C
      INDEXX=0
      IF(SIGN(1.,AXBAR).NE.IX) INDEXX=1
      INDEXY=0
      IF(SIGN(1.,AYBAR).NE.IY) INDEXY=1
      IF((INDEXX.EQ.1).OR.(INDEXY.EQ.1)) NERROR=NERROR+1
C
C     COMPUTE PROBABILITY OF ERROR FOR THIS SYMBOL
C
      CALL PERR4(AXBAR,AYBAR,INDEXX,INDEXY,SNRDB,PEI,ENOISE,NSNR)
C
      DO 5 KK=1,NSNR
    5 PE(KK)=PE(KK)+PEI(KK)
C
      NTOTAL=NTOTAL+1
      IF(NTOTAL.NE.NSYMB) GO TO 1
      PRINT 150
  150 FORMAT(/4H SNR,10X,14HERROR OF ERROR/)
      DO 500 II=1,NSNR

  500 PEI(II)=PE(II)/FLOAT(NSYMB)
      PRINT 151,(SNRDB(II),PEI(II),II=1,NSNR)
  151 FORMAT(F5.1,10X,E13.6)
      PRINT 102,NERROR
  102 FORMAT(/2X,7HERRORS=,I5)
      GO TO 132
    1 CONTINUE
  132 LOOP=LOOP+1
      RETURN
      END
```

```
      SUBROUTINE DWEYE1(SCALA,DATA,KKK,LSTART,LSAMPL,INDEXC,IOPT,KL)
C THIS SUBROUTINE DRAWS THE EYE PATTERN DIAGRAM OF A SIGNAL ARRAY
C SCALA=MAX.+ OR - VALUE FOR FULL VERTICAL SCALE
C DATA=ARRAY NAME OF SIGNAL
C     LSTART=STARTING SAMPLE
C INDEXC=INDEX KEEPING TRACK OF WHICH CHANNEL IS BEING OBSERVED
C       =0 , X-CHANNEL EYE IS DRAWN
C       =1 , Y-CHANNEL EYE IS DRAWN
C      IOPT=1 , HALF OF THE PROCEEDING EYE AND TRAILING EYE ARE
C      ALSO DRAWN.  IF   IOPT=2   ONLY THE EYE IS DRAWN.
C
      DIMENSION DATA(512),X(512),Y(512)
      DIMENSION ANIX(512),BNIY(512)
      SAMPLE=LSAMPL
      LSAMP2=2*LSAMPL
      LHALF=IFIX(SAMPLE/2.)
      BNIY(202)=300
      BNIY(203)=13.3333
      DO 1 K=1,KKK
      J1=LSTART+LSAMP2*K
      IF(INDEXC.EQ.1) J1=J1+1
      IF(IOPT.EQ.2) GO TO 10
      JLEAD=J1-2*LHALF
      N=LSAMP2
      GO TO 11
   10 JLEAD=J1-2
      N=LSAMPL+2
   11 DO 2 J=1,N
      JJ=JLEAD+(J-1)*2
    2 Y(J)=DATA(JJ)
      FACTOR=400./SCALA
      DO 6 J=1,N
    6 X(J)=J-1
      XRANGE=N-2
      DELTA=XRANGE/200.
      ISLOPE=1
      XI=.455
      CALL INTERP(X,Y,N,XI,F,ISLOPE)
      ISLOPE=0
      IY=400+IFIX(F*FACTOR)
      IX=1
      ANIX(1)=IX
      BNIY(1)=IY
      DO 9 I=2,201
      IX=(I-1)*5+1
      ANIX(I)=IX
      XU=XI+(I-1)*DELTA
      CALL INTERP(X,Y,N,XU,F,ISLOPE)
      IY=400+IFIX(F*FACTOR)
      BNIY(I)=IY
    9 CONTINUE
      IF(KL.NE.1)GO TO 13
       CALL PLOTS(27.0,26.0)
      CALL RECT(0.02,2.0,24.0,21.0,0.0,3)
      CALL SYMBOL(9.0,3.5,0.2,15HSYMBOL DURATION,0.0,15)
      CALL SYMBOL(0.5,10.5,0.2,9HAMPLITUDE,90.0,9)
      CALL PLOT(0.7,4.0,-3)
      CALL GRID(0.0,0.0,1.0,1.0,20,15)
      CALL GRID(0.01,0.01,2.0,3.0,10,5)
      CALL SCALE(ANIX,23.0,201,1)
       CALL SYMBOL(1.0,20.0,0.5,
     136HDIGITAL SATELLITE SYSTEM PERFORMANCE,0.0,36)
       CALL SYMBOL(3.0,19.45,0.2,
     143H(1) FILTERS' CHARACTERISTICS:CHEBYSHEV TYPE,0.0,43)
       CALL SYMBOL(3.0,19.0,0.2,
     146H    4-POLE;1/2 DB RIPPLE;85 MHZ 3-DB BANDWIDTH,0.0,46)
       CALL SYMBOL(3.0,18.55,0.2,
     152H(2) SATELLITE TRANSPONDER T#T AT  1 DB INPUT BACKOFF,0.0,52)
        CALL SYMBOL(3.0,18.10,0.2,27H(3) MODULATION SCHEME: QPSK,
     10.0,27)
       CALL SYMBOL(3.0,17.65,0.2,30H(4) TRANSMISSION RATE: 80 MB/S,
     10.0,30)
       CALL SYMBOL(3.0,17.20,0.2,16H(5) BIT DETECTOR,0.0,16)
       CALL SYMBOL(14.0,17.5,0.3,11HEYE DIAGRAM,0.0,11)
      KL=2
   13 CALL FLINE(ANIX,BNIY,-201,1,0,0)
```

```
      SUBROUTINE EQLZR(DATA,KKK,LSAMPL,LSTART,NSNR,LCCP,NSYMB,
     1PSHIFT,PNOISE)
        DIMENSION  DATA(1),H(21),HV(21),FBT(21),ISS(50),ITDT(21)
        DIMENSION IST(32,5),ITNS(32),TNS(32,2),LNG(32),ISRV(32,50)
        COMMON H(21),HV(21),FBT(21),ISS(50),ITDT(21),
     1IIST(32,5),ITNS(32),TNS(32,2),LNG(32),ISRV(32,50)
        DIMENSION ITM(6),PER1(11),PER2(11),SNR(11)
        REAL LNG
        DO 888 I=1,32
        DO 888 J=1,50
        ISS(J)=0
        ITNS(I)=0
        LNG(I)=0
  888   ISRV(I,J)=0
        DO 889 J=1,21
        H(J)=0
        HV(J)=0.
        FBT(J)=0
  889   ITDT(J)=0
        DO 890 I=1,32
        DO 890 J=1,5
  890   IST(I,J)=0
        DO 891 I=1,32
        DO 891 J=1,2
  891   TNS(I,J)=0
        LH=LSAMPL
        READ 5,LH,(H(I),I=1,LH)
    5   FORMAT(I3,6(1X,F7.4),/,6(1X,F7.4))
        PRINT 11,LH,(H(I),I=1,LH)
   11   FORMAT(///,1X,'L=',1X,I3//,1X,'H(I),I=1,LH=',14(F7.4,1X))
        READ 6,LV,(HV(I),I=1,LV)
    6   FORMAT(I2,3(1X,F7.4))
   63   PRINT 64,LV,(HV(J),J=1,LV)
   64   FORMAT(///,1X,'V=',1X,I2//,1X,'HV(J),J=1,LV=',3(F7.4,1X))
        IF(LV.EQ.1.OR.LV.GT.6.OR.HV(1).NE.H(1))GO TO 100
  150   FORMAT(/1X,'SNR',10X,'PROBABILITY    OF .   ERROR',/16X,
     1'(DFE)',8X,'(DFE-MLSE)'/)
        II=0
        DO 107 KK=4,12
        II=II+1
        SNR(II)=KK
        CALL DFETAP(LH)
        NU=LV-1
        NST=2**NU
        DO 43 L=1,NU
        IST(1,L)=0
   43   CONTINUE
        DO 45 M=2,NST
        M1=M-1
        DO 39 I=2,NU
        IST(M,I)=IST(M1,I)
   39   CONTINUE
        IST(M,1)=IST(M1,1)+1
        DO 45 N=2,NU
        N1=N-1
        IF(IST(M,N1).NE.2)GO TO 45
   44   IST(M,N1)=0
        IST(M,N)=IST(M,N)+1
   45   CONTINUE
        DO 21 I=1,NST
        ITNS(I)=(I-1)/2+1
   21   CONTINUE
        DO 26 J=1,NST
        DO 23 K=1,NU
        ITM(K)=IST(J,K)
   23   CONTINUE
        ITM(LV)=0
        SUM=0.
        DO 24 L=1,LV
        IT=ITM(L)
        IF(IT.EQ.0.)GO TO 24
        SUM=SUM+IT*HV(L)
   24   CONTINUE
        TNS(J,1)=SUM
        ITM(LV)=1
```

```
      SUM=0.
      DO 25 M=1,LV
      IT=ITM(M)
      IF(IT.EQ.0)GO TO 25
      SUM=SUM+IT*HV(M)
   25 CONTINUE
      TNS(J,2)=SUM
   26 CONTINUE
      DO 96 K=1,50
      ISS(K)=0
   96 CONTINUE
      LNG(1)=0.
      DO 98 M=2,NST
      LNG(M)=10.E10
   98 CONTINUE
      DO 13 J=1,50
      ISRV(1,J)=ISS(J)
   13 CONTINUE
      DO 17 K=1,LH
      ITDT(K)=ISS(K)
   17 CONTINUE
      SUM=0.
      DO 48 J=1,LH
      HJ=H(J)
      SUM=SUM+HJ*HJ
   48 CONTINUE
      SNR=NSNR
      EGY=SQRT(SUM)
      STDV=EGY*10.**(-SNR(II)/20.)/2.
      KNT1=0
      KNT2=0
      NER1=0
      NER2=0
      KT1=0
      KT2=0
      KV=0
      NV=50
      KNT1=KNT1+1
      CALL IPUSH(KS,ISS,50)
      RCV=DATA
      FNS=PNOISE
      RCV=CHANEL(LH)+FNS
      CALL DFE1(RCV,LH,KTDT)
      IF(KTDT.NE.ISS(1))NER1=NER1+1
      KT1=KT1+1
      CALL IPUSH(KTDT,ITDT,LH)
      CALL DFE2(RCV,LH)
      CALL VITERB(NST,RCV)
      KV=KV+1
      IF(KV.NE.NV)GO TO 88
      CALL MERG(NST,IDX,NUM)
      DO 82 L=1,NUM
      LB=51-L
      IF(ISRV(IDX,LB).NE.ISS(LB))NER2=NER2+1
      KNT2=KNT2+1
      IF(KNT2.EQ.NDATA)GO TO 91
      KT2=KT2+1
      IF(KT2.NE.1000)GO TO 82
      P2=FLOAT(NER2)/KNT2
      KT2=0
   82 CONTINUE
      KV=0
      NV=NUM
      REF=LNG(IDX)
      DO 83 M=1,NST
      LNG(M)=LNG(M)-REF
   83 CONTINUE
   88 IF(KT1.NE.1000)GO TO 89
      P1=FLOAT(NER1)/KNT1
      KT1=0
   89 IF(KNT1.EQ.NDATA)PER1(II)=FLOAT(NER1)/NDATA
      GO TO 33
   91 PER2(II)=FLOAT(NER2)/NDATA
      PRINT 12,SNR(II),PER1(II),PER2(II)
   12 FORMAT(/,1X,F3.0,4X,E15.3,6X,E10.3)
  107 CONTINUE
```

```
      CALL PLOTS(25.0,27.0)
      CALL RECT(4.5,0.0,26.7,20.0,0.0,3)
      CALL PLOT(6.0,1.0,-3)
      CALL SCALE(SNR,16.0,9,1)
      CALL AXIS(0.0,0.0,22HSIGNAL-TO-NOISE  IN DB.-22,16.0,
     10.0,SNR(10),SNR(11))
      CALL SCALG(PER2,25.0,9,1)
      CALL LGAXS(0.0,0.0,20HPROBABILITY OF ERROR,20,25.,90.0,
     1PER2(10),PER2(11))
      CALL PLOT(0.0,25.0,3)
      PER1(10)=PER2(10)
      PER1(11)=PER2(11)
      CALL LGLIN(SNR,PER1,9,1,0.0,1)
      CALL WHERE(RXPAGE,RYPAGE,RFACT)
      CALL SYMBOL(RXPAGE,RYPAGE,0.2,' DFE',0.0,4)
      CALL PLOT(0.0,25.0,3)
      CALL LGLIN(SNR,PER2,9,1,0.0,1)
      CALL WHERE(RXPAGE,RYPAGE,RFACT)
      CALL SYMBOL(RXPAGE,RYPAGE,0.2,' DFE-MLSE',0.0,9)
      CALL SYMBOL(8.0,24.5,0.5,17HDIGITAL SATELLITE,0.0,17)
      CALL SYMBOL(8.0,23.75,0.5,18HSYSTEM PERFORMANCE,0.0,18)
      CALL SYMBOL(8.1,23.20,0.2,
     143H(1) FILTERS' CHARACTERISTICS:CHEBYSHEV TYPE,0.0,43)
      CALL SYMBOL(8.1,22.75,0.2,
     146H    4-POLE;1/2 DB RIPPLE;85 MHZ 3-DB BAND-WIDTH,0.0,46)
      CALL SYMBOL(8.1,22.30,0.2,
     152H(2) SATELLITE TRANSPONDER TWT AT  1 DB INPUT BACKOFF,0.0,52)
C     CALL SYMBOL(8.1,22.30,0.2,
C     127H(2) WITHOUT NON-LINEARITIES,0.0,27)
      CALL SYMBOL(8.1,21.85,0.2,27H(3) MODULATION SCHEME: QPSK,
     10.0,27)
      CALL SYMBOL(8.1,21.40,0.2,
     141H(4) EQUALIZATION/DETECTION SCHEME: HYBRID,0.0,41)
      CALL PLOT(0.0,0.0,999)
  100 RETURN
      END
C
C
      SUBROUTINE DFETAP(LH)
      COMMON H(21),HV(21),FBT(21)
      DO 16 K=1,LH
      FBT(K)=H(K)-HV(K)
   16 CONTINUE
      RETURN
      END
C
C
      SUBROUTINE IPUSH(IN,IV,N)
      DIMENSION IV(50)
      DO 92 J=2,N
      NJ=N-J+1
      IV(NJ+1)=IV(NJ)
   92 CONTINUE
      IV(1)=IN
      RETURN
      END
C
C
      FUNCTION CHANEL(LH)
      COMMON H(21),HV(21),FBT(21),ISS(50)
      SUM=0.
      DO 39 L=1,LH
      IS=ISS(L)
      IF(IS.EQ.0)GO TO 39
      SUM=SUM+IS*H(L)
   39 CONTINUE
      CHANEL=SUM
      RETURN
      END
```

```
      SUBROUTINE DFE1(RCV,LH,KTDT)
      COMMON H(21),HV(21),FBT(21),ISS(50),ITDT(21)
      SUM=0.
      DO 49 M=2,LH
      IT=ITDT(M-1)
      IF(IT.EQ.0)GO TO 49
      SUM=SUM+IT*H(M)
   49 CONTINUE
      TRCV=RCV-SUM
      KTDT=1
      IF(TRCV.LT.0.5)KTDT=0
      RETURN
      END
C
C
      SUBROUTINE DFE2(RCV,LH)
      COMMON H(21),HV(21),FBT(21),ISS(50),ITDT(21)
      SUM=0.
      DO 59 N=2,LH
      IT=ITDT(N)
      IF(IT.EQ.0)GO TO 59
      SUM=SUM+IT*FBT(N)
   59 CONTINUE
      RCV=RCV-SUM
      RETURN
      END
C
C
      SUBROUTINE VITERB(NST,RCV)
      COMMON H(21),HV(21),FBT(21),ISS(50),ITDT(21),
     1IST(32,5),ITNS(32),TNS(32,2),LNG(32),ISRV(32,50)
      DIMENSION TLNG(32),ITSV(32,50)
      REAL LNG
      DO 77 I=1,NST
      DIF1=RCV-TNS(I,1)
      PLUS1=DIF1*DIF1
      DIF2=RCV-TNS(I,2)
      PLUS2=DIF2*DIF2
      ISUB=ITNS(I)
      TST1=LNG(ISUB)+PLUS1
      ISUB=ISUB+NST/2
      TST2=LNG(ISUB)+PLUS2
      IDX=ITNS(I)
      IF(TST1.GT.TST2)IDX=ISUB
      DO 76 J=2,50
      ITSV(I,J)=IST(I,J)
   76 TLNG(I)=AMIN1(TST1,TST2)
   77 CONTINUE
      DO 78 L=1,NST
      LNG(L)=TLNG(L)
   78 CONTINUE
      DO 79 I=1,NST
      DO 79 J=1,50
      ISRV(I,J)=ITSV(I,J)
   79 CONTINUE
      RETURN
      END
C
C
      SUBROUTINE MERG(NST,IDX,NUM)
      COMMON H(21),HV(21),FST(21),ISS(50),ITDT(21),
     1 IST(32,5),ITNS(32),TNS(32,2),LNG(32),ISRV(32,50)
      REAL LNG
      IDX=1
      DO 41 I=1,50
      IB=51-I
      IRF=ISRV(1,IB)
      DO 41 J=2,NST
      IF(IRF.NE.ISRV(J,IB))GO TO 51
   41 CONTINUE
   51 NUM=I-1
      IF(NUM.NE.0)RETURN
      NUM=25
      TST=LNG(1)
      DO 42 K=2,NST
      IF(LNG(K).GE.TST)GO TO 42
      IDX=K
      TST=LNG(K)
   42 CONTINUE
      RETURN
      END
```

```
      SUBROUTINE INTERP(X,Y,N,XU,F,ISLOPE)
C
C THIS SUBROUTINE MUST BE USED WITH CARE
C IT SHOULD NOT BE USED TO EXTRAPOLATE DATA BECAUSE IT USES A
C QUADRATIC APPROXIMATION AT THE EDGE OF THE ARRAY ALSO IT SHOULD
C BE MADE CERTAIN THAT NO TWO Y(I) ARE THE SAME BECAUSE WHEN THE SLOPES
C ARE CALCULATED ERROR MODE 2 C OCCUR
C
C INTERPOLATES THROUGH N POINTS . ISLOPE=1 ON FIRST CALL
C F RETURNS THE FUNCTION VALUE . USES PIECE WISE CUBIC APPROXIMATION
C
      DIMENSION SLOPES(512),X(512),Y(512)
      IF(ISLOPE.EQ.0) GO TO 1
      CALL SLOPE(X,Y,SLOPES,N)
    1 IF(XU.LT.X(1).OR.XU.GT.X(N)) GO TO 12
C
C     FIND OUT BETWEEN WHICH TWO POINTS XU IS
C
      DO 4 I=2,N
      J=I-1
C
C     1.0E-4 IS AN ARBITRARY FIGURE USED IN THIS PARTICULAR CASE
      IF(ABS(XU-X(I)).LT.1.0E-4) GO TO 10
      IF(ABS(XU-X(J)).LT.1.0E-4) GO TO 11
      IF(XU.GT.X(J).AND.XU.LT.X(I)) GO TO 5
      GO TO 4
    5 IF(I.EQ.2) GO TO 6
      IF(I.EQ.N) GO TO 7
      CALL CUBIC(A,B,C,D,X(J),Y(J),SLOPES(J),X(I),Y(I),SLOPES(I))
      XA=XU-X(J)
      F=A*XA**3+B*XA**2+C*XA+D
      RETURN
    6 CALL QUAD(A,B,C,X(J),Y(J),X(I),Y(I),SLOPES(I))
    8 F=A*XU**2+B*XU+C
      RETURN
    7 CALL QUAD(A,B,C,X(I),Y(I),X(J),Y(J),SLOPES(J))
      GO TO 8
    4 CONTINUE
      PRINT 9
    9 FORMAT(5HERROR)
      F=0.
      RETURN
   10 F=Y(I)
      RETURN
   11 F=Y(J)
      RETURN
   12 F=0.
      PRINT 3
    3 FORMAT(5X,'WARNING,X OUTSIDE RANGE OF POINTS')
      RETURN
      END

      SUBROUTINE LCAC4(DATA,KKK,LSAMPL,NX,NY,I,JLAST,JTAP,LDIM)
      DIMENSION DATA(512),DADA(512),NX(11),NY(11)
C
      DO 1 K=1,KKK
      IF(I.EQ.JLAST) I=0
      I=I+1
      J=I-JTAP
      IF(I.LE.JTAP) J=J+JLAST
      IX=NX(J)*NX(I)
      IY=NY(J)*NY(I)
      NX(I)=IX
      NY(I)=IY
      JA=2*LSAMPL
      JB=K*JA
      J1=JB-JA+1
      J2=JB-1
      DO 2 J3=J1,J2,2
      DATA(J3)=IX
    2 DATA(J3+1)=IY
    1 CONTINUE
C
C     THE REMAINING DATA ARE SET TO ZERO FOR SPILLOVER EFFECT
C
      JS=J2+2
      DO 205 JJ=JS,LDIM
  205 DATA(JJ)=0.
      RETURN
      END
```

```
      SUBROUTINE PERR4(AMPLIX,AMPLIY,INDEXX,INDEXY,SNRDB,PEI,
     *PNOISE,NSNR)
      DIMENSION PEI(25),SNRDB(25)
      DO 1 M=1,NSNR
      SNR=EXP(SNRDB(M)*.23026)
      SCALE=SQRT(SNR/PNOISE/2.)
      XX=AMPLIX*SCALE
      ABSX=ABS(XX)
      CALL TTERFC(ABSX,EX)
      EX=EX/2.
      IF(INDEXX.EQ.1) EX=1.-EX
      YY=AMPLIY*SCALE
      ABSY=ABS(YY)
      CALL TTERFC(ABSY,EY)
      EY=EY/2.
      IF(INDEXY.EQ.1) EY=1.-EY
    1 PEI(M)=EX+EY-EX*EY
      RETURN
      END

      SUBROUTINE CFICEL(SBANDW,FBANDW,TF,LDIM)
      DIMENSION TF(512)
      NH=LDIM/2
      NQ=LDIM/4
      DW=FLOAT(NQ)*FBANDW/SBANDW
      LW=IFIX(DW)
      PRINT 3,SBANDW,LW
    3 FORMAT(/10X,'SBANDW=',F8.3,'LW=',I3/)
      DO 2 I=1,LDIM
    2 TF(I)=0.
      DO 1 I=2,LW
      I2=I*2
      I1=I2-1
      TF(I1)=1.
      TF(I2)=0.
      I2=2*(NH-I+2)
      I1=I2-1
      TF(I1)=1.
      TF(I2)=0.
    1 CONTINUE
      TF(1)=1.
      TF(2)=0.
      TF(NH+1)=0.
      TF(NH+2)=0.
      RETURN
      END

      SUBROUTINE BISINC(DATA,TF1,TF2,LSAMPL,NSTART,LSTART,LDIM)
      DIMENSION DATA(512),TF1(512),TF2(512)
      INDEX=0
      DO 1 I=1,LDIM
    1 DATA(I)=0.
      LSAMP2=2*LSAMPL
      I1=LSAMP2-1
      DO 2 I=1,I1,2
    2 DATA(I)=1.
      CALL FILTER(DATA,TF1,256,LDIM)
    5 SUM=0.
      DO 3 K=1,481,2
      I2=K+LSAMP2-2
      TSUM=0.
      DO 4 I=K,I2,2
    4 TSUM=TSUM+DATA(I)
      IF(TSUM.LT.SUM)GO TO 3
      SUM=TSUM
      KSTART=K
    3 CONTINUE
      INDEX=INDEX+1
      IF(INDEX.GT.1)GO TO 6
      NSTART=KSTART
      CALL FILTER(DATA,TF2,256,LDIM)
      GO TO 5
    6 LSTART=KSTART-(NSTART-1)
      PRINT 36,NSTART,LSTART
   36 FORMAT(2(5X,I3))
      RETURN
      END
```

```
      SUBROUTINE TTERFC(Y,Z)
      DIMENSION A(10),P(8),Q(9)
      DATA C/1.1283792/
      DATA A(1),A(2),A(3),A(4),A(5),A(6),A(7),A(8),A(9),A(10)
     1/1.,-0.33333333,0.1,-0.02380952E0,0.4629629E-2,
     2-0.75757576E-3,1.0683761E-4,-1.3227513E-5,1.4589169E-6,
     3-1.4503855E-7/
      DATA P(1),P(2),P(3),P(4),P(5),P(6),P(7),P(8)
     1/883.47894,1549.6793,1347.1941,723.04,255.5049,
     259.24001,8.3765311,.5641956/
      DATA Q(1),Q(2),Q(3),Q(4),Q(5),Q(6),Q(7),Q(8),Q(9)
     1/883.47894,2546.5785,3337.2214,2606.712,1333.57,
     2460.28512,165.5025,14.647012,1./
      KRET=1
    5 X=Y
      MD=0
   10 ISW=2
      IF(X.GE.0.)GO TO 15
      ISW=1
      X=-X
   15 IF(KRET.NE.2)GO TO 20
      IF(X.LE.5.5)GO TO 20
      Z=1.
      IF(ISW.EQ.1)Z=-1.
      GO TO 100
   20 IF(X.LE..47)GO TO 45
      KRET=1
   25 SN=P(8)
      SD=Q(9)
      DO 30 J=1,7,1
      I=8-J
      SN=SN*X+P(I)
   30 CONTINUE
      DO 35 J=1,8
      I=9-J
      SD=SD*X+Q(I)
   35 CONTINUE
      Z=SN/SD*EXP(-X*X)
      IF(KRET.NE.1)GO TO 40
      Z=1.-Z
      IF(ISW.NE.2)Z=-Z
      GO TO 100
   40 IF(ISW.NE.2)Z=2.-Z
      IF(MD.NE.0)Z=.5*Z
      GO TO 100
   45 XX=X*X
      Z=A(10)
      DO 50 J=1,9
      I=10-J
      Z=Z*XX+A(I)
   50 CONTINUE
      Z=C*Z*X
      IF (KRET.NE.2) GO TO 55
      IF (ISW.NE.2) Z=-Z
      GO TO 100
   55 Z=1.-Z
      GO TO 40
   60 IF(X.LE.9.)GO TO 65
      Z=0.
      GO TO 40


   65 IF(X.LE..47)GO TO 70
      KRET=2
      GO TO 25
   70 IF(X.GT.1.E-15)GO TO 45
      Z=1.
      GO TO 40
  100 RETURN
      END
```